

## **DISCLAIMER**

**This report was prepared as an account of work sponsored by an agency of the United States Government. Neither the United States Government nor any agency thereof, nor any of their employees, makes any warranty, express or implied, or assumes any legal liability or responsibility for the accuracy, completeness, or usefulness of any information, apparatus, product, or process disclosed, or represents that its use would not infringe privately owned rights. Reference herein to any specific commercial product, process, or service by trade name, trademark, manufacturer, or otherwise does not necessarily constitute or imply its endorsement, recommendation, or favoring by the United States Government or any agency thereof. The views and opinions of authors expressed herein do not necessarily state or reflect those of the United States Government or any agency thereof. Reference herein to any social initiative (including but not limited to Diversity, Equity, and Inclusion (DEI); Community Benefits Plans (CBP); Justice 40; etc.) is made by the Author independent of any current requirement by the United States Government and does not constitute or imply endorsement, recommendation, or support by the United States Government or any agency thereof.**

# The National Diagnostic Plan (NDP) for HED Science September 2025

D Bradley

November 2025



## **Disclaimer**

---

This document was prepared as an account of work sponsored by an agency of the United States government. Neither the United States government nor Lawrence Livermore National Security, LLC, nor any of their employees makes any warranty, expressed or implied, or assumes any legal liability or responsibility for the accuracy, completeness, or usefulness of any information, apparatus, product, or process disclosed, or represents that its use would not infringe privately owned rights. Reference herein to any specific commercial product, process, or service by trade name, trademark, manufacturer, or otherwise does not necessarily constitute or imply its endorsement, recommendation, or favoring by the United States government or Lawrence Livermore National Security, LLC. The views and opinions of authors expressed herein do not necessarily state or reflect those of the United States government or Lawrence Livermore National Security, LLC, and shall not be used for advertising or product endorsement purposes.

This work performed under the auspices of the U.S. Department of Energy by Lawrence Livermore National Laboratory under Contract DE-AC52-07NA27344.

## **The National Diagnostic Plan (NDP) for HED Science September 2025**

**Abstract:** This documents the National Diagnostic Plan as of September 2025. The major changes in this version compared to the NDP document issued in 2024 are the new schedules and the text for the national transformative diagnostics - section III. The many local diagnostics for our three Inertial Confinement Fusion (ICF) facilities; NIF, Z and OMEGA are also updated and captured in section V.

**Summary:** The National Nuclear Security Administration (NNSA) has made significant investments in major facilities and high-performance computing to successfully execute the Stockpile Stewardship Program (SSP). The more information obtained about the physical state of the plasmas produced, the more stringent the test of theories, models, and codes can be, leading to increased confidence in our predictive capability. To respond to the increasing sophistication of the ICF program, a multi-year program to develop and deploy advanced diagnostics has been developed by the expert scientific community. To formalize these previously collegial activities NNSA directed the formation and duties of the National Diagnostics Working Group (NDWG) for HED Science.

The NDWG has identified nine transformational diagnostics, shown in Table 1, that will provide unprecedented information from experiments in support of the SSP at NIF, Z and OMEGA. Table 2 shows how the missions of the SSP experiments including materials, complex hydrodynamics, radiation flow and effects and thermo-nuclear burn and boost will produce new observables, which need to be measured using a variety of the largely new diagnostic technologies used in the ten transformational diagnostics. The data provided by these diagnostics will validate and improve the physics contained within the SSP's simulations and both uncover and quantify important phenomena that lie beyond our present understanding.

Transformative diagnostic	Collaborating Institutions	New capability
Pulse Dilation and Drift Tube Imaging	SNL, GA, LLNL, LLE, LANL	Multi-dimensional shape and spectra with unprecedented time and space resolution for fusion, Pu strength, and radiation effects sources
Ultraviolet Thomson Scattering (UVTS)	LLE, LLNL, LANL, NRL	Localized plasma conditions and turbulence in hohlraums and Laser Direct Drive ablation plasma. Additional uses include plasma conditions at low density for rad flow studies and many discovery science applications.
3D n/gamma imaging (NIS)	LANL, LLNL, SNL	3D shape & size of both burning and cold compressed fuel, as well as remaining carbon ablator
Gamma spectroscopy (GCD/GRH)	LANL, AWE, GA, LLNL, SNL, NNSS	Fusion burn history allowing inferred pressure with increased precision and measured truncation of burn from degradation mechanisms such as mix and loss of confinement.
Time resolved neutron spectrum (MRS-time)	MIT, LLNL, GA, LLE	Time evolution of the fusion burn temperature and areal density
Time resolved diffraction (XRDt)	SNL, LLNL, LLE	Time evolution of material structure (including weapon materials) and compression at high pressure. Also enables more efficient facility use through multiple measurements on a single shot.

High Resolution Velocimeter (HRV)	LLNL, LLE, SNL	High resolution line-imaging velocimetry measurements including higher accuracy (<1%) material EOS at high pressure. Also enables more efficient facility use through multiple high-fidelity measurements on a single shot.
>15 keV X-ray detection (DHEX)	LLNL, LLE, SNL	Multiple-frame time resolved detection of high energy (>15 keV) x-rays with high detection efficiency.
hCMOS	SNL, LLNL	Multi-frame, burst mode imaging sensor capable of capturing images on the nanosecond timescale and nanosecond gated single frame radiation hardened image sensors.

Table 1: The ten transformational diagnostics, institutional involvement & capability.

Mission	New Observable	Technique	Acronym
Materials	Strength vs time of compressed Pu	>4 images/costly target	SLOS, hCMOS
	Phase change of compressed Pu - rates	Time resolved x-ray diffraction	XRDt
	EOS of compressed Pu	High resolution VISAR velocimetry	HRV
Hydro and Properties	High energy x-ray images of Structure	Detection of High Energy x-rays	DHEX
	T <sub>e</sub> of Marshak wave	Deep U.V. Thomson Scattering	UVTS
Outputs and Survivability	Hard spectrum vs space & time	SLOS	hCMOS
TN Burn and Pursuit of High Yield	Time history of burn	Ultra-fast Cerenkov detector	GCD
	3D T <sub>e</sub> and density vs time	Dilation tube	HYXI, hCMOS
	3D burn, 3D mix vs time	3D neutron/y imaging	NIS
	T <sub>ion</sub> and areal density vs time	Neutron spectrum vs time	MRS-time
All	Hohlraum density & T vs space & time	Deep U.V. Thomson Scattering	UVTS

Table 2: How the missions of the SSP will be enhanced by new observables measured by the ten transformational diagnostics being developed under the guidance of the NDWG.

In addition to the transformational diagnostics, there are:

- (1) a set of broad diagnostics coordinated across the ICF sites,
- (2) a large number of local diagnostics associated with the three large facilities: NIF, Z and OMEGA.

This document is an update of the NDP as of 9/30/2025. The activities of the NDWG and its organization and leadership are summarized in section II. The organization, progress, and plans for the transformational diagnostics are in section III. The activities of the broad diagnostics are in section IV. Finally, the progress and plans for the local diagnostics on NIF, Z and OMEGA are in section V.

## **II: Recent activities of the National Diagnostic Working Group (NDWG)**

### **IIa: ICF and HED Diagnostics: Background and Mission**

ICF and High Energy Density (HED) physics experiments involve phenomena that occur on timescales measured in picoseconds and spatial scales measured in micrometers (or microns). Observable information is conveyed in photons with energies ranging from visible light to MeV gamma rays, and in charged and neutral

particles from fusion reactions. Progress in ICF and HED has been dependent for decades on the development and innovation of new instruments and techniques to measure the observables with increasing temporal, spatial, and energy resolution, and with the ability to gather more data in a single experiment.

Since 2008 there have been regular NDWG meetings, initially to foster national participation in the diagnostics for the NIF and recently to coordinate research and development of HED diagnostics across the ICF sites for NIF, Z and OMEGA. ***By coordinating efforts, each site is able to capitalize on the advances made at the other sites, share expertise, and incorporate new techniques into their own programs.***

The national diagnostics development effort is divided into three groups:

- Transformational Diagnostics: diagnostics requiring a major national effort with the potential to transform experimental capability for the most critical science needs across the complex.
- Broad Diagnostics: diagnostic efforts and techniques requiring significant national efforts which will enable new or more precise measurements across the complex.
- Local Diagnostics: important diagnostics that implement known technology for a local need and are identified by facility management responding to the needs of the local user community.

The NNSA ICF and HED programs supports stockpile stewardship through the four principal missions shown in Table 2. The facilities also support National Security Applications (NSA) with other national agencies and basic science conducted mainly in collaboration with universities. The decisions on which new diagnostics to develop depends on a combination of the diagnostic usage at the various facilities, the prioritized needs of the programs, the status of technology, and the requests from the user community. Each facility has a different process for making these decisions for local diagnostics. For transformational and broad diagnostics, the development activities are prioritized, advocated for, and concerns are raised as appropriate by the appointed leaders of the NDWG. The core leadership of the NDWG as appointed by the ICF Execs are David Bradley (Lawrence Livermore National Lab, LLNL), Sean Regan (Laboratory for Laser Energetics, LLE), Eric Harding (Sandia National Laboratories, SNL), and Tana Morrow (Los Alamos National Laboratory, LANL) with consistent support from Joe Kilkenny (General Atomics, GA), Alastair Moore, and Andy Mackinnon(LLNL), Maria Gatu Johnson (Massachusetts Institute of Technology, MIT), Chuck Sorce and Steven Ivancic (LLE), Michael Jones (SNL), and Eric Loomis and Yong Ho Kim (LANL).

### **IIb: Recent activities and organization of the NDWG**

- (i) The Dec. 2024 NDWG meeting was hosted by Los Alamos National Laboratory. A total of 131 registered participants, representing institutions from around the world, came together to discuss diagnostic development and progress.
- (ii) The NDWG leadership group met via video teleconference in March 2025 to review progress.
- (iii) The NDWG leadership group met video teleconference June 2025 to review progress and discuss initial plans for the December meeting which will be hosted by Sandia National Laboratory.
- (iv) The NDWG leadership group met via video teleconference in Sept 2025 to review progress and re-plan technical progress according to the expected budget for FY26. This document includes new updates based on the plan formulated during that meeting.

### **III: Transformational Diagnostics**

Section IIIa is an overview of the transformational diagnostics. Section IIIb is a summary of the achievements and plans for each of the transformational diagnostics.

#### **IIIa: Overview of the Transformational Diagnostics**

The NDWG defined Transformational Diagnostics as those requiring a major national effort with the potential to transform experimental capability for the most critical science needs across the complex. In early 2015 a set of eight transformational diagnostics were identified. This set of diagnostics was reviewed by an independent group of experts in 2015 who reported to NNSA on the relative merit and urgency of each proposed capability (report is available). The NDWG monitors, on a quarterly basis, progress on these transformational diagnostics, as described in section II, and makes recommendations to the sites in terms of development priority and resource requirements. As diagnostics are commissioned and work is completed, that diagnostic is no longer tracked as part of the NDP. New diagnostics are added by agreement of the NDWG Leadership. There is a simplified description of these diagnostics starting on page 41 of NNSA's 2016 Inertial Confinement Fusion Program Framework DOE/NA-0044, and in Appendix C.

Each category of transformational diagnostics can mean many actual diagnostics at some or all three of the major facilities. The plans for implementation consist of many phases. Table 3 is the updated top-level schedule for the transformative diagnostics as of September 2025. More details are in Section IIIb. These schedules are largely consistent with the expected budgets but can be affected by both the implemented annual site allocations by NNSA and the distributions relative to other funding priorities by each of the site managers.

UPDATED Notional PLAN 103125		FY25	FY26	FY27	FY28	FY29
NDP						
Pulse dilation(SLOS/TRIXI/ HYXI)		▲	▲	▲	▲	▲
TRL-5		Ω 3rd LOS (TRIXI)	HXYI_IP		HXYI_Hyperion	HXYI_2_Hyperion
Ultra-Violet Thomson Scattering		▲		▲	▲	▲
TRL 5 - TRL-8			NIF OTSL workshop	NIF OTSL 4w/ 5w RR	OTSL 4w/ 5w PDR	OTSL 4w/ 5w FDR
3D Neutron/Gamma Imaging		▲		▲▲	▲	
TRL-6		Gm Img 1 LoS NEMESIS (Z) OQ	Gm LOS_2	Add RIF imaging 1 LoS		
Gamma Spectroscopy		▲		▲		▲
TRL-4		GRH-10+MJ assessment		GRH-20+MJ PDR		Install GRH-20+MJ
Time Resolved Neutron Spectrometer			▲		▲	
TRL-1 - TRL-3			test options at Omega		CDR for NIF diagnostic	PDR for NIF diagno
High Resolution Velocimetry			▲	▲	▲	▲
TRL-6		HY VISAR on NIF PDR		HY VISAR FDR	Install High Yield VISAR	Upgrade VISAR
Time Resolved X-Ray Diffraction		▲		▲		
TRL-5		Fiddle-A PQ		Commission Fiddle-B		
>15 KeV X-ray Detection				▲		
Photo diode/Roics/MCP/Struc PC				MCP with Streak		
TRL-4						
hCMOS		▲		▲	▲	
TRL-9, Daedalus TRL-6, Tantalus & Hyperior	Tantalus		Hyperion_1		Hyperion_2	

Table 3: Schedule for the transformational diagnostics. The acronym definition is below.

*SLOS*– Single Line Of Sight X-ray imager

*TRL* – Technical readiness level on a scale of 1-9 with 9 being further developed (details in the appendix).

*Ω SLOS-TRXI*- x-ray imager on OMEGA consisting of a time dialation tube in front of a hCMOS detector

*0,0 Scattered LOS* – Imaging of down-scattered neutrons from (near) the north pole.

*Z-High E* – Single frame diffraction on Z at >10 keV

*Daedalus V2*: Next generation ROIC with tiling capability and deeper electron well for extended spectral range for spectroscopy.

*Tantalus*: First ROIC to be manufactured in an external foundry with integration times of around 500ps. Keystone for commercialization.

*SFS*: Single Frame Sensor a hCMOS sensor with <500ps temporal resolution (now named *Hyperion*)

*HYXI*: High Yield X-ray Imager a hCMOS based pulse dilation imager for x-ray hot spot self-emission for use on 10MJ+ NIF experiments.

### IIIb: Achievements and plans for each of the nine transformational diagnostics.

### IIIb-1: Pulse-dilation Drift Tube

Two key technologies developed within the ICF program are revolutionizing gated x-ray detectors. These technologies are pulse-dilation tubes developed in collaboration between General Atomics, Kentech Instruments, and LLNL, and fast-gated hybrid complementary metal-oxide-semiconductor (hCMOS) sensors developed at SNL. The scope of the hCMOS development has caused this effort to be covered in a new section specifically addressing hCMOS ROICs and diodes, see hCMOS section. Pulse-dilation coupled with hCMOS sensors provides a transformative capability of time gating for multiple frames along a single line-of-sight (SLOS) at gate times as short as 10 ps. Pulse-dilation coupled with other high-speed photodetectors, such as photomultiplier tubes, provides a manner in which to provide instrument response functions as short as a few ps.

Used on its own, the hCMOS sensor can provide direct detection of multi-keV x-rays or electrons at gate times  $\geq 1$  ns as well as visible to near IR laser beams. Pulse-dilation SLOS framing cameras are transformative because they enable multiple time-gated detection of x-ray images or spectra at frame rates never before possible. Spectra are recorded using curved crystals. Images are recorded with curved crystals or multi-layer mirror optics, which can have superior spatial resolution and energy selectivity over pinhole/slit optics, but are too expensive or take up too much space to create an array of many images along many lines-of-sight. hCMOS sensors are transformative because they provide multi-frame direct detection of x-rays at nanosecond frame-rates from the same active area (pixel) in a technology that can be customized for the x-ray energy. Existing sensors have good sensitivity for x-rays with a photon energy up to  $\sim 10$  keV and new technology development is planned for capability up to  $\sim 50$  keV.

The hCMOS and SLOS technologies are establishing themselves as critical tools for the NNSA stockpile stewardship program across nearly all the science campaigns and ICF. For thermonuclear burn experiments, SLOS technology enables time-resolved 3D imaging with sufficient spatial resolution to diagnose failure modes of high convergence implosions. In opacity experiments, hCMOS sensors enable time-resolved measurements of the plasma evolution essential for addressing systematic differences between models and data. In strength and phase experiments of high-pressure plutonium, hCMOS sensors will enable time-sequence measurements on a single shot (instead of using multiple shots to map out the evolution), which improves the accuracy through elimination of shot-to-shot variability and reduces the overall use of Pu on the facilities. In hostile environment experiments, high-energy hCMOS sensors will enable more detailed understanding of x-ray source physics through enhanced imaging capability that will improve the fidelity of the x-ray test environment for more precise evaluation of component survivability. There are now more than 10 diagnostics using hCMOS/SLOS technology with several more in the development phase.

While the SLOS cameras, both at the NIF and at the Omega laser facility have unlocked new experimental capabilities and have demonstrated how collaboration on diagnostic technologies at the national level leads to innovation, they are not in fact the first type of instruments leveraging the pulse-dilation drift tube technologies. Since 2014, the Dilation X-Ray Imager (DIXI) is providing X-ray imaging for ICF experiments with a temporal resolution under 10 ps that is more adequate to resolve the rapid evolution of imploding DT capsules than the 100 ps temporal resolution achieved by MicroChannel Plate (MCP) based framing cameras. HCMOS technology was not available at the time of the commissioning of DIXI, which instead uses a traditional MCP detector as a backend detector. In 2021, a second DIXI camera was installed on NIF. Located near the target chamber pole (hence named Polar DIXI, or PDIXI), it supplements DIXI to provide a second X-ray imaging line-of-sight on high-yield ICF experiments. As the implosions' performance has increased, the PDIXI camera has been steadily upgraded to continue provide high-quality data and support the National Science Goal 5.2, "Experimentally assess 10 MJ class platform on NIF" of the HED&IS 10-year plan. In FY25, PDIXI has routinely delivered time-resolved images of multi-MJ implosions, including on record energy gain shot N250406. The modifications applied to PDIXI have been retrofitted to the DIXI camera in FY24 and FY25, with the expectation that both instruments will serve as the primary time-resolved X-ray imaging lines of sight on 10 MJ class implosions starting in FY26.

The High Yield X-ray Imager (HYXI) is being developed at LLNL as an evolution from the DIXI cameras, leveraging hCMOS technology, and also with the objective to support the goal identified in paragraph 5.2 of the FY24 HED&IS Program Plan, "Experimentally assess 10 MJ class platform on NIF", while serving as the first step to evaluate the feasibility and the technology developments required to support higher implosion yields (paragraph 5.14, "Experimentally assess 30 MJ class platform on NIF"). HYXI is the first time-resolved gated x-ray detector designed with the intent to provide high-quality data on ICF shots delivering fusion yields at or above 10 MJ. HYXI will allow the collection of a series of snapshots of the DT capsule emission throughout the implosion, which will be used to measure its size and shape with 15 ps resolution. One of the performance requirements of HYXI is to provide images with signal-to-background ratios (S/B) of 25 on 10 MJ shots. This will be a major improvement compared to the current NIF capability based on the DIXI detectors, which have demonstrated S/B of ~16 at 3 MJ on the first fusion ignition experiment in December 2022. To achieve this, HYXI will leverage both the pulse-dilation drift tube and hCMOS sensor technologies. The former permits greater control of the location of the detector elements sensitive to neutron-induced background, which can be placed further away from the source and shielded from direct line-of-sight particles, while the latter has demonstrated excellent radiation tolerance on previous NIF experiments and other radiation testing facilities. A new hCMOS sensor design named HYPERION is being developed as part of the HYXI project, which will bring additional radiation tolerance by reducing the interaction cross-section of several internal components with neutrons and gamma rays. A Final Design Review (FDR) of HYPERION was held in May 2024, and the delivery of the first sensors is scheduled for Q3 FY26. HYXI will be commissioned in successive phases on NIF. The

first one (Q3 FY25) will be implemented in Q4 FY25 and allows for time-integrated data collection using imaging plates, along an orthogonal line of sight to the ones currently being used/provided by the DIXI cameras. The first experiment utilizing this capability is scheduled for Q1 FY25. The second phase (Q3 Q4 FY26) will bring the ability to collect initial time-resolved images using the existing backend gated detector used in the DIXI cameras, however images meeting the full HYXI performance requirements will only be obtained during phase 3, with the integration of the HYPERION sensor at the end of Q4 FY26 FY27. The FDR for HYXI is ~~was held~~ scheduled for the end of September 2024. Procurement of long lead time items, such as the high voltage pulser electronics, has already begun, with some prototype parts already delivered.

The Omega Hot-Spot X-ray Imager (XRHSI) will provide a 3<sup>rd</sup> time-resolved x-ray line of sight for the OMEGA laser system in support of the goals in Section 5.7 of the HED&IS Program Plan “Determine the limit of implosion efficiency (X) on OMEGA”. The XRHSI builds on lessons learned in the development cycle of SLOS instruments employing a longer drift region and modest demagnification. The XRHSI completed a Preliminary Design Review in April 2024 and a Statement of Work was submitted to General Atomics for the design and fabrication of the drift tube, anticipated to be completed in FY25. The x-ray imager design is anticipated to be complete in Q1 FY25 and the overall system will have a Final Design Review by Q2 FY25.

The OMEGA cryo campaign now reaches yields that make high bandwidth DT-gamma measurements possible with a pulse-dilation (PD-PMT) enhanced gamma-ray history diagnostic (GRH). The GRH with PD-PMT will provide a 10 ps instrument IRF. This will make measuring burn width of 10 ps and shot to shot variations in burn width of 5 ps possible. A project to integrate a GRH at OMEGA was kicked off in FY 24 to support a campaign for improving understanding of the energy balance of the hot-spot in LDD implosions and how it relates to the gamma reaction history. Hardware was procured and engineering to adapt the improved NIF design to the omega chamber will be done in FY26. The Omega GRH will also support diagnostic development for NIF detectors and analysis for the LANL double shell campaign (Section 5.8 in the HED&IS 10-year plan). Work done on NIF GRH PD-PMT is explained in section **IIIb-4**.

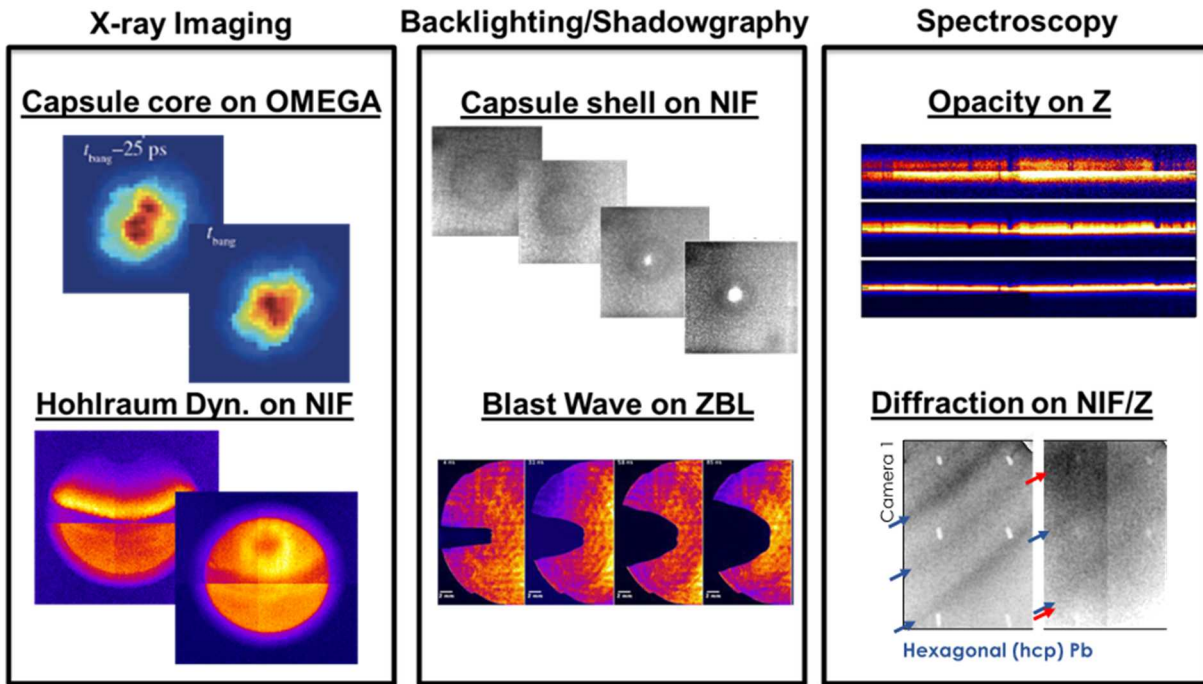


Figure 1: Example applications of SLOS- and hCMOS-enabled capabilities on NIF, Z (and the Z Beamlet Laser, ZBL) and Omega.

### IIIb-2: Ultraviolet Optical Thomson Scattering (UVTS)

UVTS on NIF will be used to measure the electron density, electron temperature, ion temperature and flow velocity of hohlraum plasmas in a well-defined localized region. The current NIF diagnostic suite is unable to reliably measure these parameters. The data is required to properly benchmark modeling of ICF hohlraums, in support of the ICF program goal for developing a predictive hohlraum model. The development of a predictive hohlraum model supports the following goals identified in the FY24 HED&IS ICF 10-year science plan:

Goal	Description
5.2	Experimentally assess 10 MJ class platform on NIF
5.4	Assess prospects for high yield with Laser Indirect Drive and Laser Direct Drive
5.14	Experimentally assess 30 MJ class platform on NIF

Generally, optical Thomson scattering measures the spectrum of the light scattered from a mono-chromatic probe beam by a plasma, to make temporally and spatially resolved measurements of the key parameters of plasmas such as temperature, density, and flow velocity. It is the gold standard measurement for plasma properties used in tokomaks and at lower densities in ICF.

On NIF, Z, and OMEGA a sub-critical density plasma produces high pressures to drive shocks or to inhibit hohlraum wall motion for all SSP programs. There are currently no direct measurements of the parameters of these plasmas. The behavior of these plasmas

needs to be better understood. Measurements of the plasma environment are critically important to better understand hohlraum behavior, and to benchmark radiation hydrodynamics codes that presently fail to predict the complex dynamics inside hohlraums. On NIF an ultra-violet probe laser beam makes Thomson Scattering a transformative diagnostic, allowing it to probe to high density. UVTS can also be used to access plasmas parameters for laser direct drive on the NIF.

The time evolution of the hohlraum plasma density ( $n_e$ ), temperature ( $T_e$ ), flow velocity and turbulence levels are critical parameters for understanding the x-ray drive for all HED hohlraum applications. Likewise, in long scale length plasmas such as Laser Direct Drive (LDD) on NIF, measurements of  $n_e$ ,  $T_e$ , and turbulence above the critical density are important for understanding the drive pressure and its uniformity. These fundamental parameters will be uniquely measured, without recourse to integrated rad-hydro models, using Ultraviolet Thomson Scattering (UVTS) on the NIF. These parameters need to be measured at high densities ( $n_e$  is calculated to be  $> 10^{21}$  e/cc in a NIF hohlraum) and in the presence of the powerful NIF heater beams. These requirements drive the need for a vacuum ultraviolet Thomson scattering probe laser beam, in order to avoid significant absorption and refraction in the plasma and so that the signal is not swamped by scattering of the 351 nm NIF drive beams. Background plasma emission and other sources of non-Thomson scattered light indicate that to exceed a signal-to-noise of unity the Thomson scattering probe laser must be 1-10J in 1ns at 210 nm, see J. S. Ross et al., Rev. of Sci. Instrumen. **87**, 11E510 (2016).

There are also many less challenging experimental configurations which can benefit from  $3\omega$  UVTS on the NIF and are benefitting from  $4\omega$  UVTS on OMEGA [for example see J. Katz et al., Rev. Sci. Instrumen. **83**, 10E349 (2012)]. These include source development for radiation effects experiments, experiments designed to study energy transport in foams, and collision-less shocks in counter-streaming plasmas. OTS has been implemented on Nova, Trident, JLF and OMEGA although in less stressing conditions than an ignition hohlraum and LDD on NIF. UVTS on the NIF is therefore a transformative diagnostic because the short wavelength of the probe opens new windows in plasma density even after five decades of Thomson scattering from high-temperature plasmas.

The detector for UVTS is a dual spectrometer multiplexing onto an ultraviolet sensitive streak camera. The detector was designed and built in FY16 [P Datte et al., (IFSA 2015) IOP Publishing], and is shown in Fig 2. It has already been used for a range of successful  $3\omega$  OTS measurements on the NIF, measuring the parameters of relatively low-density plasma for planar laser plasma instability experiments, Magnetized Liner Inertial Fusion (MagLIF) experiments, and discovery science laboratory astrophysics experiments. Data

collected by the NIF UVTS detector during Discovery science experiments investigating the formation of collisionless shocks has recently been published in *Nature Physics* (volume 16, pages 916–920 (2020)). More recently it has been used to make background measurements in ICF hohlraums. Initial issues with signal transmission below 180 nm have recently been resolved. These issues were tracked down to contamination of a gas volume in the streak camera. An actively pumped gas scrubbing system has been designed and installed and successfully tested. Improvements to the spectrometer housing have lead to continuous improvements in the background rejection, and changes in the mode of operation have allowed us to make the first successful simultaneous measurements of the IAW and EPW spectra on the NIF in FY22.

In FY23 a series of  $5\omega$  probe experiments were conducted to commission the diagnostic for ICF hohlraum experiments. These experiments initially used warm hohlraum targets and later a simplified LEH membrane target. None of these experiments were successful. Post shot investigations of the final shot did not reveal an underlying cause for the lack of data. One remaining possibility is that the beam focus quality at TCC is insufficient to deliver the required energy to the scattering volume, however there is insufficient data available to test this hypothesis.

In early FY24 development of the  $5\omega$  probe laser system for OTS was placed on hold due to a redirection of resources to higher priority NIF efforts. Experiments that had previously been scheduled to attempt a  $5\omega$  TS measurements were instead repurposed to attempt  $3\omega$  TS measurement in hohlraum relevant plasmas. Initial measurements in an LEH membrane plasmas produced both IAW and EPW data and indicated that measurements “through” an LEH membrane plasma were viable – this had previously been proposed as the cause of the lack of  $5\omega$  data. A final experiment in a gas filled halfraum target produced the first EPW data inside an ICF target. IAW data was also recorded but was saturated. A second experiment was deferred due to issues at the facility.

A review of the project was started in late FY24 to determine the best path forward. While no successful  $5\omega$  measurements having yet been made, successful measurements using a  $3\omega$  probe beam indicate that there is no underlying physics reason why a Thomson measurement inside a hohlraum is unfeasible. Instead, it seems likely that our current system is unable to simultaneously meet the extremely tight coalignment, timing and focusing requirements required for the  $5\omega$  probe system to collect data. While the



Figure 2: OTS detector for a DIM on the NIF.

techniques used to make  $3\omega$  TS measurements work well very early in the experiment when laser drive power is low, they are not expected to scale well as measurements are made at later times with higher drive powers. Further development of an alternative probe beam will still be required to meet ICF program needs.

In FY25 we carried out a study of alternative Thomson scattering probe beam options. This review focused on development of a probe design that would allow a significant relaxation of the requirements for coalignment tolerance and wavefront quality, greatly increasing the probability of measurement success compared to the tightly spaced  $5\omega$  system. The review concluded that a  $4\omega$  (263 nm) probe beamline launched from a dedicated laser port has the potential to provide much greater probe energy ( $\sim$ kJ) compared to the  $5\omega$  scheme ( $\sim$ 1J), allowing a significant relaxation of pointing, wavefront and timing requirements for the OTS probe beam. This system would leverage the alignment scheme used for the 192 NIF beams to reduce shot cycle time and therefore opportunity cost of OTS experiments. The additional probe energy available with a larger beamline also allows us to extend the duration of OTS measurements from 1ns to perhaps a full 8ns NIF laser pulse, greatly increasing the amount of data that we are able to collect in a single experiment.

A  $4\omega$  scheme had previously been investigated but was rejected due to fears of high background in the required waveband. With the OTS spectrometer DLPs now routinely collecting good quality data this issue will now be directly addressed via dedicated experimental background measurements in the required waveband, to be completed in early FY26.

The  $4\omega$  probe scheme as outlined in our review has received broad support from our external Thomson scattering expert group, and we are currently in the process of developing physics requirements for the system and preliminary discussions of the potential laser architecture with the LLNL laser science groups. It is expected that the new beamline will reuse the existing OTSL Pre-Amplifier Module (PAM) and some of its laser amplifiers, and should be able to be built in the existing OTSL laser room in SW1. We expect to propose an engineering project to implement the probe capability starting FY27.

### **IIIb-3: 3D Neutron Imaging System**

Three-dimensional (3D) imaging of thermonuclear (TN) burn provides the size and shape of the burning region and cold fuel, which has been instrumental in guiding the ICF campaigns by helping identify design changes used to improve drive symmetry or mitigate the effects of engineering features like fill tubes and tents. Gamma imaging capability under development will indicate the location of the ablator material, where it has mixed into the fuel, and provide data that can be used to validate mix modeling.

Nuclear imaging systems have been installed on two equatorial lines of sight (LOS) at the National Ignition Facility (NIF) - NIS1 on 90-315 and NIS3 on 90-213 - and one polar LOS, NIS2 on 5-22 (see Figure 3). Each system consists of two main components: a pinhole aperture (PHA) array that is used to form the neutron and gamma images, and a detector system that records the images formed by the PHA. Currently, the NIS2 lacks an active camera system and employs only image plate as detectors. Thus, the NIS2 neutron images are energy integrated with the signal dominated by the greater number of un-scattered primary neutrons.

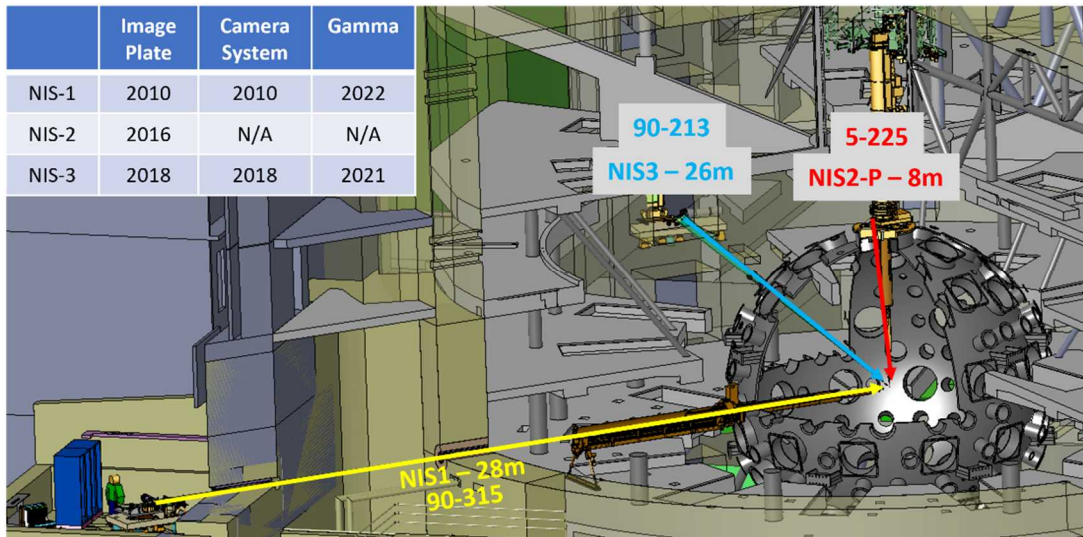


Figure 3: The Neutron Imaging System on NIF with current capabilities of each LOS identified in the table

In contrast, the two existing equatorial lines-of-sight use scintillator-based detectors with time-gated cameras in addition to image plates. The gating allows particles to be separated by time of flight. Since the active systems currently have three cameras, they can collect up to three independent images from the LOS. Typically, one camera is gated to capture an image of the 14 MeV neutrons and serves as the primary neutron imager, providing information on the size and shape of the fusion burn region. The second camera is gated to capture an image of the neutron that have scattered and lost energy and serves as the down-scattered imager, providing information on the distribution of the cold fuel. These down-scattered neutrons, typically in the 6-12 MeV range, are fewer in number and arrive after the 14 MeV neutrons. A third camera is gated earlier at the photon arrival time and acts as a gamma ray imager, providing information on the remaining ablator by imaging the 4.44-MeV gamma rays produced by inelastic scattering of the 14 MeV neutrons in the ablator material through the  $^{12}\text{C}(\text{n},\text{n}\gamma)$  reaction.

Computational tomography techniques have also been developed to use neutron and gamma images from multiple lines-of-sight to allow the generation of three-dimensional reconstructions of the burn region (see Figure 4), eventually of the cold fuel and remaining ablator. These reconstructions provide a measure of the 3D structure of the hot spot and cold fuel and full implementation of gamma imaging will allow measurement of remaining ablator distributions. The collection of these data enables the study of the effect of 3D asymmetry on the stagnation phase physics and guides the development and validation of 3D models and simulations.

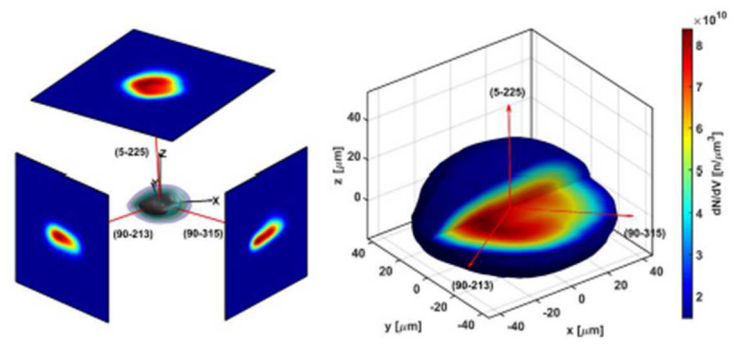


Figure 4: Neutron images from three lines of sight can be utilized to create three-dimensional reconstructions of the neutron source region and the distribution of fuel in the implosion.

## Existing Priorities

The NIS team currently has four major existing priorities:

### 1. Operation of the current systems – setup, analysis, and repairs

The NIS currently operates up to eleven separate detectors on ICF shots, this requires constant effort for setup and is a significant continuous activity to NIS team.

The NIS also produces many images on each shot and those images require sophisticated analyses, making the current NIS image analysis process labor-intensive and relatively slow. To address this challenge, the NIS team is developing new procedures, automated analysis and computational techniques to allow prompt analysis of NIF shots. For instance, a convolutional neural networks (CNN) method was recently applied to reconstruct the outer contours of simple source geometries in a timely manner. It can be applied to rapidly localize the source in the field of view of the aperture array, which is a crucial and time-consuming step in the data analysis. In a recently published paper in Rev. Sci. Instruments 95, 083559 (2024), comparisons between the quick CNN method and the current process show the performance of the CNN on both non-noisy and noisy data.

The NIS has also experienced failures of three MCP gating units and four cameras in the last three years. These failures have consumed time and energy to replace or repair and for recalibration, but these efforts are mandatory to maintain operation of the NIS and the calibrations are an ongoing effort.

## 2. Preparation for 20 MJ operation – snout upgrades, detector upgrades, possible camera system upgrades

The NIF mandated that the NIS systems be upgraded for use on shots with up to 20 MJ of yield by the end of FY25, an effort that has stretched to FY26. This complex effort involves three separate projects to upgrade snouts that hold the NIS1, NIS2, and NIS3 apertures as well as a project to upgrade the detector systems. These projects are all in progress and involve the manufacture of new snouts, a possible new aperture, repositioning of image plates and the addition of tungsten filtering on the NIS2 LOS. It is not believed that displacement damage or neutron interrupts are involved in the damage of the camera systems or that they would be significant even at 20 MJ.

## 3. Gamma-ray imaging

The systems' original plastic scintillators are not optimal for the gamma imaging. In FY25, we were able to install a better gamma-ray scintillators (GYGAG) on NIS1 with to improve the sensitivity and resolution of the system. We also found that the system requires improved collimation to perform well, and a project has been started to design and install a collimator inside DIM 90-315.

## 4. The NEMESIS project for technology transfer to Z

A technical transfer project known as NEMESIS is underway to provide neutron imaging for the Sandia Z facility. The technology developed on NIF is being used to develop a Phase A high-resolution neutron imaging system for the Sandia Z facility. In FY25, LANL completed the fabrication of the Phase A pinhole array and began metrology. In FY26, LANL will complete the pinhole array metrology, assemble the pinhole array in the cradle, and deliver it to LLNL. LLNL will perform cradle metrology and deliver it to the Z facility. Note: there were vendor manufacturing delays during manufacture of the cradle. LANL will also use the metrology data to forward model the as-built pinhole array, which will enable data analysis for NEMESIS. Classified data analysis capability is ready.

## Proposed Transformative Thrusts

There are also five major proposed transformative thrusts:

1. Advanced Neutron Modalities: Mix imaging including RIF imaging, Spatially resolved Ion Temperature.

Measuring where and how much the ablator mixes with the fuel would provide crucial data for validating mix models, and there are potential alterations to the NIS that could improve the sensitivity of the system to where the ablator mixes with the fuel. With ignition achieved and neutron yields reaching over  $1 \times 10^{18}$ , a fourth—

currently unused—camera location on both equatorial lines of sight can be used to add critical physics information such as capturing the first up-scattered (reaction-in-flight) neutrons or the spatial distribution of ion temperature, both are sensitive to mix in the cold fuel. An immediate test of RIF imaging can be performed on an existing camera, but an additional camera should be installed in the 4<sup>th</sup> NIS1 camera location to allow additional testing for other measurements. The 4<sup>th</sup> NIS3 camera location could initially be held for other measurement tests such as tests of an ion temperature diagnostic. Routine failure of existing cameras has delayed opportunity of adding new cameras for this purpose.

## 2. High-Resolution imaging

To increase spatial resolution, a new PHA may need to be designed. The current spatial resolution of NIS is limited, with neutron resolution around 10  $\mu\text{m}$  and gamma resolution around 15  $\mu\text{m}$ . It may be possible to attain a spatial resolution of 5  $\mu\text{m}$  or finer to more effectively extract mix information, a capability that may be particularly useful for the double shell campaign. To do this requires study of the effect of the existing metrology on the resolution and possible changes to aperture design and metrology that could improve it. The spatial resolution of the neutron and gamma imaging system will be enhanced through the simulation and design (FY26), and potential fabrication (FY27), and deployment (FY28) of a new pinhole aperture on one of the equatorial NIS systems (NIS1 or NIS3).

## 3. Classified data acquisition capability

A need has been identified to allow acquisition of classified data with the NIS. This capability does not exist and has not been designed into the existing NIS. If a project to allow classified operation is created, it may require changes to hardware, possible extensive addition of cabling and changes to operation. A thorough examination of the need and assessment of the effort and cost is needed to understand the scope and ultimate activities of the project.

## 4. Advanced Gamma-ray Modalities (framed and energy-resolved)

The path to 10 MJ+ takes advantage of increased NIF energy using thicker shelled capsules and more mass remaining to increase confinement. Understanding the stagnation of the carbon shell on the fuel during burn is therefore increasingly important. Two advancements in gamma-ray imaging will be explored; one with time-resolved framed imager and the other with an energy-resolved approach.

Imaging at several times can inform on asymmetries and degradations of burn, therefore can tell how the burn dies at late time. In FY26 we would like to perform *non-interfering* ride-along measurements on the NIS optical table to optimize and characterize the performance of a Cherenkov based optical radiator (quartz,

undoped YAG etc), and perform supporting calculations (GEANT4, HYDRA, LASNEX) to determine the requirements of a framed gamma imager system at NIF..

The energy-resolved gamma-ray imaging has the potential to revolutionize the conventional approach to scintillator-based systems, which lack of energy selection capabilities. The main concept of this proposal involves enhancing imaging system by incorporating an aerogel-based Cherenkov detector, inherently equipped with energy thresholding capabilities. This advancement will enable both energy and spatial resolution in gamma-ray diagnostics, offering a direct observable for validating numerical simulation benchmarks.

Preliminary studies suggest that the current yield does not make this applicable for any of the current designs. Work to quantify requirements for future designs was delayed due FY25 CR budget pullbacks

## 5. NIS2 upgrade to complete 3D nature of the systems

The existing 3D reconstructions of the burn region use the energy-integrated image from the NIS2 rather than a time-gated image, and no down-scattered or gamma-ray images can be obtained from the polar direction. The next significant improvement to the 3D neutron and gamma imaging would be to develop a gated active system on NIS2, providing true three-axis views for neutrons and gammas. Facility siting studies have been performed with the conclusion that the likely location of the system would be on the roof of the NIF, a challenging and expensive location, barring development of faster high-resolution scintillators and camera development. In FY28 and FY29, a series of requirement and design reviews will be conducted to determine the optimal path forward for neutron imaging at the NIF facility.

## Conclusions

The existing NIS has a complex set of current priorities and potential additional goals. Table I provides a summary of the timeline for those priorities and goals.

Table 1: Nuclear Imaging System (NIS) out-year plan

Priorities and goals		FY26	FY27	FY28	FY29	FY30
Existing priorities	Analysis	Down-scatter analysis + automated calibration system	Automation of IP reconstruction	Automation of down-scatter analysis		
	Electronic Repair	Calibrations and repair		SGEMP assessment		

	20 MJ Upgrades	Snout and detector upgrades	Snout and detector upgrades			
	Gamma-ray imaging	GYGAG installation NIS1	Testing NaI for NIS3			
	NEMESIS tech transfer to Sandia	fabrication for	Aperture delivery to Z			
Proposed transformative thrusts	Classified Data Acquisition		Need and scope assessment	CDR	FDR	
	NIS2 Active System				CDR	FDR
	Mix: RIF imaging			Demonstration on existing camera system	Install NIS1 Camera 4	
	Mix: Ion Temperature				Install NIS3 Camera 4	NIS3 (2D)
	Mix: High-resolution imaging		Physics review		CDR & FDR	(L2) Fabrication & OQ
	Advanced gamma-ray imaging			Testing Cherenkov based radiator	Testing aerogel radiator	

#### IIIb-4: Gamma Spectroscopy (GCD)

High-energy  $\gamma$  rays generated from inertial confinement fusion (ICF) experiments provide unique and important information for studying the dynamics of the nuclear phase of ICF process, because the energy spectra and amount of  $\gamma$  rays produced are a direct signature of the nuclear fusion reactions themselves. For example, the 16.75 MeV  $\gamma$ -ray line originating from the nuclear fusion reaction between deuterium (D) and tritium (T) can offer reaction history information, such as the time of peak reaction rate (i.e., bang time) and how long thermonuclear conditions are maintained (i.e., burn width). Due to their high-energy and penetrating nature,  $\gamma$  rays are the most unperturbed fusion products which can preserve the original birth information of the fusion process. Fusion  $\gamma$  rays provide a direct measure of nuclear reaction rates (unlike x rays) without being compromised by Doppler spreading (unlike neutrons). The metrics the GCD/GRH observe are routinely used a baseline, fundamental metrics to understand the basic implosion trajectory and energy balance of the formed fusion hot spot. Additionally, the yield of 4.44 MeV  $\gamma$ -rays from the inelastic scattering of the 14 MeV neutrons on the ablator material

measure the compression and mass remaining of the remaining ablator, HT fusion yield and short pulse MeV photon spectra are all measured by the GRH/GCD. Table I summarizing the physics values.

Table I: Overview of the physics values generated by GRH/GCD diagnostics

Physics Metric	Purpose	Types of implosion	Typical uncertainty
Nuclear bang time	<ul style="list-style-type: none"> <li>- Highly constraining value, vital for benchmarking simulations</li> <li>- Estimate shell velocity + laser energy absorbed in the capsule</li> <li>- Use to infer <math>P_1</math> net flow of implosion)</li> </ul>	All DT, HT, D <sup>3</sup> He implosions	± 30 ps
Nuclear burn width	<ul style="list-style-type: none"> <li>- Duration of thermonuclear conditions</li> <li>- Informs assembly and disassembly of hot spot</li> <li>- Challenges for simulations</li> </ul>	All DT, HT, D <sup>3</sup> He implosions with sufficient yield ( $> 10^{14}$ DT)	± 15 ps
Fusion burn shape and profile	<ul style="list-style-type: none"> <li>- Skew, structure of rising and falling edge of fusion burn</li> <li>- Constrain evolution of temperature and density of hot spot</li> </ul>	DT implosion $> 3 \times 10^{14}$	Currently ± 12 %, in future ± 6 %
Shell areal density and timing	<ul style="list-style-type: none"> <li>- Compression and mass remaining of ablator or inner shell</li> <li>- Can infer the rate of change and velocity of the shell near bang time</li> </ul>	DT implosion: carbon shell, Mo/W Double shell, PSS	Currently ± 25 %, in future ± 10 %
HT yield and $\gamma$ -inferred DT yield	<ul style="list-style-type: none"> <li>- HT yield from duded (hydrogen added) and mix implosions</li> <li>- DT yield thru independent technique, less scattered, <math>4\pi</math> averaged with no perturbation from flows or shell asymmetry</li> </ul>	All DT, HT, D <sup>3</sup> He implosions	± 25 %
Short-pulse (ARC) MeV photon spectra	<ul style="list-style-type: none"> <li>- Constrain multi-pulse MeV photon shape and flux</li> <li>- Informs understanding of high energy photon production</li> <li>- Feed-in to radiographic images</li> </ul>	ARC pulses	Total flux ± 25%, Spectrum shape ± 0.2 MeV

Two types of gamma spectroscopy diagnostics are currently operational on NIF (see Figure 5): the four-channel Gamma Reaction History (GRH) instrument and the single-channel, torpedo-like Gas Cherenkov Detector (GCD). The GRH uses a folded design, requiring it to be operated outside the target chamber, but allowing the photomultiplier tube (PMT) to be better shielded from x rays or other sources of background radiation, such as neutron-induced secondary  $\gamma$  rays. Since the inception of National Ignition Campaign in 2010, the folded-design GRH diagnostic on NIF has measured time-resolved measurements of fusion  $\gamma$  rays from implosions. While Cherenkov conversion process and its optical collection together provide a 10 ps temporal response, however, GRH is limited in temporal resolution by ~ 100 ps due to temporal response of the PMT.

As a testbed, the linear-design GCD has been developed to improve temporal resolution down to 10 ps by incorporating a Pulse Dilation (PD) PMT technology. High band-width  $\gamma$  reaction histories measured by the GCD/PD-PMT confirmed that the fusion burn widths measured by the slower instrument, GRH/PMT, are still in good agreement with the faster GCD/PD-PMT data. However, the 10 ps GCD/PD-PMT measurements (using CO<sub>2</sub>) have been limited by the presence of a long-

duration ( $\sim 500$  ps) tail on the fusion signal, which is not observed on the better-shielded folded-design GRH (also using CO<sub>2</sub>). It has been confirmed that the long-duration tail is produced in the gas cell and is not an artifact of the PD-PMT or recording system. The current hypothesis is that the tail is caused by sub-threshold  $\gamma$  rays (i.e.,  $\gamma$  rays with energy lower than GCD's energy threshold at given gas pressure) which induce scintillation in the gas. These sub-threshold  $\gamma$  rays are likely caused by neutron-induced secondary reactions on the hohlraum wall and thermomechanical package (TMP) used in indirect-drive cryogenic NIF implosions. The folded-design GRH does not see the tail due to the convoluted optical path used in the GRH, which efficiently transports the forward-directed Cherenkov radiation, but may not be efficiently collecting the scintillation, which is isotropic. As a near-term resolution, neon (Ne) gas was used in the GCD/PD-PMT because Ne produces enough late-time tail signal so it can be measured at high thresholds without the Cherenkov signal (i.e.,  $> 17$  MeV), and its longer decay time makes the temporal signature distinguishable from the DT gamma signal. This effort was abandoned because of high cost of Ne.

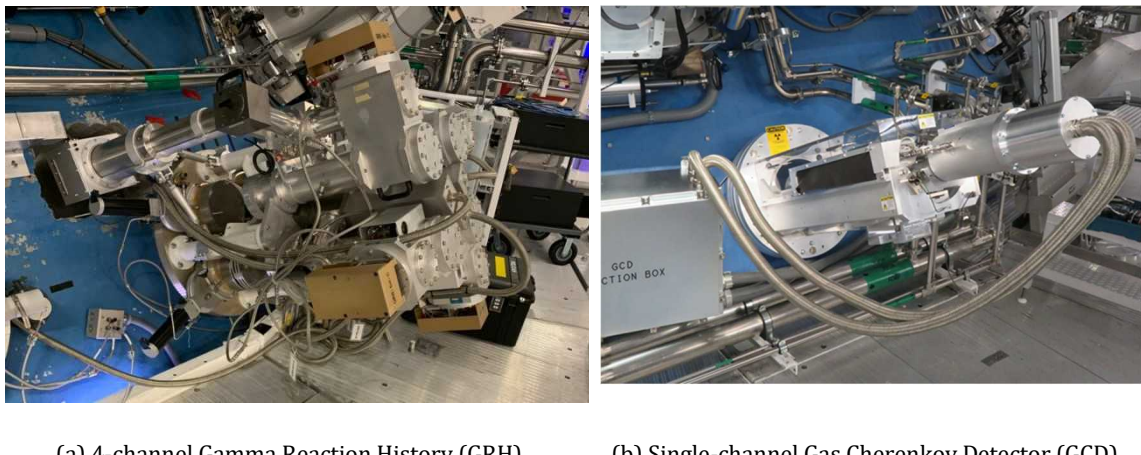


Figure 5: (a) Gamma Reaction History (GRH) installed on NIF (1 cell is coupled with a 10 ps PD-PMT) and (b) Gas Cherenkov Detector (GCD) coupled with a PD-PMT

Table II shows the operational summary of GRH and GCD including temporal-resolution, sensitivity, and energy threshold used. Two GRH channels (i.e., cell A and cell D) are dedicated to measure the burn history by setting an energy-threshold at 10 MeV or 12 MeV. The remaining two GRH channels (i.e., cell B and cell C) have been used to isolate the 4.44 MeV  $\gamma$  rays generated from (n, n'γ) reactions on the <sup>12</sup>C ablator by setting one  $\gamma$ -ray detector threshold just below 4.44 MeV, and another just above it, and then subtracting the signals.

Table II: Operational summary of single-channel GCD and four-channel GRH

	GRH-A	GRH-B	GRH-C	GRH-D / PD-PMT	GCD / PD-PMT
Goal	Fusion reaction	12C ablator	Hohlraum	Fusion Reaction	Fusion reaction
Gas	CO <sub>2</sub> @ 42.5 psia	SF <sub>6</sub> @ 215 psia	CO <sub>2</sub> @ 187 psia	CO <sub>2</sub> @ 42.5 psia	Neon @ 235 psia
Energy-threshold	10 MeV	2.7 MeV	4.5 MeV	10 MeV	11.5 MeV
PMT/PDPMT	PMT	PMT	PMT	Pulse Dilution PMT	Pulse Dilution PMT
Temporal-resolution	100 ps	100 ps	100 ps	10 ps	10 ps
Minimum DT yield for 100 $\gamma$ detection	$> 3 \times 10^{13}$	$> 10^{13}$	$> 2 \times 10^{13}$	$> 3 \times 10^{14}$	$> 3 \times 10^{14}$

## Existing Priorities

The GRH team currently has three major existing priorities:

1. Improving temporal resolution of one-channel of GRH

In addition to tests utilizing the GCD, further tests involved installing a PD-PMT on one channel of the GRH, which was completed in early FY23 and has allowed direct comparison of high-temporal resolution GRH and GCD signals. The GRH PD-PMT was fielded on several near-ignition shots and compared with GCD. These tests essentially confirmed the GRH PD-PMT removed or substantially reduced the tail signal seen on GCD, however additional measurements and characterizations of the dilation window are needed to explain some unexpectedly long burn width seen by GRH PD-PMT. Space charge has been identified as a source of burn width measurement broadening. A characterization of the space charge effect as a function of electrons in the PD-PMT drift tube has been performed in FY24. Changes to the GRH setups were implemented to reduce the number of electrons in the drift tube and mitigate the space charge effect. We also discovered that charge depletion at the MCP can occur with increasing fusion yield, which needs investigation and possibly mitigation, since it prevents precise measurement of electrons in the drift tube and therefore space charge correction. Due to continuing resolution in FY 25, LANL lost funding to contribute to these investigations and hopes to start again in FY 26. Additional shielding for GRH is investigated to reduce the generation of early-time background that contributes to charge depletion. Other possible sources of

background are the pressure window and PD-PMT input window. A baffle was fabricated in FY 24 to mitigate background and therefore charge depletion from the pressure window but the installation has been delayed. Work on gating out and therefore reducing cumulative background has been performed and will be tested on upcoming high yield shots.

## 2. Operation of the current systems at NIF, Omega and Z machine – setup, analysis, and repairs

The NIF GRH/GCD run on about ~40 implosions per year. The GRH and GCD currently operates up to five separate detectors on ICF shots, each detector transfers data through two or three Mach-Zehnder electrical-to-optical converters which feeds into 4 channels of data for each detector, totaling 20 channels of data for each implosion. The Double Shell pusher areal density measurements require GCD to provide low energy threshold data. The Double Shell pusher areal density measurements require GCD to provide low energy threshold data. The set up, analysis, maintenance and replacement of all components requires constant effort and continuous activity at LANL and LLNL. Furthermore, with the GCD & GRH now being over a decade old, many components have started failing and need to be replaced.

Omega has 3 separate detectors that are fielded on all LANL hot spot physics shots. The detectors are 20 years old and require reauthorization to continue use. The OMEGA cryo optimization campaign would benefit from use of these detectors in the future given improved temporal resolution (as explained in Section IIIb-1).

There is one detector on the Z machine, it was installed almost 10 years ago. It is ran on 8 DT shots a year. Work was done to mitigate the increased background levels compared to NIF and Omega. Work is beginning in FY 26 to design the next generation Gamma Reaction History detector which will be optimized for pulsed power.

## 3. Preparation for 10 MJ and higher operation – fiducials and background

Very high ignition yields pose problems for the GRH to continue reporting physics values. At high yields, the signal difference between the injected optical fiducials and the physics signal is so great that both cannot be measured on the same channel – without the optical fiducial, the uncertainty in the timing increases significantly. A 1-omega fiducial directly injected onto the scope has been implemented in FY25 and mitigates the issue. Upgrades to the MZ system could increase the dynamic range and improve signal to noise of GRH measurements.

As NIF performances are now routinely reaching above 1 MJ yield, GRH background improvement is necessary to prepare 10 MJ+ operation. Previous studies at Omega and NIF have identified two major sources of GRH background: the vacuum window

of the PMT and the pressure window of the gas cell. To address these issues, mitigation techniques are being developed, such as reducing the thickness of the PMT vacuum window and modifying the surface roughness of the gas cell to scatter the background signal from the pressure window, as well as additional shielding, and a baffle to reduce internal reflection.

## Proposed Transformative Thrusts

There are also five major proposed transformative thrusts:

### 1. High-dynamic range GRH (HIDALGO)

The current GRH achieves a signal-to-background up to  $\sim 12$  due to its design, the high radiation environment in the NIF target bay and its weight constrain. Due to their limited signal-to-background, only the peak of the fusion burn is measured and measurements cannot detect the earlier onset of alpha heating, where the slope of reaction history changes the most abruptly. To record the onset of alpha heating, a yield-rate coverage of at least 1000 will be needed.

HIDALGO, is proposed to be a high dynamic range detector with low background and will provide reaction history data at higher signal-to-background ratio than is possible with the existing GRH. To accomplish this improvement, the optical detectors (i.e., PMT or PD-PMT) must be protected from the high radiation environment in the target bay because the direct interaction of x rays and neutron-induced  $\gamma$  rays are dominant background sources. The existing GRH diagnostic was designed to operate below 1 MJ to give optimum performance on the path to ignition. Implementing the PD-PMT on GRH has extended the operating yield limit, but at the 3-4 MJ yield range we are again approaching the operational limit. The HIDALGO diagnostic is a necessity for extending reaction history measurements beyond the 10 MJ range into 30MJ.

### 2. Exploring alternative ultra-fast detector concepts

Despite the achieved unprecedented  $\sim 10$  ps time resolution achieved, high gain, highly igniting ICF implosions are predicted to have extremely narrow burn widths (15 to 20 ps), where even the current detector may not be enough. Furthermore, if even faster time resolution could be achieved, new physics phenomena - like observing the movement of rattling, rebounding shocks – could be temporally observed.

There are a couple advanced concepts that could achieve single or sub-picosecond temporal resolution. One example led by General Atomics and LLNL is an etalon technique, an optical cavity with transmissive media and parallel reflecting surfaces,

that is sensitive to the incident radiation. Energy deposited in the etalon by the radiation changes the index of the media quasi-instantaneously (of order a picosecond), changing the global reflectance and transmittance of the etalon. The cavity, with length dimension  $\ll 1$  mm, can have response time  $< 10$  ps.

Another example, using charge-induced optical etalons or converting the measurement into a THz radiation pulse where the spectrum, as opposed to the temporal evolution, could be measured instead at much higher fidelity. These techniques often forego electronic techniques entirely and remain purely optical. It remains to be seen whether these techniques could be successfully utilized, but a future detector could further push the frontier of understanding the dynamics and interactions of a burning plasma.

### 3. Time-dependent ion temperature

In ICF, the fusion process is highly sensitive to the ion temperature, as the deuterium-tritium (DT) fusion rate is proportional to the third or fourth power at keV temperatures. Furthermore, the processes that affect the ion temperature — alpha particle deposition, radiation, and conduction transfer — evolve quickly compared to the hydrodynamic evolution of the imploding capsule. Measuring how the ion temperature evolves near peak implosion is closely connected to the performance and energy balance of the implosion. Although the burn-averaged ion temperature is routinely measured using neutron time of flight techniques, a time-resolved ion temperature is currently not measured. Techniques have been suggested, such as a time-resolved magnetic recoil spectrometer [MRS(t)], which development continues and extremely fast reaction history measurements. Here, we propose an alternative technique to utilize a differential fusion gamma ray and neutron measurement to attempt to measure the time dependence of the neutron Doppler broadening in order to infer the time-resolved ion temperature. This technique leverages Cherenkov gamma-ray detectors, specifically for their high temporal resolution.

### 4. Gamma-to-Electron magnetic Spectrometer (GEMS)

GEMS is a gamma ray spectrometer, giving up the fast time resolution of the Cherenkov technique for energy resolution of the created gamma ray spectrum, allowing novel physics measurements. The GEMS would allow the first time measurement of the MeV spectra created from ICF implosions. It would have a slower time response ( $\sim 1$  ns) and so would be integrated over the implosion. GEMS would answer fundamental physics questions about the nuclear physics reactions that create the MeV spectra, which currently have high uncertainty. GEMS would give very precise ablator areal density of arbitrary materials.

### 5. Classified data acquisition capability

A need has been identified to allow acquisition of classified data with the GRH. This capability does not exist and has not been designed into the existing GRH. If a project to allow classified operation is created, it may require changes to hardware, possible extensive addition of cabling and changes to operation. A thorough examination of the need and assessment of the effort and cost is needed to understand the scope and ultimate activities of the project. This has implications for some ICF platforms as well applications of ignition measurements.

## Conclusions

Table III outlines key areas for improvement in Reaction History Diagnostic to enhance our ability to capture and analyze the onset of ignition and trace the evolution pathway of ignition conditions. Experience from improved NIF GCD and GRH PD-PMT operations will be fed into the final phase of a NIF-specific HIDALGO which can better handle the harsh radiation environment associated with indirect-drive and will increase dynamic-range by a few orders-of-magnitude. The development of the dynamic range of the reaction history instrument was delayed by the FY25 CR budget cuts to LANL. It will be expanded through the Phase-A design (FY26) for testing inside the target bay in FY27, followed by the Phase-B design (FY28) and installation outside the target bay in FY29. The goal is to achieve a dynamic range of 1000 or greater to accurately capture the evolution of temperature and areal density of hot spot.

Table III: Gamma Spectroscopy (GRH/GCD) out-year plan

Priorities and goals		FY26	FY27	FY28	FY29	FY30
Existing priorities	GRH PD-PMT	Charge depletion mitigation				
	Operation	GCD with shell rhoR, Mach-Zehnder improvements				
	Background reduction	GRH baffle, shielding				
Proposed transformative thrusts	Classified Data Acquisition	Need and scope assessment	CDR	FDR		
	Hidalgo	FDR: Phase A (target bay)	OQ: Phase A (target bay)	FDR: Phase B (bio shield)	OQ: Phase B (bio shield)	
	Time-dependent ion temperature	FDR	OQ			

GEMS				CDR	FDR
Alternative fast detector	Physics review				

### IIIb-5: Time resolved neutron spectrum

The goal of the proposed transformational **time resolved neutron spectrum** (TRNS) diagnostic is to infer neutron yield ( $Y$ ), ion temperature ( $T_{ion}$ ), compression (through the down-scatter ratio,  $dsr$ ) and directional flow ( $v_{flow}$ ) as a function of time. Current neutron spectrometers all make a single burn-integrated measurement of these quantities. The top-level physics requirement for TRNS were summarized in Kunimune et al, 2021 [A], which concluded based on ensemble simulations that  $d\rho R/dt$  should be measurable to  $\pm 60$  mg/cm<sup>2</sup> / 100ps and  $dT_{ion}/dt$  to  $\pm 1.9$  keV/ 100ps at bang time. While the exact numbers depend on ignition dynamics, any time-resolved information for these quantities that could be obtained would be more than currently available; there is no hard cut off below which time resolved information would not be useful. TRNS output would strongly constrain simulations and our understanding of ignition physics (see Fig. 6 Ref. [B]), providing critical information towards the long-term goals of the ICF program of increasing gain ( $G \gg 1$ ) and understanding the limits of gain at the NIF.

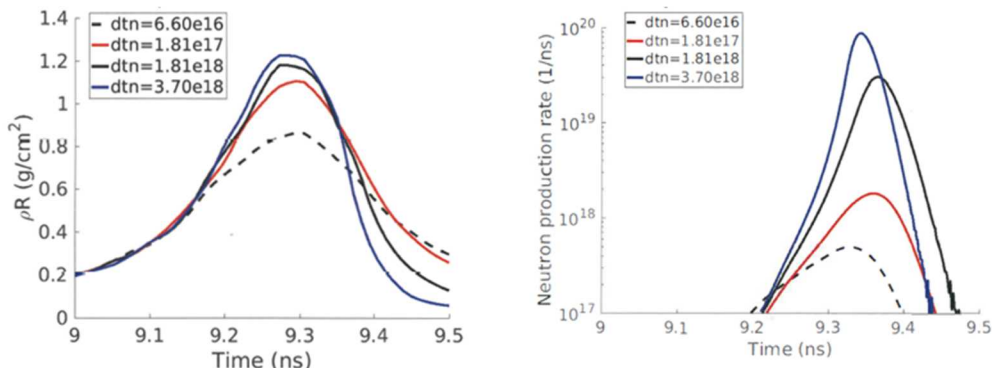


Fig. 6. xRAGE simulations by Brian Haines at LANL showing (left)  $\rho R$  vs time and (right) neutron production rate vs time for implosions below, at and above the “ignition cliff”. Below the cliff, burn occurs mainly at peak compression. On the cliff, burn occurs during disassembly, and the disassembly quenches the burn. Above the cliff, burn takes off rapidly and disassembles faster. Time-resolved neutron spectra would enable direct measurement of peak  $\rho R$  for these implosions (not just burn-weighted  $\rho R$ ), direct measurement of confinement time, and a determination of when the capsule ignites (using  $\rho R$  vs time and  $T_{ion}$  vs time). This information would be highly constraining for simulations and for our understanding of ignition physics. Reproduced from Ref. [B].

Key information that would be obtained includes:

- Plasma conditions at the start of ignition from  $T_{ion}(t)$ . This would be used to evaluate the timing of cross-over into the ignition regime. More robust implosions can ignite before peak compression, which changes the relative timing of burn and peak compression. For example, N210808 is believed to have ignited right at

peak compression, which is the latest you could possibly ignite, leading to burn substantially after peak compression and burn as the capsule is exploding. This trend has continued with more recent ignition shots on the NIF. As NIF laser capabilities increase in power and energy, the ability to drive implosions harder could lead to ignition on

- Confinement time inferred from the width of  $dsr(t)$ . Pure burn width measurements currently made are in some sense unrelated to confinement because they do not correlate with compression.
- Peak compression inferred from the max of  $dsr(t)$ . In contrast, a time-integrated  $dsr$  is neutron weighted and will sometimes provide information about peak compression, sometimes not; this measurement is not comparable between shots.

Currently, THD implosions are frequently used as a surrogate to address some of these questions, but this is not a perfect method, due to the high sensitivity to small target imperfections. TRNS would also eliminate the need for THD implosions to determine “burn-off” conditions, saving of order \$1M per configuration.

In summary, TRNS would provide an unprecedented window into the dynamic energy balance of implosions not accessible with any current diagnostics, and can be anticipated to uncover “unknown unknowns” [C].

Historically, the primary technique pursued for making this measurement has been time-resolved Magnetic Recoil neutron Spectrometry (MRSt). While much progress has been made towards an MRSt design [A, D-L], there is substantial uncertainty about the feasibility of the proposed backend detector concepts, and further development of MRSt has been put on hold pending a resolution to this question. In FY25, development work was undertaken on a simplified proposed MRSt backend detector concept using printed circuit board (PCB) technology, proposed by LLNL’s Clement Trosseille. The idea of the PCB concept is to split the MRSt focal plane into 1cm wide bins each covering  $\sim 100\text{keV}$  energy, with the signal within each bin passively time-aligned using varying-length PCB traces (Fig. 7) before recording each bin on a fast digitizer channel. Prior to the PCB, a multi-channel plate (MCP) will be used to convert incident deuterons to electrons. The FY25 effort involved investigating how to minimize cross talk between and impedance match PCB traces all while considering size constraints. Progress was made as reported in a qualifying exam paper by MIT graduate student Audrey DeVault [M], but more work remains to prove this technology as an MRSt backend detector concept.

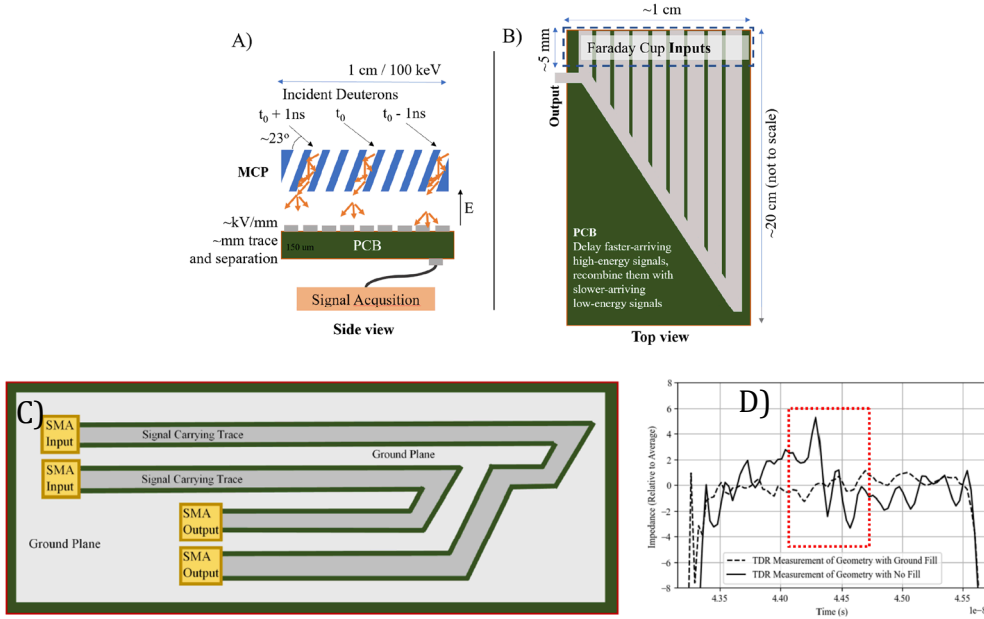


**Fig. 7. (a)** Side-view of a single PCB “bin” geometry, also showing the MCP used to convert incident deuterons to electrons. **(b)** Top view of the PCB bin, showing how varying length traces are used to time-align signals arriving at different positions/energies within the bin. **(c)** Simplified diagram of board used to test impedance matching (minimization of reflections), and **(d)** time-domain reflectometry results showing successful implementation of ground fill for impedance matching.

An alternative proposed technique is the so-called tomographic neutron time-of-flight (nTOF) technique, which uses multiple time-of-flight detectors along a single line of sight but located at different distances from the source [N-Q]. During FY25, Appelbe and Crilly at Imperial College developed a mathematical framework relevant to this technique using a moments method to analyze nTOF signals recorded by two or more collinear neutron detectors located at different distances from a pulsed neutron source [R].

Appelbe also tutored two students, Audrey DeVault at MIT and Charlotte Stewart at the University of Oxford, in how to use this methodology. In FY26, these two students will continue recently started complementary efforts using different methodologies to establish whether the tomographic nTOF technique will work with realistic detector noise and time resolution. The goal is to use synthetic data to test whether this technique can meet the top level TRNS physics requirements as outlined above and then to evaluate whether to move on to hardware implementation.

A national TRNS working group convened by Chad Forrest (LLE) has been continuing monthly meetings during FY25, and plans to meet regularly to monitor progress in FY26 as well in anticipation of reaching a conclusion on feasibility of tomographic nTOF. Other concepts, which at the moment look like they might be able to provide subsets of the desired information, also continue to be investigated by the working group, including a General Atomics fast burn history concept using a rad optic design (which would only provide burn history, or which could be used as one step in a tomographic nTOF chain) and a Los Alamos National Lab effort to infer  $T_{ion}(t)$  using a multi-puck gamma detector concept.

Progress towards implementation of TRNS hinges on a decision on path forward along with funding allocations. Within current funding levels, progress will remain slow.

## References:

- [A] J.H. Kunimune et al., "Top-level physics requirements and simulated performance of the MRSt on the National Ignition Facility", *Rev. Sci. Instrum.* 92, 033514 (2021).
- [B] B.M. Haines et al., "Simulated signatures of ignition", *Phys. Plasmas* 31, 042705 (2024).
- [C] J. D. Kilkenny et al., "The crucial role of diagnostics in achieving ignition on the National Ignition Facility (NIF)", *Phys. Plasmas* 31, 080501 (2024).
- [D] J.A. Frenje et al., "The Magnetic Recoil Spectrometer (MRSt) for time-resolved measurements of the neutron spectrum at the National Ignition Facility (NIF)", (presented at HTPD-2016) *Rev. Sci. Instrum.* 87, 11D806 (2016).
- [E] T.J. Hilsabeck et al., "A stretch/compress scheme for a high temporal resolution detector for the magnetic recoil spectrometer time (MRSt)", (presented at HTPD-2016) *Rev. Sci. Instrum.* 87, 11D807 (2016).
- [F] C. Wink et al., "Signal and background considerations for the MRSt on the National Ignition Facility (NIF)", (presented at HTPD-2016) *Rev. Sci. Instrum.* 87, 11D808 (2016).
- [G] C. W. Wink, "Characterization and Optimization of Signal and Background for the Time-Resolving Magnetic Recoil Spectrometer on the National Ignition Facility", M. Sc. Thesis, MIT (2017).
- [H] A. Sandberg, "Shielding Design for the time-resolving Magnetic Recoil Spectrometer (MRSt) on the National Ignition Facility (NIF)", M.Sc. Thesis, MIT (2019).
- [I] C. Parker et al., "Implementation of the foil-on-hohlraum technique for the magnetic recoil spectrometer for time-resolved neutron measurements at the National Ignition Facility", *Rev. Sci. Instrum.* 89, 113508 (2018).
- [J] C. Parker et al., "Response of a lead-free borosilicate-glass microchannel plate to 14-MeV neutrons and  $\gamma$ -rays", *Rev. Sci. Instrum.* 90, 103306 (2019).
- [K] J. Kunimune et al., "Phased plan for the implementation of the time-resolving magnetic recoil spectrometer on the National Ignition Facility (NIF)", *Rev. Sci. Instrum.* 93, 083511 (2022).
- [L] G.P.A. Berg et al., "Design of the ion-optics for the MRSt neutron spectrometer at the National Ignition Facility (NIF)", *Rev. Sci. Instrum.* 93, 033505 (2022).

[M] A. Devault et al., “A Printed Circuit Board (PCB) Backend Detector Concept for the Time-Resolving Magnetic Recoil Neutron Spectrometer (MRSt) for the NIF”, Qualifying Exam paper, MIT (2025).

[N] J. Catenacci, et al., “Tomographic Reconstruction of the Neutron Time-Energy Spectrum From a Dense Plasma Focus”, IEEE Trans. Plasma Sci. 48, 3135 (2020).

[O] A. S. Moore, et al., “Constraining time-dependent ion temperature measurements in inertial confinement fusion (ICF) implosions with an intermediate distance neutron time-of-flight (nToF) detector”, Rev. Sci. Instrum. 93, 113536-1 (2022).

[P] D. J. Schlossberg, et al., “Design of a multi-detector, single line-of-sight time-of-flight system to measure time-resolved neutron energy spectra”, Rev. Sci. Instrum. 93, 113528-1 (2022).

[Q] J. M. Mitrani, et al., “Simultaneous analysis of collinear neutron time-of-flight (nToF) traces applied to pulsed fusion experiment”, Rev. Sci. Instrum. 95, 083529 (2024).

[R] Brian D. Appelbe, Aidan J. Crilly, “The neutron spectral moments method in the time-of-flight domain”, <https://doi.org/10.48550/arXiv.2411.12414> (2025).

### IIIb-6: High Resolution Velocimeter (HRV)

The current VISAR instrument on NIF is a highly reliable, versatile, high precision diagnostic which is run as a primary diagnostic on 100+ shots per year. It provides space- and time-resolved measurements (in one spatial dimension) of the velocities of free surfaces, shocks in transparent media and the motion of internal interfaces behind windows in dynamically driven targets. The two-dimensional data sets can be analyzed to infer space- and time-resolved pressure in the driven target as a function of time. The velocimeter can therefore be regarded as a high precision pressure gauge. About a dozen shots per year are devoted to shock tuning for the ICF program which help to set the timing and initial symmetry of the drive on the capsule. Such tuning experiments are required every time a new target design is developed. The bulk of VISAR shots are devoted to various of the stockpile assessment platforms indicated in more detail below. In all cases these platforms require precise and accurate measurements of target pressure history.

New programmatic needs that exceed the current capabilities were identified which motivated the inception of a new High Resolution Velocimeter (HRV) instrument including a new High-Resolution 1D VISAR, as well as a new High-Resolution 2D VISAR capability together with a visible streaked pyrometry system. The 2D VISAR can provide important data sets on the seed-level non-uniformities that underlying the Richtmyer-Meshkov and Rayleigh-Taylor instabilities commonly found to occur

in dynamically-driven targets in the context of ICF, and which are of general interest in the HEDS community.

The current NIF Velocimetry Velocity (Doppler) Interferometer System for Any Reflector (VISAR) can track the velocity of a moving reflecting surface with sub % precision using a visible Laser probe at 660 nm and an interferometer to transform Doppler shift into a fringe phase shift proportional to the velocity of the reflector. A time-delay element (etalon) determines the velocity sensitivity. Specifically, the NIF VISAR is a line-imaging (1D) instrument: a f/3 optical-relay images the target onto the entrance slit of a streak camera fitted with a CCD detector. The system therefore records the velocity time-history for ~100 resolution elements corresponding to different spatial positions onto the target. Two field-of-view options are available: 1mm and 2 mm. The spatial resolution is currently limited by the streak cameras. Space-time distortion inherent to streak-tube technology are also strongly limiting the performance near the edges of the field of view. The time-resolution is currently around 30 ps over a 30 ns streak.

The ICF program needs to accurately track the relative timing and speed of the multiple shock waves launched into ICF capsules (shock timing experiments) to benchmark radiation-hydrodynamic simulations of high-yield DT implosions. There is also a need to understand capsule and shock-front non-uniformities which degrade implosion quality as even very small velocity variations can seed major degradation in the implosion quality. There is therefore a need to document the velocity distribution in-flight, with micrometer spatial resolution and meter-per-second velocity sensitivity.

HED Stockpile Stewardship Science programs perform critical experiments to study the Equation of State (EOS), strength, phase transitions and short range microstructure of High-Z materials using the PHPEOS, RampEOS, RMStrength, TARDIS and EXAFS platforms which all use VISAR as a primary diagnostic. There is a need for sub-% accuracy in velocity, ps timing accuracy and high-fidelity imaging and recording that exceed the current capabilities. Higher spatial, timing and velocity resolution 1D VISAR would boost the data return per shot, reduce the number of NIF shots necessary to obtain the required accuracy in the EOS data (which currently requires averaging data from 3-5 shots) and would also enable new science.

Based on the programmatic needs and discussions with the users' community the new NIF High Resolution Velocimeter (HRV) instrument will have several channels to allow simultaneous recording of 1D and 2D VISARs plus Streaked Optical Pyrometry data and room to grow not to preclude future improvements. The new High-Resolution 2D-VISAR will feature f/2 and f/3 collection systems, a picosecond laser, two interferometers and 4-records per snapshot on a CCD detector. The new High-Resolution 1D VISAR will feature 4 interferometer channels for higher resolution and higher dynamic range, data redundancy and increased flexibility. A new push-pull detection scheme for higher velocity and spatial resolutions will be

tested on one channel initially, before being extended to all channels. Two nanosecond lasers (blue, red) will allow us to obtain a two-color system for improved optical properties measurements. The improved Streaked Optical Pyrometry (SOP) will feature optimized stray light rejection and a detector gating to mitigate background. Overall, this combination of new and unique capabilities will make the High Resolution Velocimeter at the NIF a transformative diagnostic for the HED community.

After completing a PDR, the project was paused due to lack of available funding. The N221204 implosion with a 3 MJ neutron yield reinforced the need for enhanced neutron resilience for NIF diagnostics. The team evaluated deployment options including expanding on the existing system in the Target Bay, using the current VISAR laser room or building a new instrument on two new floors located in the NIF switchyard. While more costly and complex to deploy initially, only the deployment in the switchyard meets the programmatic needs and neutron shielding requirements from high-yield implosions moving forward. The second option, deployment in the current VISAR laser room, appears to be more easily achievable in the near term with current budget constraints. It will allow for operation outside of the shield wall which will relieve the operational burden of moving the streak cameras during high yield experiments. However, this option will likely have reduced scope for meeting the performance specifications originally envisioned for the HRV.

During FY25 engineering design work on the second option, deployment of the existing VISAR system to the VISAR laser room in the OSB began and has passed the conceptual design review stage. The engineering team identified a feasible design path for an image relay that is able to use the current neutron image wall penetration with routing of the optical relay from the switch yard area into the optical sciences building (OSB) VISAR laser room. Design is proceeding towards a preliminary design review expected to occur in early FY26, with final design completed by late FY26. The new implementation is expected to match or exceed all of the specifications and capabilities of the current VISAR and will be implemented in a way that allows a seamless transition from the current VISAR to the new system.

### **IIIb-7: Time-Resolved X-ray Diffraction**

X-ray diffraction is a well-established technique to identify phases and document phase transitions in compressed materials of interest to the SSP. X-ray diffraction is the most discriminating method to identify the phase of a solid material because it reflects the distances between atoms with high precision. The technique has now been developed for use in HED experiments at NIF, OMEGA, and Z.

Early work on NIF has been limited to using TARget Diffraction In-Situ (TARDIS) to obtain one or two snapshots per very expensive laser shot. Time-resolved x-ray diffraction will build on the demonstrated success of the platform to provide a significant enhancement to the HED materials diffraction program by providing multiple snapshots during a single laser shot with one target. The first diagnostic commissioned in the XRDt campaign was the Gated Diffraction Development Diagnostic (G3D); this diagnostic was developed to confirm the feasibility of hCMOS sensors to be used in the NIF environment. The Flexible Imaging Diffraction Diagnostic for Laser Experiments (FIDDLE) was built and was fielded on NIF for the first time in 2023 (Figure 8 left).

The ability to observe material phase at multiple times during a solid-solid or solid-liquid phase transition within a single laser experiment will substantially constrain equilibrium material phase boundaries and enhance our understanding of kinetic effects that drive or inhibit phase transformation in materials at high densities. Moreover, we anticipate that the time-gated quality of these measurements will improve the signal to noise of measurements as background signals (which are substantial) are not integrated over the entire experiment. With this platform our facilities will be able to make multiple diffraction measurements of a solid material compressed to multi-Megabar pressures over timescales as long as tens of nanoseconds.

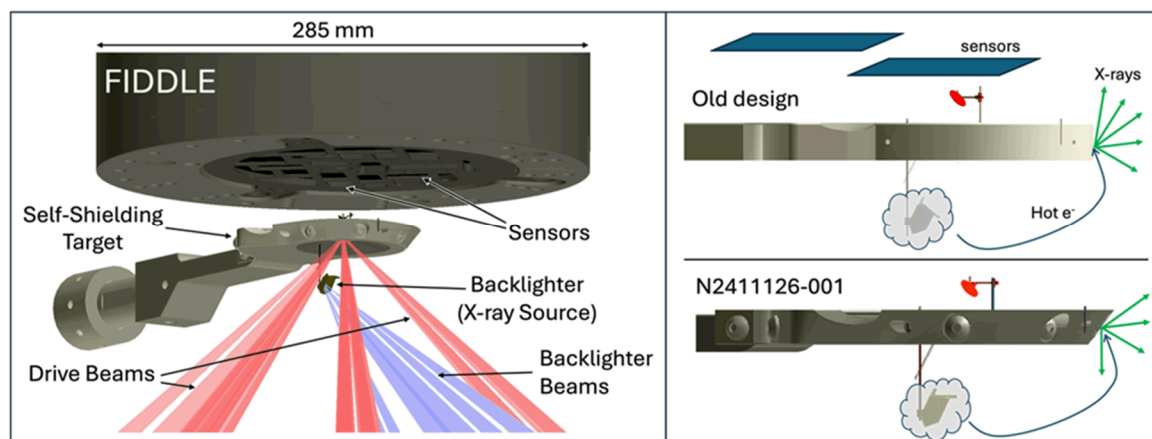


Figure 8. Time-resolved X-ray diffraction platform at NIF showing the redesigned XRDt target with a time-resolved diffraction diagnostic. Left. FIDDLE. Right. Updates to the target design during the reporting period which significantly lowered background on sensors.

## Completed 2024 Milestones related to Time Resolved x-ray diffraction at NIF

### Milestone 10.3 #7453, Q2 FY24

**Title:** Capability for time-resolved diffraction for material phase in extreme conditions  
**Completion Criteria:** Demonstrate >3 frame diffraction diagnostic on a high-pressure material platform (FIDDLE)

**Status:** Written milestone report was submitted and accepted in April, 2024.

## Milestone 10.8 #7469, Q4 FY24

**Title:** Diffraction of a phase transition with uncertainty analysis

### Completion Criteria:

1. Demonstrate time-dependent diffraction measurements of a solid-solid phase transition on a single shot.
2. Perform error analysis to determine uncertainties in time, **density**, pressure and phase boundaries.

**Status:** Milestone oral report (presentation) and peer review was submitted and accepted 16 October 2024.

### Status update, 2025

Several notable advancements were made with the FIDDLE diagnostic during FY25 which improved the signal to noise in the X-ray diffraction measurements. One of the most significant developments was the introduction and testing of a new self-shielding target design, which was first evaluated in shot N240717-001 and then fully utilized in N241126-001 (Fig. 9, right). This design led to a substantial reduction in background noise on the Icarus sensors, yielding the highest quality diffraction data recorded by FIDDLE to date. The background on the sensors typically increases as an experiment progresses, often overwhelming observable diffraction in later frames. This increase is attributed to hot electrons generated in the backlighter plasma, which travel to the target and collide with its sides and top, producing secondary X-rays through bremsstrahlung processes. While the new target does not decrease the generation of these secondary X-rays, it effectively shields the sensors from direct exposure to the sides of the target, thereby reducing the background interference and enhancing data clarity (Fig. 10).

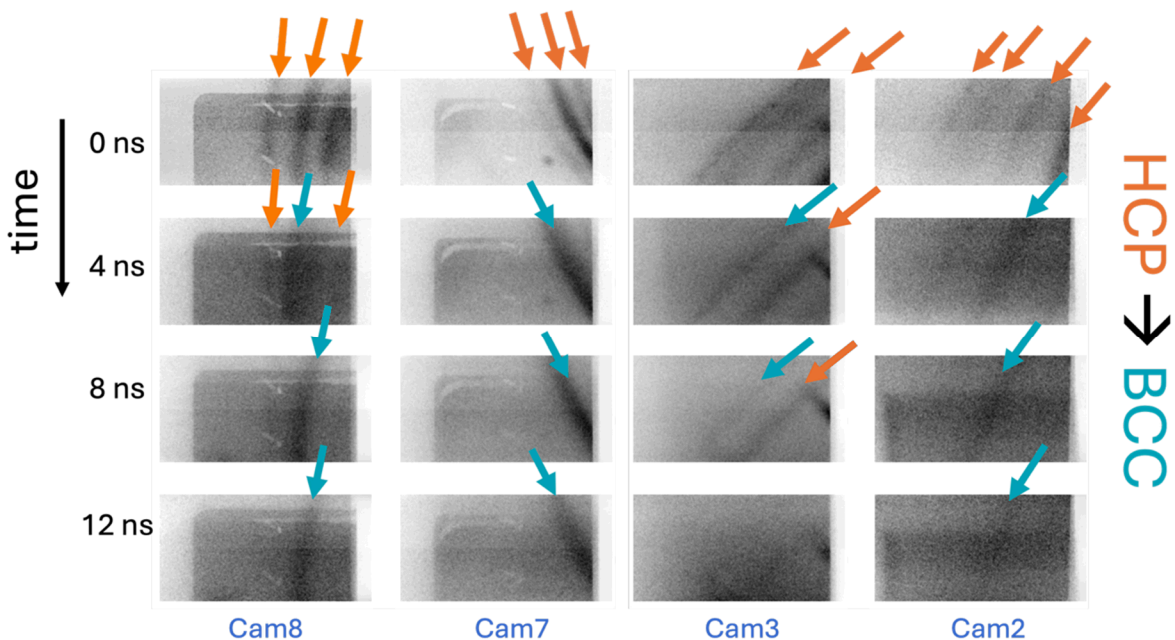


**Figure 9. X-ray diffraction of Pb during NIF shot N241126-001.** Hexagonally close-packed Pb is observed to transform into a body-centered cubic structure over approximately 8 ns. Diffraction peaks are labeled with arrows (orange for hcp; cyan for bcc.)

In addition to improvements in target design, an undriven shot was performed on cerium oxide ( $\text{CeO}_2$ ), a commonly used X-ray diffraction standard, under shot N240402-002 and N250403-002. This experiment aimed to assess the in-situ alignment of the FIDDLE diagnostic relative to the target. The results showed that the calibrated position of FIDDLE was within one millimeter of its predicted location, as determined by the ATLAS alignment system, confirming the precision of the setup and the reliability of the alignment methodology.

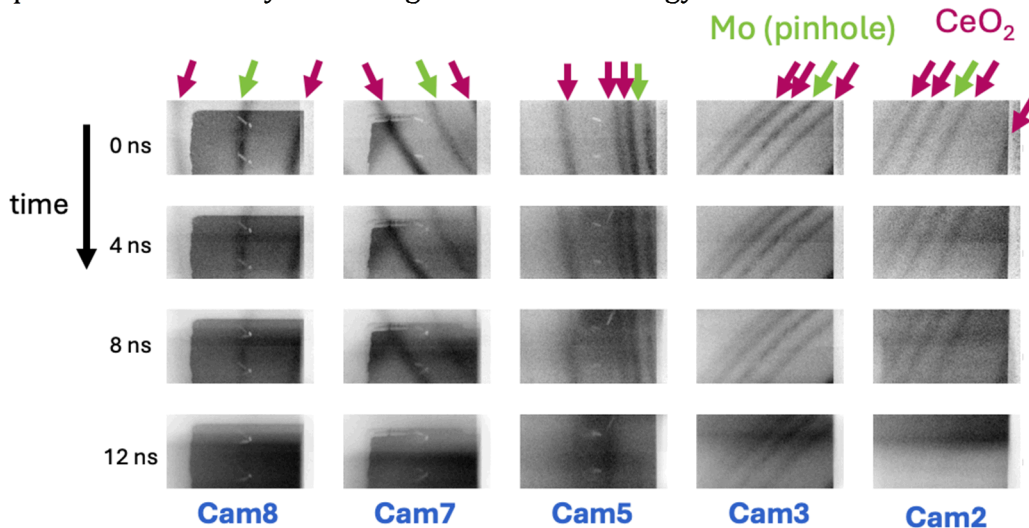


**Figure 10. X-ray diffraction of  $\text{CeO}_2$  during NIF shot N250403-002** with expected peak positions shown in the grey dashed line.

Another key development was the adoption of a new backscatterer pulse shape, extending the pulse duration from 10 nanoseconds to 14 nanoseconds. This modification allowed for a longer record length of diffraction data and contributed to a reduction in X-ray background levels. As a direct result, diffraction was observed for the first time on the image plate in FIDDLE during shot N240717-002, marking an important milestone in the diagnostic's capabilities.

The team also engineered a novel pinhole imaging snout for FIDDLE, enabling the first timing shot for this diagnostic, recorded as N241126-002. By capturing pinhole images from a series of short laser pulses on a gold sphere, the timing of each Icarus sensor was characterized with improved precision, reducing the timing uncertainty to less than half a nanosecond. This advancement is crucial for synchronizing data acquisition and improving the temporal resolution of the measurements.

To further enhance reliability, new multiplexing boards were installed for the timing monitors in FIDDLE prior to the November shots (N241126-001 and N241126-002). These boards utilize low voltage differential signaling (LVDS) inputs, which are more resistant to electromagnetic pulse (EMP) noise. The implementation of

these boards effectively eliminated the previously observed EMP-induced timing shifts, which could be as large as ten nanoseconds, thereby stabilizing the timing system and improving overall data accuracy.

Our continued focus is to continue to improve the quality of the diffraction data by further reducing X-ray background and driving down uncertainties in timing and spatial calibration. We are also planning a new version of FIDDLE (FIDDLE-B) with significant new capabilities to meet programmatic needs, including next-generation hCMOS sensors (Daedalus), an X-ray streak camera, the ability to rotate the diagnostic about its axis, and the ability to acquire classified data, which will be of specific interest to the SSP.

### **IIIb-8: >15 keV X-ray Detection (DHEX)**

Efficient detection of high-energy X-rays (DHEX) with multi-frame capability is crucial for advancing high energy density (HED) applications and programs. This capability is essential as experiments increasingly probe plasmas with higher density, temperature, or larger volume, requiring higher X-ray energies. The development of these detectors aligns with the HED&IS 10-year plan by enhancing diagnostic capabilities to support stockpile stewardship and scientific progress.

Goals:

- Efficient x-ray detection at high energies (>15keV)
- GHz, Multiple frames & high data rate, fast detection

Developing high-energy X-ray detectors with multi-frame capability is crucial for numerous HED facilities worldwide. This capability would enable the observation of a single driven target's evolution on a sub-nanosecond timescale, enhancing data quality by consolidating what would typically require multiple shots into a single sequence and eliminating uncertainties from variations in target and laser conditions. This advancement would similarly benefit HED science in NNSA missions, such as time-resolved diffraction for diagnosing the material properties of shocked materials at high strain rates. A high quantum efficiency detector operating at >10 keV with sub-nanosecond frame duration and multi-frame capability would reduce the number of experiments needed to map material phase space as a function of pressure. This would lower experimental costs and minimize uncertainties from comparing trends across multiple experiments.

Ways to detect high-energy (HE) X-rays can be put into two categories, bulk (diode) and electron (photocathode) detection. These two approaches differ in temporal resolution, ns vs 10s of ps scales.

Currently available photodiode-based detectors use 25 and 50  $\mu\text{m}$  thick Si diodes which only work well for  $\sim$ 5 keV X-rays. Moving to thicker, 100  $\mu\text{m}$  - 200  $\mu\text{m}$  Si diodes would increase the absorption for HE X-rays. Unfortunately, a thicker photo diode (PD) detector structure results in slower performance and blooming between pixels and though Si has a very high technology readiness level (TRL), for HE X-ray detection it requires an

unfeasible thickness. This causes as slow temporal response in the 5ns to 10ns range, and the expected absorption is only about 10% at 25 keV.

Other PD materials that are currently under development such as GaAs and Ge are of lower TRL but are promising with regards to improved X-ray detection at higher energies while having a fast expected temporal response. Ongoing work at SNL includes pixelated GaAs diodes with 40  $\mu\text{m}$  thickness, and expected 40% absorption @25 keV, and 0.44 ns expected temporal response. LLNL was working with UC Davis on a Ge pixelated diode with expected 50% absorption @ 25 keV for 60  $\mu\text{m}$  Ge with a temporal response of 1 ns.

The diodes can be integrated with fast Read Out Integrated Circuits (ROICs), which are large and contain millions of pixels. For hard X-rays, the generated electron-hole pairs can quickly saturate the readout. To address this, strategies such as increasing full-well capacities and implementing charge dumping schemes are being explored. Recent efforts have focused on using high-k dielectrics like HfO<sub>2</sub> and Al<sub>2</sub>O<sub>3</sub> in MIM Capacitors to enhance the full-well capacity of existing ROICs, achieving up to a fivefold increase without requiring major redesigns. In FY22, 20  $\mu\text{m}$  GaAs diode arrays were integrated with ICARUS V2 sensors, but a packaging issue prevented functionality. In FY23, a new batch was successfully packaged, resulting in the first testable GaAs hCMOS sensor. Although nanosecond-fast framing is not yet possible due to a shorting issue, preliminary images and gate profiles were obtained. Efforts continue to demonstrate a fully functional nanosecond-fast GaAs imager next year, and the potential of InP for even higher QE at >30 keV is being investigated. As of FY25, yield issues and defects in GaAs diode production remain an active area of investigation. The team continues to analyze defect sources and process variables that impact yield, with ongoing small-batch fabrication and in-house testing to identify and mitigate these issues. Improvements in wafer quality, packaging, and process control are being prioritized to enhance overall device reliability and yield.

Plasma and material research often require temporal resolution beyond the nanosecond scale, where photocathode approaches are more suitable. Streak cameras and pulse dilation aided framing cameras, both transformative diagnostics, offer short integration times. Current state-of-the-art X-ray detectors use photocathodes and diodes made from traditional materials, which struggle with poor detection efficiencies at higher X-ray energies, making detection of >10 keV X-rays challenging. An ideal photocathode material would have high X-ray stopping power, low electron pulse height distribution, large escape depth for secondary electrons, and minimal primary contribution. Ideally, it would absorb all photons and produce only one low-energy electron per photon. However, existing X-ray photocathodes often produce noisy images, as each photon can generate a wide range of electrons, leading to high pulse height distributions. Additionally, their detection sensitivity typically decreases by an order of magnitude between 5 and 15 keV, resulting in a Detective Quantum Efficiency (DQE) of less than 0.5% for the X-ray energies in question.

One approach to enhance the Quantum Efficiency (QE) of photocathodes is through geometric structuring, such as microchannel plates (MCPs) and structured PCs, which

increase the effective X-ray path length. Initial results with gold structured photocathodes have shown up to a  $3.4\times$  improvement in QE at 7.5 keV, with potential for further gains at higher energies. However, temporal fidelity and coating methods for alkali halide materials require further study, and the overall impact on signal-to-noise ratio and dynamic range is still being characterized. Current efforts are focused on MCP-based photocathodes due to their promising performance characteristics.

Efforts to develop higher quantum efficiency photocathodes using microchannel plates (MCPs) as PCs remain paused due to ongoing resource limitations. Although a modified streak camera test apparatus has been assembled to measure electron transit time spread and energy distribution, further experimental progress is currently on hold. In addition, detecting high-energy photons generates a large number of primary and secondary electrons per absorbed photon, which can lead to excess charge buildup, space charge effects, and reduced dynamic range in detectors. Mitigation strategies are necessary to address these space charge issues. Although some work is underway, further efforts are needed to fully characterize and resolve these challenges. Particle-in-Cell codes are valuable for modeling the behavior of these instruments. Additional effort is required to adapt existing codes and develop new tailored models to better understand these critical issues.

An additional effort has been initiated to evaluate fast scintillator materials for high-energy X-ray detection, with particular relevance for radiography of ICF-driven samples. These applications require area detectors capable of nanosecond-scale time resolution and sensitivity to X-rays exceeding 100 keV. Lead tungstate ( $\text{PbWO}_4$ ) and barium fluoride ( $\text{BaF}_2$ ) are among the primary candidates under consideration.  $\text{PbWO}_4$  offers a fast decay time and is well-suited for higher energy detection, while  $\text{BaF}_2$  provides higher optical yield for lower energy backlighters. The effectiveness of these scintillators for a multi-frame record on the same line of sight depends on their ability to decay sufficiently between exposures (whether that's between a package drive pulse and a backlighter pulse, or between consecutive backlighter pulses). The scintillator must also be formable as either a thick, optically transparent slab, or as segmented array, and must exhibit sufficient sensitivity and low enough effective pulse height distribution for the required numerical aperture to provide the required signal to noise. Testing at the LLNL's MegaRay and UCB/LBNL Scintillator Characterization Lab is planned for FY26, to obtain sensitivity and decay curve measurements.

To evaluate the feasibility of a multi-frame single line-of-sight ARC radiograph of a high-yield hohlraum driven sample at  $>50\text{keV}$  using such an scintillator and associated readout (either image relay of a large area scintillator, or hollow core fibers on a segmented scintillator array), we will use Geant4 Monte Carlo simulations to model the photon interactions, energy deposition, and optical photon yield. This simulation capability is essential for evaluating noise characteristics and guiding material selection for future diagnostic systems. As simulation requirements grow, a key challenge is the limited number of staff proficient in Geant4.

This transformative diagnostics effort directly enables advanced high energy density (HED) diagnostics, including radiography and high-energy X-ray detection for ICF-

driven samples. By advancing detector optimization and modeling, this work supports the HED&IS 10-Year Science Plan's objectives for future facilities and assessment platforms. Specifically, it addresses the plan's call for innovative diagnostic technologies to improve measurement precision, reduce experimental uncertainties, and expand the experimental capabilities required for next-generation science-based stockpile decisions and inertial confinement fusion applications.

### **IIIb-9: hCMOS**

The hCMOS technology developed at Sandia's Microsystems Engineering Science & Applications (MESA) facility is the world's fastest, multi-frame, burst mode imaging sensor capable of capturing images on the nanosecond timescale. The hCMOS technology provides three key benefits to many ICF and HED diagnostics under development: time-sequenced imaging from the same sensor area, background reduction through time gating, and operation under high neutron fluences (i.e., sensors are radiation hardened). The hCMOS sensors and supporting camera electronics are currently the most radiation tolerant imagers on NIF and Z. This radiation tolerance and ability to gate out unwanted background is a growing benefit to the programs for both high yield and high background experiments that are frequently encountered at NIF, Z, and Omega.

For thermonuclear burn experiments, hCMOS (in conjunction with SLOS technology) enables time-resolved 3D imaging with sufficient spatial resolution to diagnose failure modes of high convergence implosions. In opacity experiments, hCMOS sensors enable time-resolved measurements of the plasma evolution essential for addressing systematic differences between models and data. In strength and phase experiments of high pressure plutonium, hCMOS sensors will enable time-sequence measurements on a single shot (instead of using multiple shots to map out the evolution), which improves the accuracy through elimination of shot-to-shot variability and reduces the overall use of Pu on the facilities. In hostile environment experiments, high-energy x-ray sensitive hCMOS sensors enable more detailed understanding of x-ray source physics through enhanced imaging capability that will improve the fidelity of the x-ray test environment for more precise evaluation of component survivability. There are now more than 25 diagnostics using hCMOS/SLOS technology.

The development of new hCMOS sensors continues to evolve now that a private company known as Advanced hCMOS Systems (AHS) has been formed by a group individuals who left Sandia. AHS supports existing sensors and designs new sensors in collaboration with scientist and engineers at MESA. Wafers continue to be fabricated using the radiation-hard, hCMOS7 process that is provided by MESA. The largest investment is in a new single frame sensor known as Hyperion. This sensor is specifically designed for the new High Yield X-ray Imager at NIF for use on experiments with >10 MJ of neutron yield. The new imager is expected to be

deployed in FY26 and other diagnostics such as x-ray streak cameras will later benefit from the new Hyperion sensor. This work is a collaboration primarily between LLNL and AHS. Similar efforts are underway for continued development of the Kraken hCMOS sensor, which is collaboration primarily between AHS and Nevada National Security Sites (NNSS).

Other research efforts continue as a collaboration between the Pulsed Power Sciences Center at Sandia, AHS, MESA, and LLNL. This work includes the following:

- Faster photodiodes through novel electrode designs
- GaAs photodiodes for high-energy x-ray detection.
- Improved fabrication yield for Daedalus V2
- Evaluation of non-MESA fabricated sensors (e.g., Tantalus).

All of these efforts are important for the broader community of hCMOS users.

Fabrication costs continue to rise. The fabrication of a twelve-wafer lot costs around two-million dollars. If new sensor designs are needed the required labor from AHS or Sandia will increase the cost substantially. This large price tag will likely require cooperation and cost sharing across multiple laboratories to in order to develop new sensors. One of the challenges is determining the requirements of a future sensor that will support multiple laboratories. This work should be stewarded by the NDWG.

#### **IV: Broad Diagnostic Efforts**

The NDWG defined a class of diagnostics or diagnostic related activities which benefits from significant national efforts and will enable new or more precise measurements across the complex. These are: Precision nToF, Mix, and Te, Image Analysis, Hard X-Ray Detectors, X-ray Doppler Velocimetry (XDV), and Synthetic Data. There is also an ongoing effort to maintain the capability to scan imaging plates with high accuracy and consistency across the complex.

One part of the precision nToF activity is to continue improving the measurement accuracy of the hot-spot velocity inferred from the nToF spectrum. Existing nToF detectors provided the first evidence that DT implosions at both NIF and Omega have a residual bulk velocity limiting the efficiency of the implosion. Both direct and indirect drive experiments have confirmed the adverse impact of residual hot-spot velocity on fusion yield and was confirmed with simulations.

Measuring the hot-spot velocity requires better than 10000:1 precision owing to the relatively small drift velocity  $\sim$ 10-100km/s that modifies the birth neutron spectrum that has a velocity associated with the 14 MeV neutron of 51233km/s. A simple hot-spot model asserts that the mean neutron energy is modified by both bulk hot-spot motion and the average kinetic energy (or ion temperature) of the D and T reactants. To characterize the 3D velocity vector and ion temperature a minimum 3 or 4 independent nToF detectors are required at quasi-orthogonal positions around the target chamber. Each of these must be sufficiently well collimated so that the neutron spectrum is not significantly impacted by the scattering environment and of sufficient temporal response to meet the precision requirements described above. This need has led to a multi-laboratory goal within the nToF community to implement more collimated lines of sight and faster fused-silica Cherenkov nToF detectors to better characterize the bulk flow. In addition adding a fifth detector on NIF has improved the accuracy of the velocity measurement as shown in

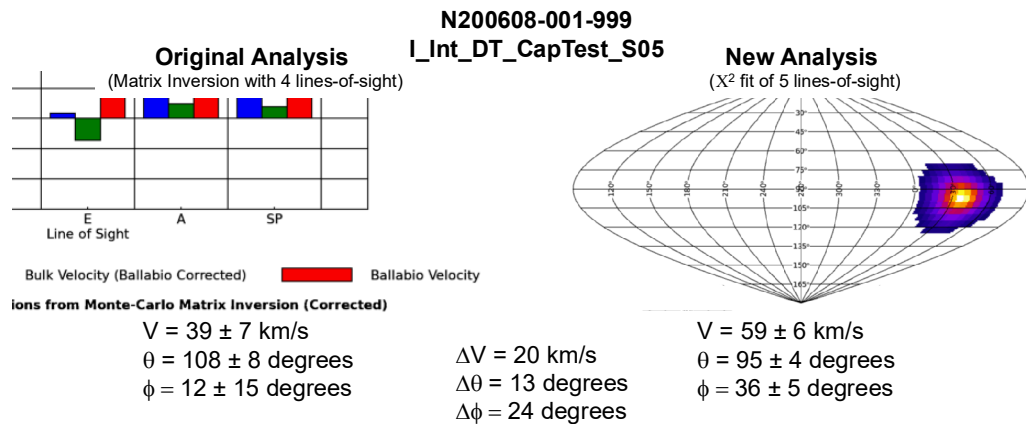


Figure 11 -Analysis of hot spot velocity using 4 NTOF LOS vs 5 LoS, which has improved both the angular precision of the velocity measurement by  $\sim 2x$ .

Fused-silica Cherenkov nToF detectors (QCD) have enabled higher precision velocity measurements illustrated in Figure 11 due to the thresholding nature of the Cherenkov process. This means that the signal measured due to gamma-rays is more directly related to the implosion bang-time and not polluted by high-energy x-rays emitted by LPI in the hohlraum or plasma surrounding the capsule.

This has revolutionized the precision with which hot-spot bulk flow can be measured and as a result, Cherenkov detectors have been deployed and tested at NIF, Omega and Z over the past 2 years. All 3 laboratories are investing in additional nToF lines of sight to better understand these effects which should lead to a significantly improved capability within the next few years.

#### NIF to Z Diagnostic Tech Transfer Effort:

After a decade of intense investment, there are well established diagnostic capabilities demonstrated at the NIF that are used to make quantitative measurements on ICF plasmas. Many of these diagnostics were developed as national collaborations toward the goal of determining the efficacy of NIF to achieve ignition. Starting in late 2020 a tech-

transfer effort was initiated to transfer key measurement capabilities and engineer for use at Z. These demonstrated capabilities on the NIF is bringing the measurement maturity for characterizing magnetic direct drive (MDD) fusion plasmas on Z up to the long-standing ability of the NIF. Three types of measurements were identified: (1) x-ray emission durations using x-ray streak cameras (SCORPIONZ), (2) improved neutron time-of-flight detectors (ZNTOF) on multiple lines of Sight, and (3) 2D-neutron imaging (NEMESIS) of Z-pinch implosions.

Nuclear burn volume, burn and confinement time, burn magnitude (and spectra), and ion burn temperature are fundamental to quantifying burn performance. At present, Z has limited capabilities to measure neutron production duration and no 2D neutron imaging capability. Routine 1D-neutron imaging is performed but is limited to a spatial resolution of 0.3 mm. In addition, there are no capabilities to disambiguate effects of motion broadening of neutron spectra from a thermonuclear ion temperature. While substantial understanding can be gained with integrated measurements, multi-dimensional spatially and temporally resolved data is critical to assess key questions on performance and scaling and to utilize burning platforms for stockpile science. The physics requirements for spatial and temporal resolution in nuclear and x-ray measurements in some MDD platforms require existing capabilities on Z to improve by roughly an order of magnitude. The technology to make each of these measurements on NIF are routine and in some cases have been deployed along multiple lines-of-sight.

The specific capabilities under development as part of this NIF-to-Z technology transfer include:

- Improved nTOF for reliable Tion and kinetic energy (ZNTOF): During the latter stages of the National Ignition Campaign (NIC), it became clear that a significant amount of residual kinetic energy (RKE) was present during the burn phase of the implosion. This RKE manifested itself in significantly shifted and broadened neutron time-of-flight signals. Quantifying the RKE requires measuring the neutron time-of-flight (nTOF) signals along multiple independent nTOF lines of sight to fully disambiguate coherent and incoherent flow, as well as the true burn weighted ion temperature, Tion. In FY25 major progress was made on one line of sight for ZNTOF using technology transferred from NIF. First data on this Line of sight with prototype detectors will be obtained in FY26 once approvals for shielding changes on the line of sight have been approved by the Z facility.
- X-ray streak bang and burn(SCORPIONZ): Understanding stagnation conditions is greatly enhanced through an analysis based on both X-ray and nuclear signatures. One gap in the X-ray diagnostic suite at the Z-facility is the lack of X-ray streak camera-based instruments. At the NIF, X-ray streak cameras are regularly used to provide high temporal resolution X-ray burn history measurements (SPIDER), high temporal resolution 1-D images of implosions (DISC), and high temporal and spatial resolution spectroscopy measurements (DISC/tConSpec). In FY25 the SCORPIONZ x-ray streak camera was installed on Z. The system is being commissioned on the Z facility and it is anticipated that first data will be obtained early in FY26
- 2-D neutron imaging (NEMESIS): At Z, there is no 2-D neutron imaging capability, while there is a 1-D capability it is limited by a spatial resolution of 0.3

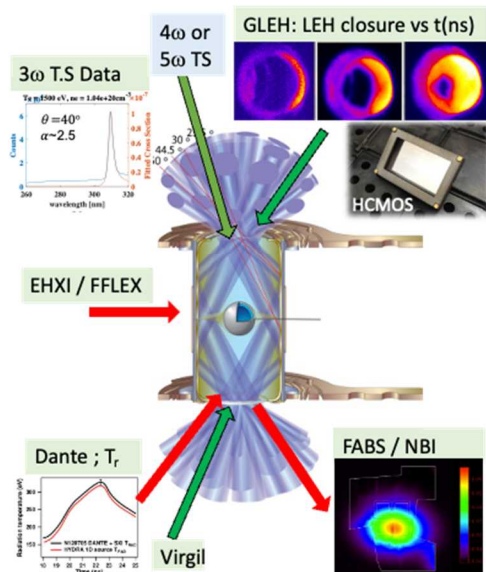
mm. A highly resolved 2-D neutron capability will be transformational to help understand and resolve fusion parameters such as the burn volume and shape, which is critical to infer ignition metrics such as P-tau. In FY25 the FDR for NEMESIS was completed and work on developing the required alignment systems for Z will continue in FY26.

## **V: Local diagnostic development efforts at NIF, Z and OMEGA**

### **V-1: Local Diagnostic Development on the National Ignition Facility**

New local diagnostic capabilities on the NIF are aimed at improving our understanding of the evolution of high energy density plasmas for stockpile stewardship, National Security applications and discovery science. The majority of the development activities in FY 25 continued to be focused on the development of x-ray, neutron and optical diagnostics for the LLNL HED science programs, including Inertial Confinement Fusion (ICF) and focused high energy density experiments, specifically: Materials research and radiation transport. For ICF NIF's local diagnostics are categorized into three general areas, (1) Hohlraum drive, (2) Capsule response and (3) Stagnation diagnostics.

#### **Hohlraum Drive Diagnostics :**



Acronym	Diagnostic	Observable
DANTE	Broadband, time-resolved x-ray spectrometer (DANTE-1 and DANTE-2)	Hohlraum x-ray conditions
EHXI	hard x-ray imager	beam pointing in hohlraum
FABS	full aperture backscatter system	backscattered light into lens / hohlraum energetics
NBI	Near Backscatter Imager	backscattered outside lenses
FFLEX	Filter Fluorescer	hot electron fraction and temperature
SXI	x-ray imager for hohlraum imaging (2x LoS)	Hohlraum laser entrance hole closure
VIRGIL	soft x-ray spectrometer	Hohlraum x-ray conditions
GLEH	1ns,gated x-ray imager for hohlraum imaging (HCMOS)	Hohlraum laser entrance hole (LEH) closure as function of time
SLTD	Scattered light temporal diagnostic	Laser to target energy coupling for direct drive
OTS-3w	3w Optical Thomson Scattering	Measure plasma density, temperature and plasma flows in hohlraum LEH region
OTS	Optical Thomson Scattering	Workshop held in FY25 to determine future path. E.g. 4ω or 5ω

**Figure 12: ICF Hohlraum Drive Diagnostics:** Hohlraum Drive Diagnostics, including example data from Gated Laser Entrance Hole (GLEH) imagers that utilize hCMOS technology, 3w Thomson Scattering, Radiation temperature measured by Dante 1 and Dante 2, backscattered light distribution measured by the NBI and FABS diagnostic. The table shows diagnostic and observables.

The hohlraum drive local diagnostics, shown in Fig.12, include soft x-ray spectrometers e.g. Dante 1&2 (time resolved) and Virgil (time integrated) to measure the hohlraum drive conditions. In addition these measurement both Dante systems also provided direct measurements of hohlraum reheating by igniting capsules. Hard x-ray emission from HED plasmas is measured by the FFLEX spectrometer., Hohlraum alignment is confirmed by

soft x-ray imagers (EHXI and SXI), while scattered light from NIF experiments is characterized by a variety of scattered light diagnostics (SLTD, FABS, NBI). The NIF scattered light time history diagnostic (SLTD) was developed for LDD to measure the azimuthal distribution of scattered light in NIF polar direct drive implosions. The gated laser entrance hole imager (GLEH-2), replaced the standard CCD camera in SXI with SNL's time gated hCMOS cameras. This now provides 1-2ns duration time gated images of the hohlraum laser entrance hole (LEH), which feeds into assessments of both laser-hohlraum energy coupling and implosion symmetry. A time resolved Thomson scattering spectrometer captures light scattered from HED plasmas. This technique is designed to provide time resolved point measurements of temperature, plasma flow and plasma ionization stage in the hohlraum plasma (this system is described in detail in transformational section). The development of deep UV Thomson scattering diagnostic using 1J of 5w energy proved to be very challenging to implement and the project was put on pause at the end of FY23. To determine the future direction of this project a workshop was held in FY25 to determine potential solutions to the challenges of deep UV Thomson scattering on hohlraum and coronal plasmas for HED science over the next few years. It is anticipated that a new plan utilizing 4w light will be developed in FY26, ready for detailed design studies in FY27. In FY25 the team continued to use the OTS spectrometer system to collect Thomson scattered  $3\omega$  light from the laser entrance hole plasma in simplified hohlraums.

### ICF Capsule response diagnostics:

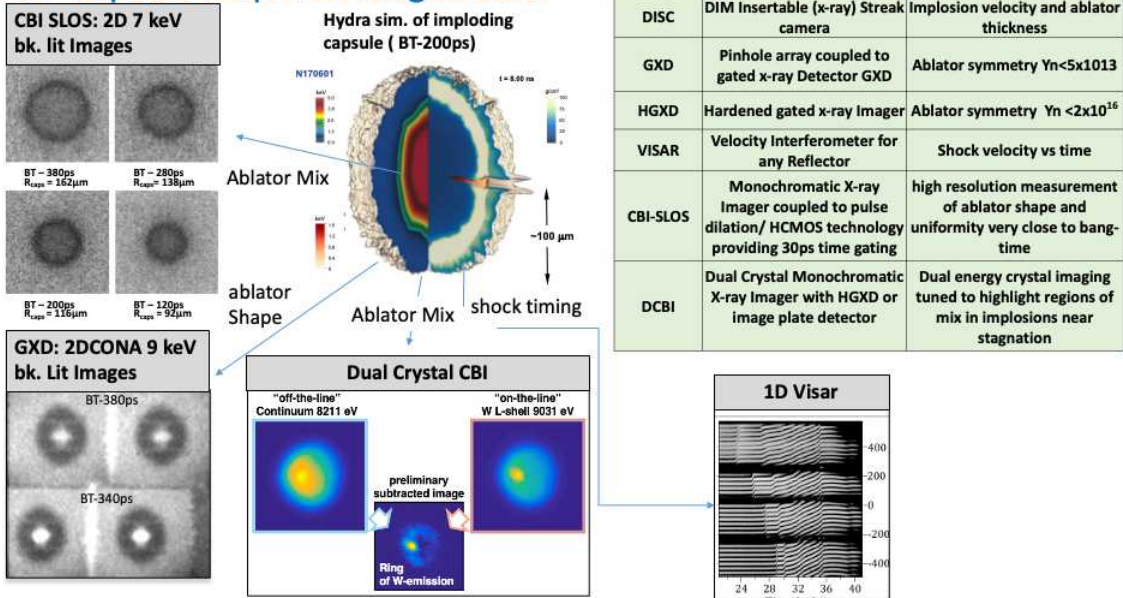


**Figure. 13: ICF Capsule Response Diagnostics**, showing a hydra simulation of a capsule within 200ps of bang time, four examples of important diagnostic measurements for Shock timing, ablator conditions and ablator mix.

## 2.2. Capsule Response Local diagnostics:

For laser indirect drive the hohlraum produces a large flux of soft x-rays which are absorbed in the capsule containing the DT fuel. The outer wall of the capsule (the “ablator”) is heated by the x-rays and expands rapidly, driving a series of shocks that travel through the ablator and fuel, leading to a quasi-spherical implosion that both

compresses and heats the DT fuel. Capsule response diagnostics are required to measure the symmetry and performance of the ablator and fuel as it implodes.

Capsule response diagnostics are shown in Fig.13. Just after the completion of NIC, the ablator uniformity, density and symmetry were measured using backlit 2D x-ray radiography (2DCONA). This technique continues to use an x-ray backlighter to provide a shadow of the ablator, which is imaged via a pinhole array onto a gated framing camera (GXD). This provides a series of radiographic in-flight images of the ablator within about 500ps of the peak compression, with an example of data shown in panel on lower left of Fig. 13. The dark ovals show compressed ablator while the bright regions in the center of the images are from capsule self-emission. This diagnostic provided critical insight into the deleterious effects of the capsule support tent, seeding a hydrodynamic instability, which led to non-uniform implosion and mixing of ablator into the fuel and hot spot. These measurements provided important data that caused the ICF program to change the laser pulse shape and minimize the thickness of the support tent. Both of these changes paved the way to the use of HDC capsules that achieved ignition in 2022..

The single line of sight imaging diagnostic (SLOS), was one of the nine NDWG transformational diagnostics, and replaced the gated x-ray imagers as the detector for 2D x-ray backlit imaging (2DCONA) for experiments that measured ablator shape. Coupling this new diagnostic with a mono-chromatic imaging crystal (CBI-SLOS) enabled ablator radiography measurements to overcome the capsule self-emission within  $\sim$ 100ps of bang-time, as shown in panel on upper left. It is the narrow bandwidth of the imaging crystal that allows greater discrimination between backlighter x-rays over the broad-band capsule self-emission, enabling ablator measurements late in the implosion, which could not be done with the previous 2DCONA technique. This system has been used to infer mixing of ablator material into the hot spot, providing valuable new information on an important ICF degradation mechanism. The SLOS prototype system has proven to be difficult to calibrate and operate in practice and so the ICF program are now using short pulse x-rays and image plates to perform these measurements. The best example of this consists of a system with dual crystals, called Dual Crystal CBI (DCBI), which was first implemented in late FY23 and has been used through FY2 / FY25. This technique uses two narrowband crystals to image emission from dopant material (tungsten) into the hot spot, using either image plates or HGXD detectors. This allows experiments that can isolate the mixing of ablator material into the hot spot. Implosion trajectory and ablator density are also measured using one dimensional x-ray backlighting techniques, which use x-rays to project a 1D slit image onto an x-ray streak camera (DISC) this platform is called 1DCONA and continues to be used by both the ICF and HED programs to provide a wealth of data on shock transit through ablator materials.

Another important diagnostic is the one-dimensional velocity interferometer (1D VISAR) that is used to characterize materials at high pressure (as shown in lower middle panel in fig.13) and to synchronize the shocks driven by the x-ray drive through both the capsule and the DT fuel. This ensures that the laser pulse drives the correct sequence of shocks to assemble the fuel. The achievement of ignition in Dec 2022 and the advent of multiple shots producing MJ of neutron yields highlight the

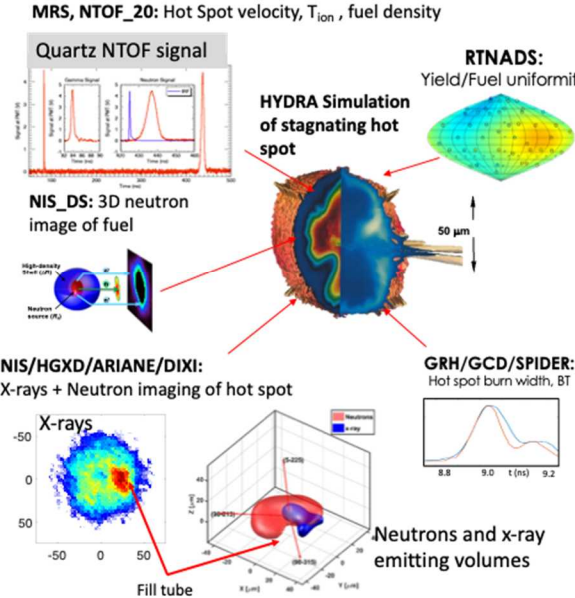
fact that the VISAR diagnostic needs to be placed in a room that is far enough from the chamber and shielded from high neutron fluxes to prevent neutron damage to the detectors. Currently the sensitive detectors are removed and replaced around every high yield shot. This is inefficient and time consuming, so a design study started in FY25 with the aim to move the existing VISAR interferometer system to a shielded room. This project aims to reach PDR/FDR stage in FY26, to with the intention to complete the relocation on the FY28 timescale.

### **2.3. Stagnation Local diagnostics:**

As the capsule approaches peak compression, the hot spot begins to approach maximum density and temperature conditions and produces copious neutrons and x-rays. These particles and photons are used to diagnose stagnation conditions  $\sim$ 100-200ps around time of peak compression. As shown in Fig.14, a large number of diagnostics were commissioned on NIF to characterize stagnation conditions during the NIC. Since then, there have been multiple advances that are greatly improving understanding of these challenging implosions. Some notable examples are; (1) the use of 5 neutron time of flight detectors to provide high precision measurements of neutron ion temperature and the bulk velocity of the neutron emitting hot spot; (2) the use of the multi-kJ, 30ps ARC laser to provide a higher energy X-ray backlight images of the compressed fuel at stagnation, via Compton scattering; (3) multiple Neutron and X-ray imaging lines of sight to provide 3D reconstructions of the neutron and x-ray emitting volume at stagnation. These diagnostics are continuing to provide powerful insights into degradation mechanisms that prevent NIF implosions from reaching their designed performance. The contribution of these diagnostics to the achievement of ignition has been described in detail in a recent Physics of Plasmas publication [ J. Kilkenny et al., ***The crucial role of diagnostics in achieving ignition on the National Ignition Facility (NIF)*** ]

*"Phys. Plasmas 31, 080501 (2024)]*

## ICF Stagnation Diagnostics



Acronym	Diagnostic	Observable
ARIANE	Hardened Gated x-ray Imager - Chamber based	X-ray hot spot size and shape for yields up to $1 \times 10^{17}$ neutrons
HGXD	Hardened Gated X-ray Detector - DIM based	Ablator symmetry $Y_n < 2 \times 10^{16}$
DIXI	Dilation x-ray imager on pole and equator	X-ray hot spot size and shape with 10ps gate time, Yields in 1-10MJ range
NIS	3D Neutron Imaging system (3x Los)	hot spot size on 3 axis + and fuel asymmetry, Gamma imaging on 2 lines of sight
NTOF_20	neutron time of flight	Ion Temperature, hot spot velocity on 5 Lines of sight
MRS	Magnetic Recoil spectrometer	Neutron spectrum for Yield, Ion temperature and fuel density
Well_NADS	Nuclear activation	Absolute neutron yield using Zr activation
RTNADS	Higher Resolution Unscattered neutron yield	Fuel symmetry using multiple Zr activation discs around the chamber
GRH	Gamma Reaction History + PDPMT on one channel	Neutron bangtime (BT) and burnwidth down to ~50ps pulsewidths
GCD	Gas Cherenkov Detector	Neutron burn history and gamma excitation from Carbon ablators
SPIDER	Streak Polar Streak camera - chamber based	X-ray BT and Burnwidth @ 10keV

**Figure 14: ICF Capsule stagnation Diagnostics**, showing a hydra simulation of a capsule at bang-time, five examples of important diagnostic measurements; neutron time of flight (NTOF\_20), down scattered neutron imaging of the dense DT fuel, RTNADS measurements of fuel uniformity, GRH/GCD measurements of implosion bangtime / hot spot burnwidth and combined 3D x-ray imaging / neutron imaging of the stagnating hot spot.

### Stagnation local diagnostic status in FY25 :

**DIXI/ARIANE:** X-ray emission diagnostics that have been hardened against the high neutron and hard x-ray fluxes are used to measure the shape and brightness of the hot spot throughout the time of peak x-ray emission. HGXD (70ps resolution x-ray framing camera) are used for this measurement up to neutron yields of  $2 \times 10^{16}$ . ARIANE is a hardened x-ray framing camera placed 6m from chamber center that is designed to provide similar x-ray shape data up to yields of  $\sim 1 \times 10^{17}$  neutrons. For time resolved data at neutron yields in the  $\sim 10^{18}$  range we have converted the CMOS detector on polar DIXI instrument to use film, with the goal to extend the useable range up to  $\sim 10$ MJ fusion yields ( $\sim 3 \times 10^{18}$ , 14MeV neutrons). In FY25 we worked on converting the equatorial DIXI to have a similar film back end detector system. This was implemented in FY25 and will be commissioned by the end of FY26 during FY26 on the NIF target chamber by diagnosing stagnation shape on implosion experiments which produced neutrons in the MJ range .

**Upgrade of NIS\_1 with GyGAG scintillator for improved gamma imaging:** This is part of the LANL neutron imaging diagnostic. This diagnostic routinely produces images of the primary neutron source(14MeV), lower energy neutrons ( $\sim 6$ -12MeV) that have been down-scattered by the DT fuel and gamma rays produced by neutrons interacting with the carbon ablator. Introduction of a sub aperture new higher resolution scintillator( GY:GAG) in FY24 improved the resolution of the gamma imager on a subscale of gamma images. Work on a full aperture GY:GAG system was completed on one line of sight in FY25 . This now allows measurements

of the shape of the neutron emitting hotspot, the DT fuel and the carbon ablator on a single line of sight. To add another constraint to the state of the stagnating plasma, in FY26 we will test gamma imaging on a second line of sight with a new Sodium Iodide scintillator.

**GRH with PDPMT :** Measurements of the time of peak emission and the neutron burn duration are obtained via fusion induced gamma emission using the Gamma Reaction History (GRH) diagnostic , which was co-developed between LANL and LLNL.. In GRH Gamma radiation from the implosion is converted into energetic electrons via the Compton effect. These electrons propagate through a gas cell ( SF6 or CO2) producing prompt Cherenkov radiation which is then detected by an optical Photomultiplier (PMT). The original GRH systemmeasures the time of peak emission to  $\pm 50$ ps and burn duration to  $\pm 100$ ps. In FY22/23 we replaced one of the PMT's on GRH with a pulse-dilation PMT with  $\sim 10$ ps temporal resolution. The detector for the GRH-PDPMT system was calibrated in an offline laser test station in FY24. In FY25 we installed the calibrated PDPMT on one of the GRH channles on NIF and ran it high yield shots. It is now regularly producing good data on MJ yield shots. Late in fY25 the LLNL/LANL GRH team installed a gated MCP to gate out neutron induced backgrounds on high yield shots. This was very successful, producing very good signal to background on multi-MJ neutron shots in FY25 (e.g. 3.6MJ yield shot N250930)..

**RTNADS:** Absolute neutron yield is measured using zirconium Nuclear Activation Detectors (Well\_NADS). DT fuel uniformity is also measured by a distribution of chamber nuclear activation detectors (RTNADS). Around 2020 RTNADS began to provide automatic analysis of low mode fuel uniformity with higher sensitivity and  $\sim 2$ x increased locations ( $\sim 40$  vs 18), which allows fuel maps to be measured with higher Legendre modal content ( $L < 4$ ) than the previous FNADS system ( $L < 2$ ). This detector is now run routinely on all high yield shots on NIF. However the LaBr detectors induced a background that takes time to decay. This puts a constraint on the amount of time between high yield DT shots ( $\sim 2$  weeks) for this background to die away before the next high yield shot. In FY24 we removed the PMT detectors from high yield shots and reinstalled them on a subset of Zr pucks after the experiment to protect the detectors from the high neutron yields. This provides a fuel uniformity map of low mode fuel ( $L < 2$ ) which is used on high yield shots to compare to downscattered neutron images from the NIS systems..

**NTOF\_20:** As described in the broad diagnostics section, a suite of five Neutron Time of Flight systems (NTOF\_20; each  $\sim 20$ m from the center of the chamber) are used to measure the ion temperature and hot spot bulk velocity via broadening of the neutrons emitted from the hot spot at time of peak compression. These diagnostics have been developed via a decade's long collaboration with scientists and engineers from LLNL, LLE, LANL and Sandia. Fig.14 shows example data from the high temporal resolution quartz detector. In addition to ion temperature and bulk velocity these diagnostics also measure the fraction of neutrons that are down-scattered by the DT fuel (the Down Scattered Ratio = DSR), giving 5 measurements of fuel density around the implosion. The five NTOFs with the

high temporal resolution quartz detectors are also used to routinely used to measure the bulk velocity of the hotspot velocity with 5km/s temporal resolution). The hot spot bulk velocity is a key degradation measurement for laser driven implosion as high bulk velocities ( >50km/s) are a leading indicator of implosion asymmetry leading to reduced kinetic energy being converted to hot spot internal energy .

## **2.4. Development of high yield diagnostics for Enhanced yield capability (EYC) and beyond:**

Diagnostic development for Multi-MJ yields is an ongoing effort at the National Ignition facility. NIF diagnostics have evolved since the early days of NIF experiments in 2010 when the neutron yields were in the ~1kJ range. Most of these improvements have involved incorporating three main elements: (a) moving detector systems to more remote locations, (b) incorporating hardened detectors, such as film, CMOS or hCMOS and (c) incorporating line of sight shielding of detector systems. Applying these elements has allowed NIF to provide critical data for HED science as the yield has increased by more than 3 orders of magnitude in the decade of NIF experiments (from <5kJ in 2012 to 8.6MJ in 2025).

For example: time resolved x-ray imaging with framing cameras evolved from non-radiation hard CCD cameras (GXD) placed 1.2m from the x-ray source to radiation insensitive optical film in HGXD at 1.2m and then optical film at 7m with the ARIANE and most recently film based pulse dilation DIXI diagnostics. A new High yield x-ray imager ( HYXI) is currently being design to push the upper yield range for time resolved imaging up beyond 20MJ on the existing NIF facility using a

Measurement or diagnostic capabilities	Existing NIF (Yn ~ 10-20MJ) status	Enhanced Yield Facility (Yn ~ 30-50MJ, 3x higher than Existing NIF )	Future Yield Facility (100-1000MJ, neutron flux ~20x higher than EYC)
X-ray Drive diagnostics	Primary diagnostic: DANTE x-ray diode low resolution spectrometers @ ~ 8m from TCC	Existing DANTE systems: evaluate detector scope upsets at 10-20MJ	Relocate DANTEs detectors to remote shielded location at ~20m from TCC to reduce neutron flux on detectors
Shock timing and Equation of state diagnostics	Primary diagnostic: VISAR	Primary diagnostic: VISAR-> Relocate Visar to shielded location, so can operate routinely and efficiently at yield up to 50MJ	Construct VISAR system with image relay to shielded room.
Hot spot imaging diagnostics - time integrated x-ray imaging	Primary diagnostics: Time integrated x-ray pinhole Imaging using image plates @ 6m	Develop yield tolerant alternative to image plates and/or move detector plane further from TCC by ~2x	Use experience learned at existing NIF/ EYC to design location of detector plane and hardened electronics ( e.g. hCMOS)
Hot spot imaging diagnostics - time resolved x-ray imaging	Primary diagnostics: Hardened x-ray framing cameras @ 7m using pulse dilation technology + optical film / yield tolerant hCMOS electronics(DIX1 / HYXI).	Primary Diagnostic: HYXI. May need to move detector plane further from TCC to ~10m for higher end of yield range	Primary Diagnostic: Move pinhole array and detector plan further from TCC ( to maintain optimum magnification). Detector plane would be around ~40m from TCC for same detector technology as HYXI. Alternative Concept: Use X-ray optic to relay x-ray image to detector at remote location at ~40m
Hot spot, DT fuel and gamma imaging diagnostics - time integrated (burn average) neutron imaging	Primary diagnostics: Neutron Pinhole Imaging onto image plate and scintillators at 20m from TCC	Primary diagnostics: Neutron Pinhole Imaging onto image plate ( more remote location) with thinner scintillators at current location ~20m ( thinner so less sensitive detector). May need to add neutron scattering filter to further reduce signal at detector at upper end of yield range	Primary diagnostics: Neutron Pinhole Imaging onto image plate and scintillators 3x further from TCC (~60m)
Neutron spectrum from stagnating hot spot	Primary diagnostics: Magnetic recoil spectrometer (MRS) and neutron time of flight (NTOF) diagnostics	Primary diagnostics: Upgraded neutron time of flight(NTOF) diagnostics with neutron scattering filter and/or reduced sensitivity detectors Secondary Diagnostic: Upgraded MRS with remote convertor foil. This may also need remote detector	Primary diagnostics: Upgraded neutron time of flight (NTOF) diagnostics with more remote detectors and /or neutron scattering filter, reduced sensitivity detectors. Lessons learned in 10-20MJ NIF will inform the changes required for 1000MJ facility
Time Resolved neutron Spectrum	No Diagnostic for the measurement: Some promising techniques. Needs more R&D and prototyping to develop viable and cost effective solution for NIF	TBD: depends on lessons learned on existing NIF	TBD: depends on lessons learned on existing NIF and experimental needs for applications of ignition, which is evolving.
X-ray burn width and BT	Primary Diagnostic: X-ray streak camera (SPIDER)	Primary diagnostic: upgraded SPIDER with hardened streak camera (HDISC). This is an R&D effort	Primary diagnostic: upgraded SPIDER with hardened streak camera at remote location. This may also required X-ray imaging optic. Will rely on lessons learned on existing NIF and EYC solution.
Neutron burn history (BW and BT )	Primary Diagnostic: Gamma reaction History (GRH) with PMT or PD-PMT	Primary Diagnostic: Gamma reaction History (GRH) with PMT or PD-PMT at more remote location (20m vs 7m)	Primary Diagnostic: Gamma reaction History (GRH) with PMT or PD-PMT or optical streak camera at more remote location (60m vs 20m)
Stagnation conditions ( e.g. mix via x-ray spectroscopy	Primary diagnostic: DIM based x-ray crystal spectroscopy (ISS) ( time integrated) of ablator dopants ( e.g. tungsten) with Image plate detector	Primary diagnostic: Chamber based x-ray crystal spectroscopy with x-ray relaying crystal and hardened streak camera (HDISC) in shielded location. R&D ongoing	x-ray crystal spectroscopy with x-ray relaying crystal and hardened streak camera type detector in shielded location. Will depend on lessons learned on current NIF
Plasma Opacity	Primary diagnostic: DIM based x-ray crystal opacity Spectrometer (OPSPEC) ( time integrated)	Need to develop a chamber based x-ray crystal opacity Spectrometer with time gating, framing or streaking that is compatible with 30-50MJ yields. R&D starting in this in FY25	Need to develop an x-ray crystal opacity Spectrometer with time gating, framing or streaking that is compatible with 100-1000MJ yields. The design of this will depend on the specific experimental need and lessons learned at 10-50MJ scale on
Applications of yield: Survivability	Survivability experiments using multiple experimental platform to expose samples to x-rays and neutrons.	Survivability experiments using multiple experimental platform to expose samples to x-rays and neutrons. Scale platforms to survive higher yields	Need positioner systems that can put samples close to neutron and x-ray sources. Tion maximize flux on target. These platforms will be informed by results from NIF and EYC in 1-50MJ range
Applications of yield: high level description	Dante has been used to diagnose reheating effect in igniting hohlraums.	Use hardened optical, x-ray and nuclear diagnostics systems to diagnose packages that are impacted by ignition. In general will need systems with 10's um spatial resolution and 10-100ps temporal resolution and able to function in high yield environments	Use upgraded optical, x-ray and nuclear diagnostics systems to diagnose packages that are impacted by ignition. The design of these systems will be informed on the specific experimental need and lessons learned at 10-50MJ scale on NIF/EYC
Applications of yield: X-ray backliters	X-ray backliters driven by either standard NIF beams or the Advanced Radiography Capability (ARC) are routinely used , but not at MJ yields because all beams are required to drive ignition hohlraums.	A dedicated X-ray backlifter beam would be ideal for EYC. This would require either a synchronized x-ray source or a dedicated laser system ( could be an additional quad) to be dedicated to driving the x-rays required for these applications	A dedicated X-ray backlifter beam would also be required for hard x-ray radiography on this facility. This would require another quad. Would need yield tolerant detectors ( similar to those for hot spot x-ray imaging)

combination of pulse dilation and a new generation of hCMOS detectors (planned for testing on NIF in FY27).

**Table 4.** High level description of status of high yield diagnostics on existing NIF and prospective development needs for EYC and high yield facility

The planned upgrade to NIF laser energy, called the Enhanced Yield Capability (EYC), is envisioned to produce neutron yields in the 30-40MJ range (which is roughly 2x higher than the maximum yield that is projected for the existing NIF facility with laser energy peaking at 2.2MJ). The next generation high yield facility which could follow NIF with EYC, will be designed to operate up to a yields roughly 10-20x higher; in range of 200-1000MJ. This will open up new parameter spaces in

HED and weapon science, and provide new challenges for diagnostics of both implosion performance and applications of 100's MJ neutron yields. Table 4 shows some the current understanding of diagnostic developments, which will be required for NIF over next 5 years, NIF\_EYC in early 2030's and the NGHED facility in the mid 2040's.

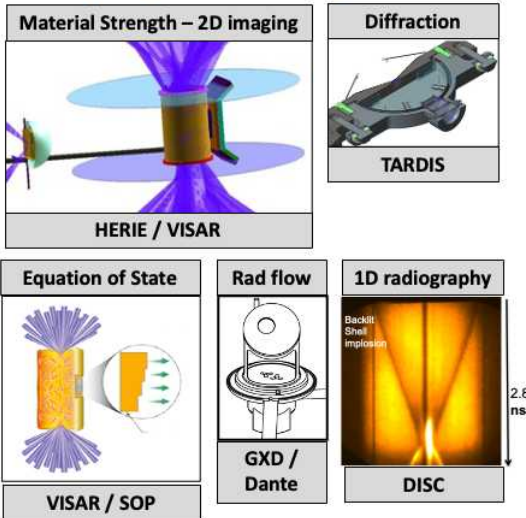
As outlined in table 4, these upgrades will require application of the same 3 elements to ensure that diagnostics can operate at these elevated backgrounds. For EYC the yield increase is roughly a factor of 2x, which will allow some diagnostics to operate with minimal modifications, possibly with the addition of radhard detectors (HYXI) or relocation to more remote shielded locations (VISAR), while other will require all three elements ( e.g. x-ray spectroscopy will require hardened detectors in a shielded remote location). The NGHED facility will also require all three elements relaying images to remote shielded locations for the diagnostics that will be required to enable the creation of implosions producing 1000MJ neutron yields and for the experiments that are currently being designed to utilize those applications. The requirements for the NGHED facility are currently being developed through multiple workshops. These workshops are identifying experiments that will be able to answer compelling science questions in the weapons design community. New diagnostic requirements will flow down from these experiments however we can use our experience learned from NIF and NIF\_EYC to chart the likely diagnostic technology that will be required at to 10-20x increase in neutron yields on NGHED. So to make progress on these definitions we will continue to work on developing diagnostics that can operate NIF diagnostics in the 10-40MJ regime and use this experience to prepare diagnostics for NGHED. The National diagnostics workshop is a critical venue for these discussions with the national and international HED diagnostic community. One of the most important objectives of these workshops will be the development of a long term diagnostics roadmap for the high yield facility.

#### **4. Local diagnostics supporting HED science experiments on NIF:**

The diagnostic suites support experiments that generate weapon-relevant HED conditions in specialized laboratory environments for NIF, Omega and Z. These are generally experiments that use a subset of the facility diagnostics to study focused physics problems relevant to weapons science in the general areas of radiation flow and material properties at high pressures (including equation of state, opacities, and material strength) as shown in Fig. 15. On NIF the VISAR system is used for shock timing in ICF implosions, and for equation of state studies that have provided important data on a range of materials for the national HED program. Planned improvements to the VISAR system on NIF will make the VISAR detection system compatible with multi-MJ yields by relocating the detector systems to a more remoted shield location in the NIF facility. X-ray diffraction is another important diagnostic that is used to directly measure the crystal structure, adding another constrain to the equation of state in HED experiments. On NIF the TARDIS diagnostic is a workhorse diagnostic that has been used to characterize the crystal structure of important materials at high pressures.

**Figure 15: The NIF diagnostic suite supports focused science experiments for the HED program**, some of the many examples are shown here. These include advanced 1D streaked x-ray radiography using DISC, 2D high energy radiography for material strength using image plates (future experiments will use ARC and high energy

## HED diagnostics supports many experimental platforms



Acronym	Diagnostic	Observable
VISAR	Velocity Interferometer for any reflector	shock velocity vs time
SOP	streaked optical pyrometer	temperature diagnostic for shock materials
DISC	DIM Insertable (x-ray) Streak camera	soft x-ray imaging and Spectroscopy
SXI	x-ray imager for hohlraum	Hohlraum laser entrance hole imaging
GLEH	1-2ns,gated x-ray imager for hohlraum imaging (HCMOS)	Hohlraum laser entrance hole (LEH) closure as function of time
HERIE	passive hard x-ray imager	image plate based imaging snout
GXD/HGXD	Time gated x-ray Detector	Soft x-ray Imaging, Radiation flow
DANTE 1	Broadband, time-resolved x-ray spectrometer	Hohlraum x-ray conditions
DANTE 2	Broadband, time-resolved x-ray spectrometer	Hohlraum x-ray conditions
VIRGIL	soft x-ray spectrum	Hohlraum x-ray conditions
TARDIS	X-ray Diffraction	crystal structure
EXAFS	Edge x-ray absorption fine structure	Temperature diagnostic for shocked materials
OPSPEC	soft x-ray spectrum	opacity
FIDDLE	time resolved diffraction	crystal structure vs time
RADChem	RAGS and solid radchem (SRC), CLOVER	activated samples from implosions

HCMOS gated detectors), material behavior at ultra-high pressures with VISAR, SOP, TARDIS, EXAFS and DIFF(t).

In FY23/24 we commissioned a more sophisticated version called FIDDLE, that has more sensors with higher well depth (SNL supplied Daedalus devices). FIDDLE provided excellent data throughout 2025 and the FIDDLE team was awarded an R&D 100 award for innovative design engineering in 2025. Gated x-ray framing cameras (GXD / HGXD) continue to be used to diagnose radiation flow via plasma self-emission and x-ray streak cameras (DISC) are used to measure material equation of state

through 1D streaked x-ray radiography on both NIF and OMEGA. Material strength at high pressure has been successfully measured using point projection x-ray backlighting and simple image plate diagnostics. In the future this experiment capability will be extended to thicker samples by using ARC or OMEGA EP to drive higher x-ray energy back-lighters. These techniques will be used to diagnose metallic ablator conditions that are relevant for double shell implosion science. The data return per experiment can be increased by using gated high energy hCMOS detectors (DHEX/HEXI) to obtain multiple frames per shot. New cathode materials that are sensitive to more energetic x-rays (>15keV) will be required for these devices. R&D work is continuing on Germanium and GaAs detectors that can provide good detection efficiency for these x-ray energies.

In FY25 the newly commissioned EXAFS II spectrometers have been used to diagnose material temperatures in Copper and Zirconium samples by measuring the spectral modulations near a K or L edge in materials that have been compressed to high pressures. These spectrometers, which have been developed in collaboration with PPPL, utilize novel x-ray crystal geometries to enable high throughput with high spectral resolution. In FY24 we commissioned a new spiral crystal system to measure Zr K shell that can be used to measure EXAFS around the Pu L shell (Pu experiments planned for FY26).

With the development of volume burn platforms that utilize opaque metal shells (pushed single shells and double shells), diagnostics capable of constraining high-Z mix are needed. Since x-rays do not escape these shells all information about the stagnation phase must use nuclear techniques. Leading detection methods of mix use charged-particle radiochemical and reaction-in-flight (RIF) neutron spectral measurements. The radiochemical products must be efficiently collected and then counted to understand the levels of mix that occurred. These capabilities exist at NIF but must be regularly maintained and improved for future use. In FY25 the NIF Gaseous radchem diagnostic (RAGS) was revamped so it can be used to provide insight into mix in double shell experiments. A prompt counting facility for solid radchem diagnostics used on LANL double shell experiments was also recommissioned on the NIF facility and has been used on multiple shots in FY25.

## **V-2: Local Diagnostic Development on Z**

The development of new local diagnostic capabilities on Z is aimed at addressing gaps in our understanding across all program areas with a particular emphasis on fusion experiments. Some of the key diagnostic development activities are given below separated by program area:

- Magnetic Direct Drive ICF
  - Gamma Reaction History (GRH) (with LANL and LLNL)
  - Neutron time-of-flight (ZNTOF) (with LLNL)
  - 2D Neutron Imaging (NEMESIS) (with LLNL and LANL)

- Dynamic Materials
  - X-Ray Diffraction
  - Pyrometry
- Multi-program
  - Multi-frame x-ray radiography
  - High-spectral resolution, time-gated x-ray spectroscopy
  - X-ray streak camera (with LLNL)

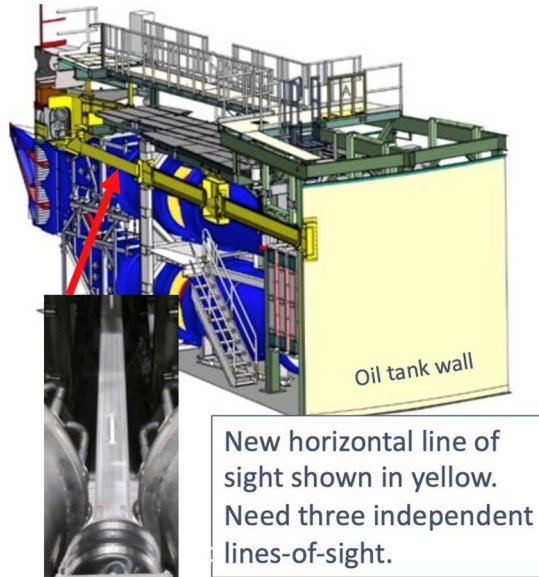
Some of these efforts are collaborations across several laboratories. As noted earlier there is a national effort to advanced diagnostics for magnetic direct drive ICF experiments on Z through a partnership with LLNL and LANL. A further emphasis on advanced neutron diagnostic was initiated in FY25. SNL kicked off the Z extended performance initiative (ZX) in FY25, which will include upgrades to the pulsed-power storage, facility, and diagnostics. The development of four key diagnostics will be accelerated to meet a FY29 completion date.

1. Gamma Reaction History (GRH)
2. ZnTOF
3. 2D neutron imaging (NEMESIS)
4. Multi-frame backlighting

Table 5 shows the present estimates of the timeline for development of the local diagnostics on Z. Not included in this table is a new facility infrastructure that will allow an equatorial view of imploding targets from distances greater than 3 meters. The transport section will extend through the water and oil sections of Z which will provide great neutron collimation for future nuclear diagnostics. Facility modifications were made in FY25 to enable the first ZnTOF line-of-sight at the 140 degree position. See the image below of the new line-of-sight and a picture of the tube installed in the water section.

Local Z Diagnostics	FY25	FY26	FY27	FY28	FY29	FY30
X-ray Diffraction (pulsed-power x-ray source)		Src. Dev.				
High-Res. X-ray Spectrometer (MONSSTR)	IV2		DV2	Tiled DV2	GaAs	
Multi-frame Backlighting		4-frame	7-frame			
Gamma Reaction History		Design	Build/Test		Comm.	
X-ray streak camera (SCORPIONZ)	Install	Comm.				
ZnTOF		Comm. 140	2nd line		3rd line	
2D Neutron Imager (NEMESIS)	Final Design		1st Line		2nd line	Gated

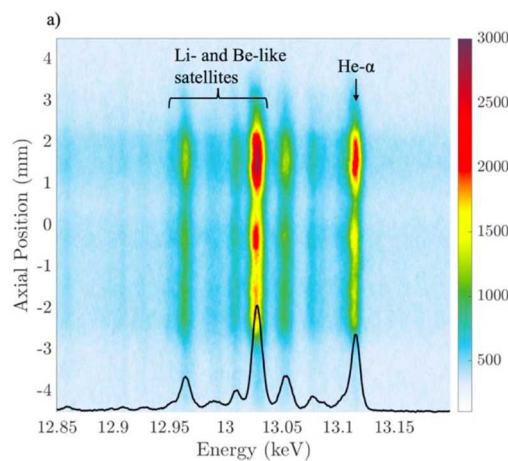
*This table shows the estimated timelines for the local diagnostic effort on Z.*



*Cutway of the Z water and oil sections. The yellow-colored tubes will provide a pathway for neutrons to exit the machine along the equatorial plane. They can then be diagnosed with the ZnTOF, GRH, or NEMESIS diagnostics.*

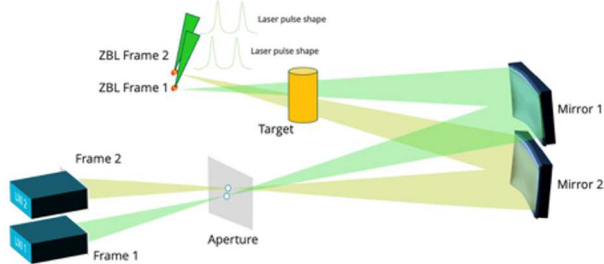
Here is a brief description of the local diagnostic capabilities being developed at Z and their applications:

**MONSSTR:** Multi-Optic Novel Spherical Spectrometer with Time Resolution is a time gated in-chamber spectrometer being developed to diagnose the evolution of mix in ICF experiments. Future plans include integrating tiled Daedalus sensors to increase the spectral range. Recording of Kr K-shell spectra from fusion experiments is enabling important pressure measurements and estimates of RKE. A example of Kr emission is shown below.



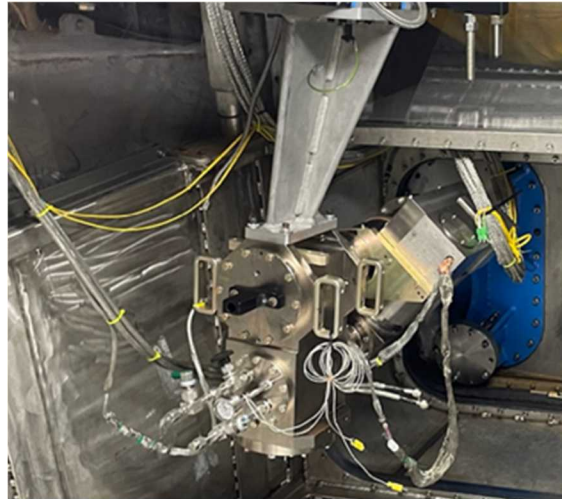
*Kr K-shell spectrum from MagLIF shot z4178, showing the Kr He-resonance and satellite lines. Date courtesy Jeff Fein and Kathy Chandler (SNL).*

**Multi-Frame Crystal Backlighting:** This is a spherical crystal backlighter coupled to an hCMOS camera with multiple laser pulses to enable multi-frame capabilities. By using the Icarus sensor we are working to obtain up to seven frames of data in a single shot. Radiography is a primary driver for abuttment of multiple hCMOS sensors to create a larger detector area. Backlighting is used for HED and ICF experiments on over 50 shots/year.



*Cartoon illustrating the operation of the four frame crystal backlighter. By adding more pulses, this technique can likely be extended 5 to 7 frames.*

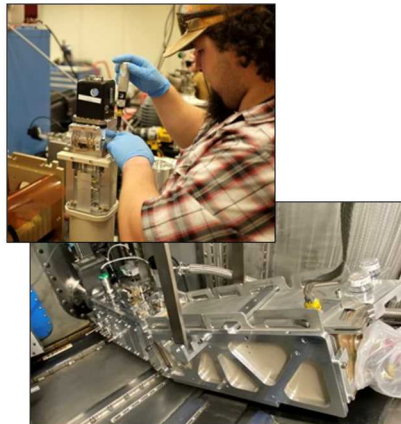
**GRH:** This is a gamma reaction history diagnostic to measure the time-history of the DT fusion production in MDD-ICF (requires ~1% tritium on Z). The conceptual development a new GRH specifically design for the Z-environment is underway. An unfolded design is being investigated. Initial deployment of the GRH on loan from Omega, revealed important differences between the laser and pulse power environments. See the image below of the current GRH installed on Z.



*GRH installed installed on Z.*

**SCORPIONZ, X-Ray Streak Camera** – Streak Camera Observatory for Radial or Polar Implosions ON Z (SCORPIONZ). Enables much faster temporal response to better resolve the target x-ray emission. The diagnostic will be commissioned in FY26, and will be used to record the x-rays from ICF and radiation producing

experiments. Steaked spectroscopy is a future advancement that may be considered after commissioning. The pictures below show the x-ray streak camera installed on Z.



*Top: LLNL technologist working on the SCOPRIONZ x-ray streak camera at SNL. Bottom: Full SCOPRIONZ assembly installed on Z.*

**ZNTOF** – Developing an advanced nTOF system that will use up to three-equatorial line of sight. One line-of-sight at 140 degrees will be commissioned in FY26. This is being developed to measure  $T_{ion}$  in fusing DD and DT plasmas.

**2-D Neutron Imager:** This is a time-integrating 2-D neutron imager optimized for primary DT neutrons from the stagnation in MDD-ICF. This diagnostic is known as NEMESIS. Other novel techniques for large field-of-view imaging are being explored. The primary purpose is to measure the volume and shape of the fusing plasma in ICF experiments.

**X-Ray Diffraction** – Measure the phase dynamics of compressed materials for materials research using a flyer-plate driven target sample. In FY25, the experimental platform abandoned laser-driven x-ray sources and is now investigating a pulsed-power source that will be compatible with containment.

### **Local Diagnostic Effort on OMEGA**

**Introduction:** Scientific advances in High Energy Density (HED) physics are realized with an innovative research and development program of visible, ultraviolet, x-ray, gamma ray, nuclear, and particle diagnostics. Inertial Confinement Fusion (ICF) and the pursuit of ignition has been a major driver for diagnostic development for decades and this has driven many advances in diagnostics that are now being used in the wider HED community. The development of many diagnostics for Laser Indirect Drive (LID), Magnetic Direct Drive (MDD) and Laser Direct Drive (LDD) on the National Ignition Facility (NIF) often starts with a prototype demonstration on the Omega Laser Facility. There is also strong constructive collaboration between diagnostic groups at the major HED facilities:

OMEGA, Z and NIF. It is coordinated through quarterly meetings of the Leadership Team for the National Diagnostics Working Group, of which LLE is an active participant.

The Omega Laser Facility is used to develop diagnostics for the three ignition approaches in ICF and HED experiments. LDD ICF implosions and focused HED experiments on OMEGA are diagnosed to understand fundamental target physics. Diagnostic development for LDD on OMEGA supports the strategic goals identified in Sections 5.1 and 5.7 of the HED&IS 10-year plan, that is supporting the delivery and measurement of laser-plasma instability thresholds with high-bandwidth laser drivers (FLUX) and determining the limits to implosion efficiency (X) on OMEGA. For ICF the key target physics areas for each of the four phases of an LDD implosion—initial plasma formation, acceleration phase, deceleration phase, and stagnation—are highlighted in Fig. 19, including laser drive uniformity, laser imprint, laser-plasma instabilities, energy coupling, shock propagation, hydrodynamic instabilities, hot-electron preheat, multidimensional effects on hot-spot formation, and residual kinetic energy. A multi-year research and development effort is being conducted for 3-D (i.e., having three or more diagnostic lines of sight) x-ray and nuclear diagnostics to study multidimensional effects on LDD implosions during all phases of the implosion. The development of primary diagnostics, including the accuracy and precision requirements, are derived from the fundamental target physics needs. In addition, the high shot rate on OMEGA and OMEGA EP is exploited to develop LID and MDD diagnostics for NIF and Z, respectively.

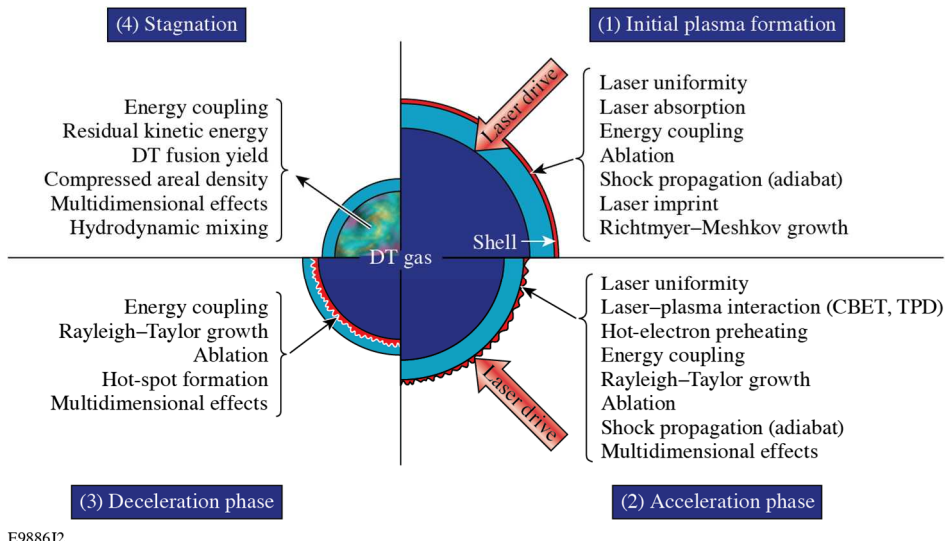


**Figure 19. The key target physics areas for each of the four phases of an LDD implosion**

The primary diagnostics associated with the key target physics of the initial plasma formation and the acceleration phase of an LDD implosion are listed in Table 1. Many synergies were realized with the VISAR diagnostic, which is used by all three approaches. Diagnostics developed for NIF on OMEGA are highlighted with an asterisk.

Target physics area	Diagnostic and measurement
---------------------	----------------------------

Laser Uniformity	Full-beam in-tank diagnostic (records the spatial distribution of UV far-field fluence inside the OMEGA target chamber) [1] X-ray target plane (infers the spatial distribution of UV far-field fluence from x-ray spots recorded on target) [2] Fixed x-ray pinhole cameras for beam pointing [3] Laser power balance measurement [4] Ultraviolet equivalent target plane [5]
Laser Absorption	Full-aperture backscatter station for time-resolved scattered light spectroscopy [6] Scattered Light Uniformity Imager (SLUI)
Ablation/Shock Propagation/adiabat	1-D VISAR (velocity interferometer system for any reflector) [7]* Refraction-enhanced X-ray radiography [8] X-ray Thomson Scattering [9] X-ray Talbot-Lau deflectometry [10]
Laser Imprint/Richtmyer–Meshkov Growth	OHVR (2-D VISAR) [11]* Through-foil x-ray radiography [12]
Laser Plasma Instabilities	Full-aperture backscatter station for time-resolved scattered light spectroscopy [6] 3/2 $\omega$ time- and space-resolved imagers [13] 2 $\omega$ and 4 $\omega$ (5 $\omega$ in future) optical Thomson scattering [14]* 4 $\omega$ interferometry [15] and angular filter refractometry [16] TOP9 beam and transmitted-beam diagnostic [17] Angularly-Resolved Thomson Scattering for electron distribution functions [18] Hard x-ray diagnostic [19]
Energy Coupling	Shell trajectory measurements using x-ray framing cameras (XRFC) [20]
Rayleigh–Taylor Growth	Through-foil x-ray radiography using Fresnel Zone Plates [21]
Multidimensional Effects	3-D in-flight ablation surface measurement using XRFC [22]

**Table 1. LDD key target physics areas and diagnostics for the initial plasma formation and acceleration phase.** \*These diagnostics were developed on OMEGA for NIF through collaborative efforts amongst scientists and engineers from LLE, LLNL, LANL, SNL, MIT, Kentech and the NDWG.

The primary diagnostics associated with the key target physics of the deceleration phase and stagnation of an LDD implosion are listed in Table 2. Diagnostics developed for NIF on OMEGA are highlighted with an asterisk.

Target physics area	Diagnostic and measurement
Hot-spot formation/ Multidimensional Effects / Hot-spot flow velocity	3-D gated x-ray imaging of hot spot [23] 16 channel gated Kirkpatrick–Baez microscope [24] Single line-of-sight time-resolved x-ray imager (SLOS-TRXI) [25]* 3-D neutron time-of-flight (nTOF) detectors [26]* Neutron imaging [27]* Penumbra imaging of knock-on deuterons (KoDI) [28] X-ray backlighting with monochromatic crystal imager at 1.86 keV [29] Spec $T_e$ [30] or x-ray penumbral imager [31] particle X-ray temporal diagnostic (PXTD) to diagnose hot-spot $T_e$ [32] High-resolution X-ray spectroscopy [33]*
Hydrodynamic Mixing	X-ray spectroscopy of high-Z dopants [34]* X-ray backlighting with monochromatic crystal imager [29] Comparison of absolute x-ray continuum emission (Spec $T_e$ ) and neutron yield from hot spot [35]
Fusion Yield	nTOF detectors (yield, $T_i$ ) [26]*, [36]* Cu activation detector [37] Neutron bang time and burn rate [38] PXTD [32]

Compressed areal density	Charged-particle spectrometer [39] Neutron spectroscopy via nTOF detectors in shielded and collimated diagnostic lines of sight [40] and magnetic recoil spectrometer [41]* X-ray backlighting with monochromatic crystal imager at 1.86 keV [30] Compton Radiography [42]* KoDI [28]
--------------------------	---

**Table 2. LDD key target physics areas and diagnostics for the deceleration phase and stagnation.**

\*These diagnostics were developed on OMEGA for NIF through collaborative efforts amongst scientists and engineers from LLE, LLNL, LANL, SNL, MIT, GA, Kentech, Sydor Technologies, and the NDWG.

In support of high energy density physics experiments conducted on the Omega Laser Facility, the National Ignition Facility, and advanced light sources, LLE pursues diagnostic developments for the following research thrusts: studying fundamental high energy density physics (i.e., equation of state, opacity, conductivity, stopping power, and viscosity), developing innovative diagnostic techniques for HEDP (e.g., THz spectroscopy, Raman Spectroscopy, streaked optical pyrometry spectrometers, high-resolution x-ray spectroscopy, and superconducting superfluid detection), and the development and application of probes for HEDP (e.g., THz radiation, X rays, Hard X rays,  $\gamma$ -rays, and particle beams). The OMEGA EP PW laser, like Z-beamlet and ARC, is combined with OMEGA to develop advanced x-ray and particle probe sources for HED plasma research. The primary diagnostics associated with high energy density physics experiments conducted at OMEGA are listed in Table 3. Diagnostics developed for NIF on OMEGA are highlighted with an asterisk.

Target physics area	Diagnostic and measurement
Equation of state	1-D VISAR (velocity interferometer system for any reflector) [7]
Opacity	X-ray spectroscopy of high-Z dopants [34]* X-ray backlighting with monochromatic crystal imager [29] High-Resolution Spectroscopy [33]* Imaging X-ray Thomson Scattering [43]
Conductivity	Streaked Optical Pyrometry [44] Streaked Spectral Pyrometry [45]
DC conductivity, phonon states, molecular structure	THz spectroscopy [46]
Stopping Power	Charged Particle Spectrometer [39]* Wedge Range Filter Module [47]* Magnet Recoil Spectrometer [41]*
Viscosity	1-D VISAR (velocity interferometer system for any reflector) [7]
Long-range Ordering	Powder X-ray Diffraction Image Plate (PXRDIP)* [48]

**Table 3. HED key target physics areas and diagnostics.** \*These diagnostics were developed on OMEGA for NIF through collaborative efforts amongst scientists and engineers from LLE, LLNL, LANL, SNL, MIT, GA, Kentech, Sydor Technologies, and the NDWG.

Progress in FY25: In FY25 several research and development efforts for diagnostics on the Omega Laser Facility were performed. They are summarized in the table shown in Table 4. Some of them involved collaborations with members of the NDWG from LLNL, SNL, MIT, Sydor, GA, and Kentech. Sustainment activities included finding a replacement sensor for the obsolete Charge Injection Device (CID) detectors and the replacement of the two Active Shock Break Out (ASBO) laser systems for OMEGA and OMEGA EP. Novel diagnostic development includes the the OMEGA X-ray Hot-Spot

Imager (XRHSI), simultaneous VISAR and X-ray Radiography on OMEGA EP, a Raman spectroscopy capability for HED samples on OMEGA, and the development of a  $4\pi$  averaged compressed areal density diagnostic.

Diagnostic	Status	Collaborating Lab
Active Shock Break Out (1-D VISAR)	Two new diode pumped solid-state laser systems have been delivered and are in the process of being installed on the OMEGA and OMEGA EP laser facilities. Qualification of these systems began in Q1FY25.	LLNL
CryoPXTD*	New scintillator array developed to simultaneously record DT-neutrons, two x-ray channels and D-3He protons to assess kinetic effects in implosions.	MIT
Long Term replacement for X-ray Pinhole camera detectors*	Prototype replacement system has been procured ride-along experiments were conducted in FY25.	SNL, Sydor
$4\pi$ pR (3-Dimensional nTOF) [49]*	Collaboration with Imperial College on MCNP simulations to determine most effective locations of additional required collimated lines-of-sight. LLE held internal workshop to refine the analysis techniques and compare different diagnostic modalities (e.g. NTOF, MRS) for assessment pR.	LLNL, Imperial
OMEGA X-ray Hot Spot-Imager (XRHSI) [50]	A multi-meter drift tube will be fabricated by General Atomics. Integration onto OMEGA chamber is expected FY25-26.	LLNL, SNL, GA, Kentech, Sydor
3-D reconstruction of hot-spot formation [23]	Novel 3-D reconstruction algorithms using hot-spot x-ray images recorded along three or four diagnostic lines of sight have been developed. Low-mode reconstructions of the hot-spot are being studied.	LANL, LLNL
Raman Spectroscopy on OMEGA [51]	Raman spectroscopy to directly measure, for the first time, novel chemistry phenomena at HED pressures, crystallographic structure of low Z materials, and temperatures lower than what is accessible to streaked optical pyrometry.	LLNL
Simultaneous VISAR and X-ray Radiography on EP	A new optical transport has been designed to enable face-on, short-pulse x-ray radiography in tandem with VISAR particle velocity measurements on OMEGA EP. This capability has been activated in Q4 FY24.	LLE, LLNL

**Table 4. Local Diagnostic Projects underway and proposed at OMEGA.** \*These diagnostics were developed on the Omega Laser Facility through collaborative efforts amongst scientists and engineers within the NDWG from LLE, LLNL, LANL, SNL, MIT, GA, Kentech, and Sydor Technologies.

Diagnostic Name	Diagnostic Status	Lead Lab	Diagnostic description
-----------------	-------------------	----------	------------------------

Omega High Resolution Velocimeter (OHRV)	Operationally Qualified	LLE/LLNL	Operationally qualified and operated on two OMEGA shot days in FY24. LLNL supplied a new laser front end integrated into the OMEGA laser bay. LLNL and LLE are working to transfer operations, specialist, and data analysis responsibilities onto LLE staff. LLE invested in diagnostic enclosure upgrades in FY25 to enhance reliability and effectiveness of the diagnostic recording system.
Multi-frame Zoneplate Imager	Operationally Qualified	LLE	A system consisting of an hCMOS sensor on OMEGA coupled to a Fresnel zone plate imaging system. LLE is collaborating with SNL on fielding the hCMOS on the Fresnel Zone Plate imager to achieve ns-resolution for hydrodynamic instability experiments.
Full Aperture Backscatter-P9	Operationally Qualified	LLE	Refurbishment project of the OMEGA backscatter station. New spectrometers were procured in FY23 and two ROSS streak camera systems were upgraded with optical calibration modules to integrate with the new spectrometers. In FY24 the project to integrate the streak cameras into OMEGA was completed.
Time-resolved X-ray Diffraction	Operationally Qualified	LLE	This project combines the powder X-ray diffraction platform with a framing camera to provide time resolution to x-ray diffraction measurements on OMEGA EP experiments.
Spectroscopy Resolved Streaked Optical Pyrometer	Operationally Qualified	LLE	With the addition of spectral resolution, the proposed SOP-Spec will be capable of measuring temperature down to 3000K, and wavelength dependent emissivity and reflectivity of compressed materials in the ~400-850 nm range with ~100 ps temporal resolution.
Phoswitch Detector	Operationally Qualified	LLE / Houghton College / SUNY Geneseo	The phoswitch detector captures reaction products and detects their decays over (10-1000 ms) using a reaction medium and photomultiplier tube with a scintillation layer sandwiched between. This technique allows in-situ measurement for samples with half-lives too short to allow retrieval and counting in a standard activation platform.
Angular Thomson Scattering	Operationally Qualified	LLE	A novel Thomson-scattering diagnostic allowing a large number of plasma frequencies to be probed simultaneously by utilizing a very large (120°) collection aperture.[52]

**Table 5. Diagnostics qualified on the Omega Laser Facility in FY24. The diagnostic name, diagnostic status, lead lab, and diagnostic description are listed in the table.**

In FY25 a number of novel local diagnostics were qualified and utilized on the Omega Laser Facility. They are listed in the table shown in Table 5 along with the diagnostic

status, lead lab, and diagnostic description. Several notable qualification experiments with their data follow below.

## UV-Raman Spectroscopy

A single-shot, nanosecond-scale Raman spectrometer is being developed for the OMEGA Laser System at the Laboratory for Laser Energetics. Raman scattering is an incredibly weak inelastic scattering process – about 1 in 10 million photons will Raman scatter. Spectrally resolving Raman scattered light provides detailed information on the structure, bond character, and temperature of materials without relying on that material’s ability to scatter x-rays. This technique is routinely implemented over longer time scales; however, the short time scales of laser-driven experiments make diagnostic design for a Raman spectrometer on a laser facility a challenge. Laser-compressed materials are probed with 1-10 mJ of a 5-ns, 266-nm laser, taking advantage of the  $1/\lambda^4$  factor in Raman intensity to produce enough signal for a measurement. The resulting Raman scattered light is spectrally resolved with 0.2 nm of spectral resolution over a 10 nm window. The implementation of Raman spectroscopy on a large-scale laser facility fills a critical gap in measurement capabilities at high energy-density conditions.

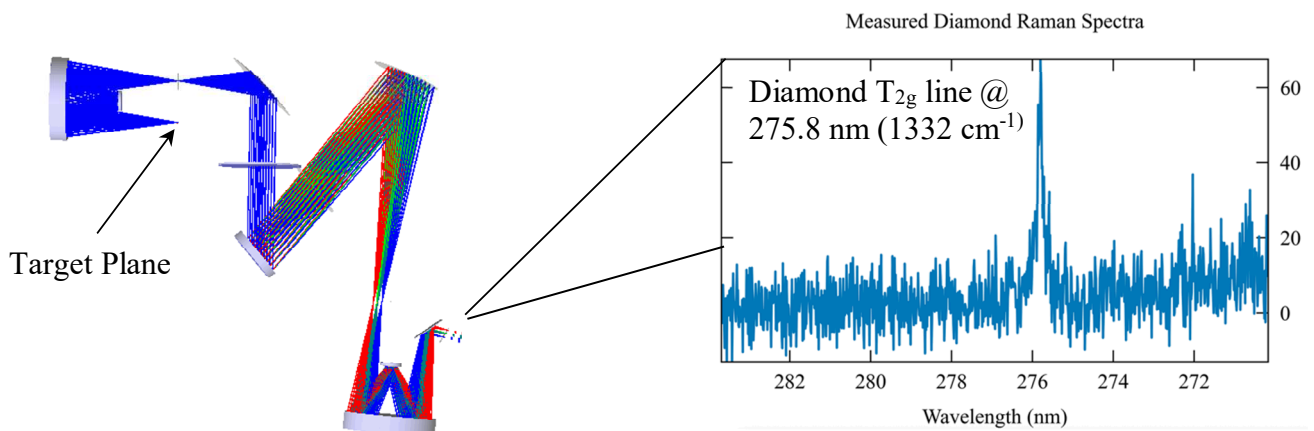


Fig 20. Development of the OMEGA Raman Spectrometer is based off an offline prototype (left). Initial experiments demonstrate single-shot, nanosecond-scale Raman spectra from a diamond target. Peak in the spectra comes from triply degenerate optical phonon mode (T<sub>2g</sub>) expected of ambient diamond located at 1332 cm<sup>-1</sup> or 275.8 nm (right)

## Time-resolved Diffraction

The first time-resolved diffraction measurements on OMEGA EP were made during the TRXRDEP-23A campaign. Principal Investigators D. Polsin, LLE, and L. R. Benedetti, LLNL, added an x-ray framing camera to the powder x-ray diffraction image-plate diagnostic (PXRDIP) and recorded the body-centered cubic to hexagonal close-packed

(bcc-to-hcp) phase transition in shocked iron. The time-resolved x-ray diffraction (XRD) measurements utilizing a 6.7-keV, 1.25-ns x-ray backlighter captured the unshocked (pure bcc), shock transit (mixed bcc and hcp phase), and shock breakout on a shot-by-shot basis [53].

The figure shows the XRD data captured on the four-strip x-ray framing camera surrounded by image plates. The framing camera strips (each with a temporal resolution of 400 ps) are in the center of each image and spatially aligned with the time-integrated image-plate data. The growth of the high-pressure hcp phase of iron out of the ambient bcc phase can be seen from left to right as the shock enters the iron (left-hand panel) and at shock breakout (right-hand panel). Acquiring high-quality and high-temporal-resolution data required mitigating sources of x-ray fluorescence in the x-ray framing camera and blocking direct lines of sight from the x-ray backlighter to the detector. This campaign represents a significant milestone in the development of an experimental platform to collect time-resolved x-ray diffraction measurements on a single laser shot.

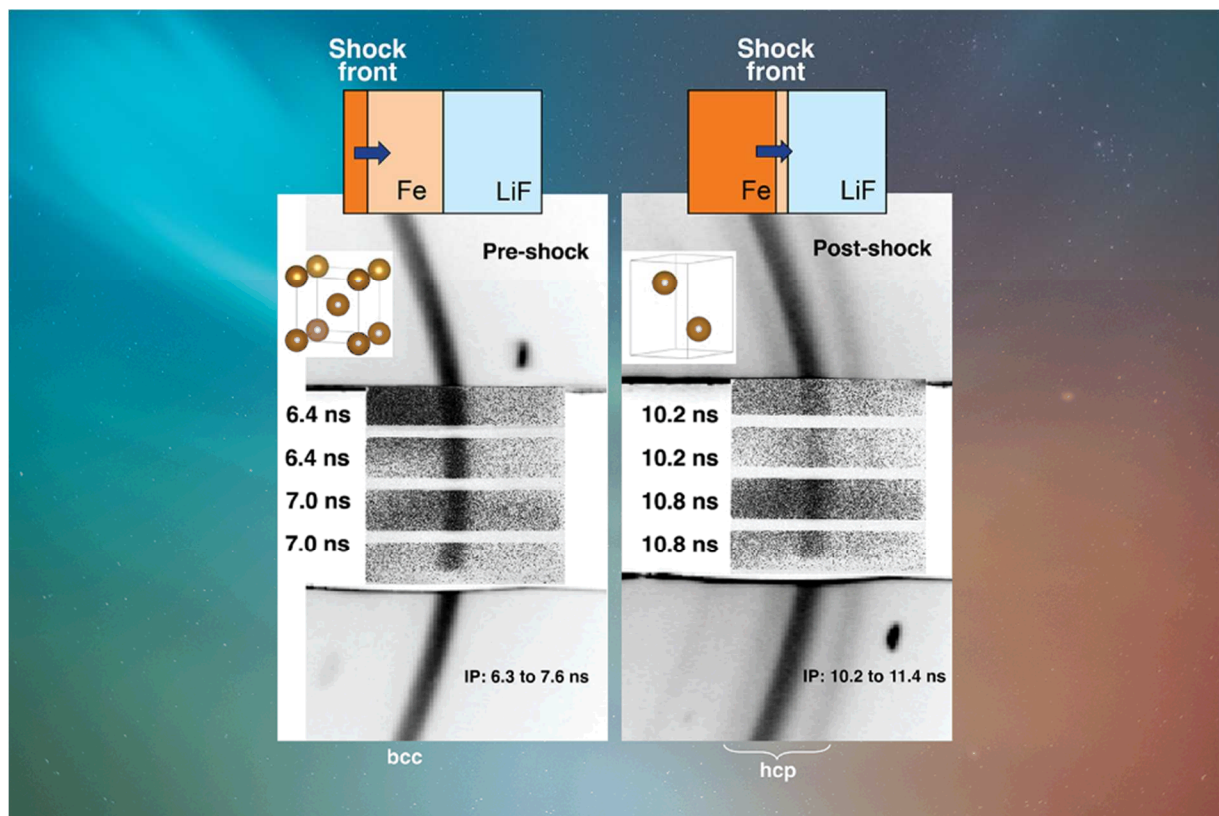
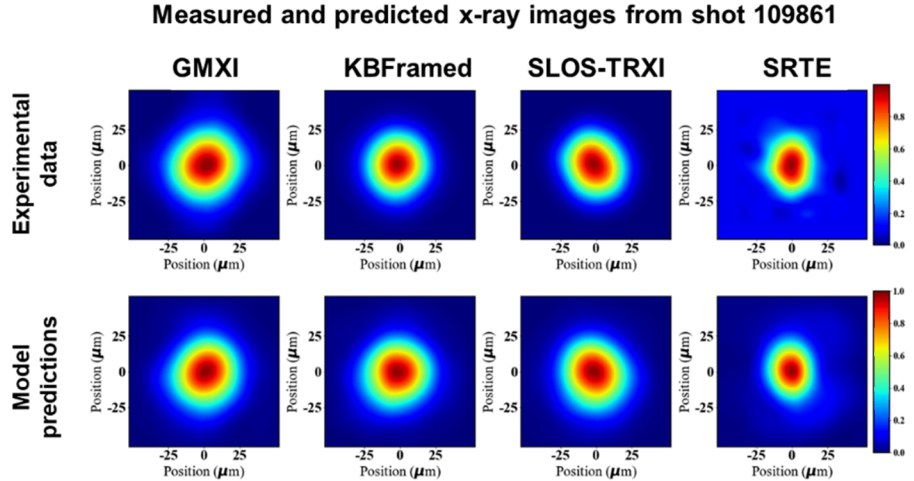


Figure 21. X-ray diffraction data showing the time-dependent transformation from bcc (right) to hcp (left) crystal structure in compressed iron as a shock passes through the sampled material.

## X-ray Hot Spot Imaging

A deep-learning convolutional neural network (CNN) has been used to infer the low-mode shape of the hot-spot emission of deuterium–tritium (DT) laser-direct-drive

cryogenic implosions on OMEGA [54,55]. The CNN was trained on a 3D radiation-hydrodynamic simulation database to relate 2D x-ray images to 3D emissivity at stagnation. The CNN accounts for the lack of an absolute spatial reference and the different bands of photon energies in the x-ray images. Previous work [26] has studied the effect of mode-1 asymmetries on implosion performance using nuclear diagnostics. The present work focuses on the effect of mode 2 inferred with x-ray diagnostics on implosion performance. A current analysis of 19 DT cryogenic implosions indicates there is a weak dependence of implosion performance on  $\bar{\omega}$  amplitude for  $\bar{\omega}$  and the mode 1 has a stronger effect on implosion performance, which is supported by 2D simulations. Figure 22 shows the result of multiple time-integrated x-ray images obtained on an OMEGA implosion shot (top) compared against a three dimensional reconstructed twin images. A contour rendering of the reconstructed emissivity model used to generate Figure 22 is shown in Figure 23.



**Fig. 22.** The measured and predicted x-ray images for implosion 109861. (a) The measured x ray data from each diagnostic and (b) the projections of the reconstructed 3D hot-spot emission. The projections of the reconstructed emission are in good agreement with the measured data.

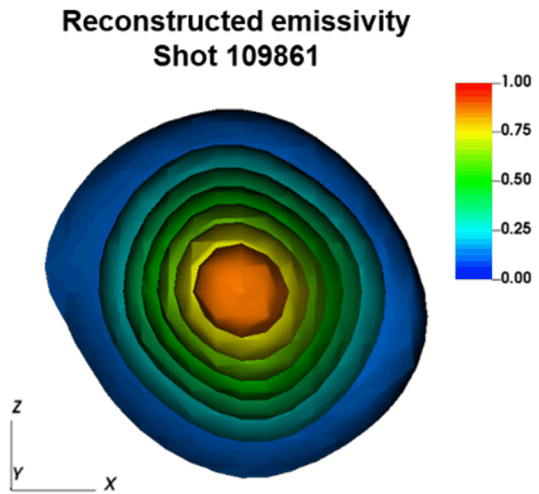


**Fig. 23.** The reconstructed emissivity for implosion 109861, shown as a 3-D contour plot.

## Nuclear Reaction Product Detection

The nuclear science community has an increased interest in the structure of light nuclei and their interactions at energies approaching 1 MeV. Many of these reactions have been previously measured in this energy range using accelerators; however, experimental results disagree and have large uncertainties. In addition, several of these product half-lives are too short (100-ms to 10 s) for removing samples and conducting activation measurements. Therefore, a technique using target normal sheath acceleration (TNSA) was developed on the Multi-Terawatt (MTW) laser to measure light-ion reactions at MeV energies that allows access to these short-lived half-lives. A successful measurement from a joint MTW experimental campaign between SUNY Geneseo, Houghton University, and LLE took place using the Houghton–Geneseo short-lived isotope counting system and the Geneseo particle time-of-flight detector. This Phoswich detector is designed to detect low-intensity, low-energy beta particles efficiently in a higher-energy ambient background. For this design, there is a combination of scintillators with dissimilar pulse shape characteristics optically coupled to each other and to a common photomultiplier tube(s). Pulse-shape analysis distinguishes the signals from the two scintillators, identifying in which scintillator the event occurred. The reaction was used to show that the proof-of-principle was  ${}^7\text{Li}(\text{d},\text{p}){}^8\text{Li}$ , for which the  ${}^8\text{Li}$  product has a half-life of 840 ms that was measured to well within the accepted uncertainty from past measurements. The nextstep in development is to field this detector on OMEGA to diagnose the  ${}^7\text{Li}(\text{t},\alpha){}^6\text{He}^*$  reaction.

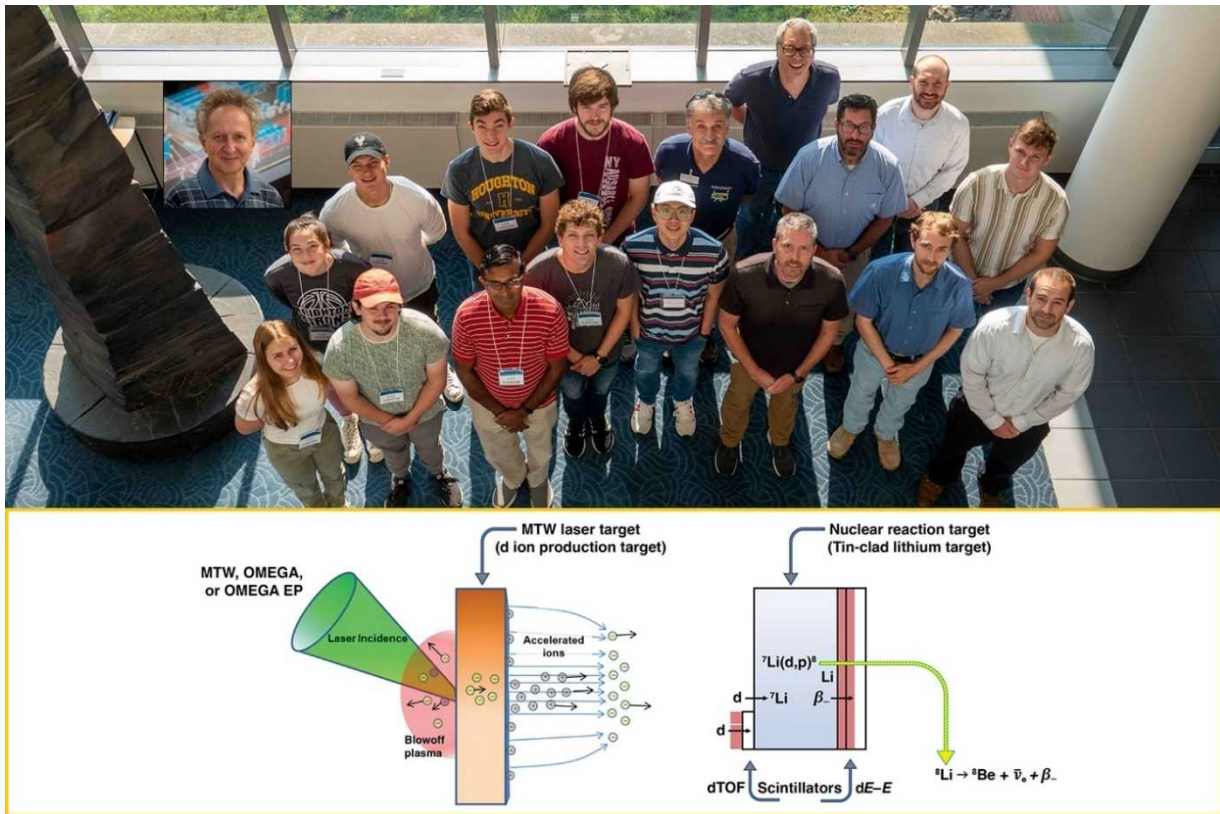
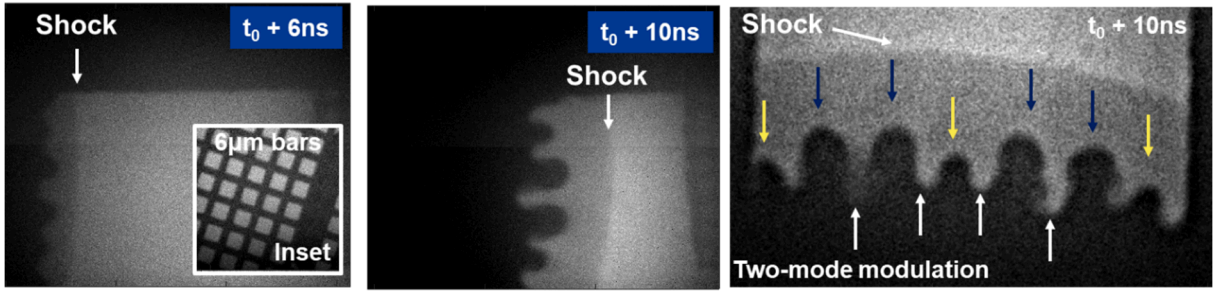


Figure 24. The MTW- Phosswitch experimental team was a collaboration between undergraduates and faculty at SUNY Geneseo, Houghton College and LLE. A schematic of the experimental set-up and phosswitch detector is shown below.

## High-resolution X-ray Imaging

In collaboration with LLNL and SNL, LLE has successfully developed and implemented an hCMOS sensor on OMEGA coupled to a Fresnel zone plate imaging system. [56] Figure 25 shows two successive radiographs measured 4-ns apart where the Rayleigh-Taylor growth of a blast-wave-driven, two-mode interface between a plastic pusher and a low-density foam was observed on a single shot with a temporal resolution of  $\sim 100$  ps and a spatial resolution of a few microns. Target development activity was carried out in collaboration with the University of Michigan and SciTech. This is a unique demonstration of coupling an hCMOS detector to a Fresnel zone plate radiography platform in a high-energy density environment by another successful multi-institutional collaboration.



**Figure 25.** Evolution of shock-driven blast waves and Rayleigh-Taylor bubble growth recorded using the Multiframe Zoneplate Imager Diagnostic. Two-mode sinusoidal modulations were imposed between the plastic pusher and low-density foam in which the instability was observed to grow.

## Spectral Pyrometry on OMEGA EP

LLE successfully carried out a preliminary qualification shot day on OMEGA EP for the SOP-Spec diagnostic, where the team measured spatially-integrated, time and spectrally-resolved, broadband pyrometry measurements from laser-driven quartz, fused silica, and diamond targets at a variety drive conditions. A representative streaked spectra obtained from the driven diamond target is shown in the Figure 26. Broadband pyrometry will enable improved temperature measurements without reliance on the grey-body model and at lower temperatures. The diagnostic will enable additional advancements in understanding emissivity and absorptivity of ramp-compressed HED materials.

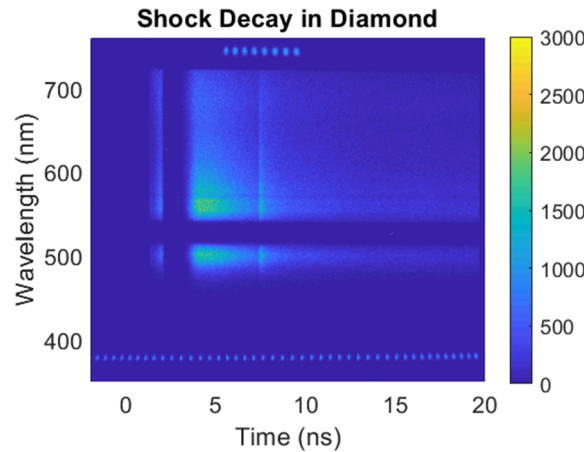


**Figure 26.** Streaked spectrum obtained from the SOP-Spectrometer instrument.

## Multi-ion Detection with the Particle and X-ray Temporal Diagnostic (PXTD)

A new four-channel scintillator for the CryoPXTD instrument was fielded on a qualification campaign on OMEGA [57], focusing on multi-ion and other kinetic effects

in thick-shell hoppe glass implosions. The experiments observe the D-<sub>3</sub>He protons, DD-neutrons, DT-neutrons and x-ray temporal evolution with individually filtered channels. Data obtained from the CryoPXTD streak camera are shown in the left panel of Figure 27 and the summed channel signals are plotted against emission time in the right panel.

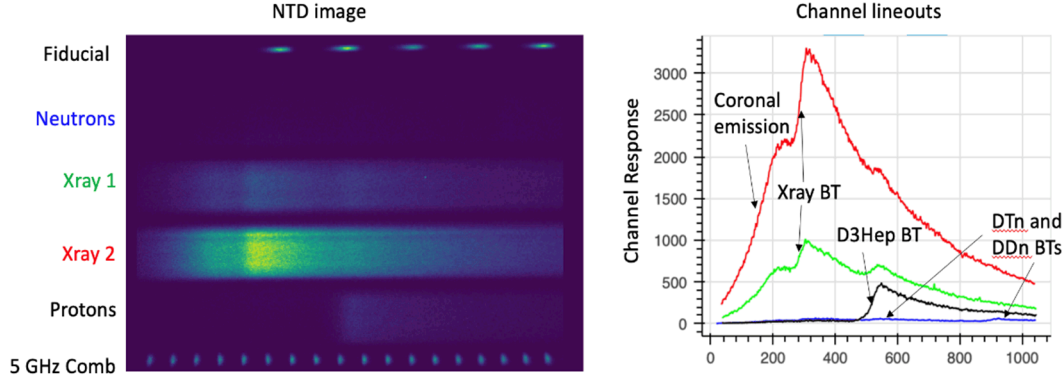


**Figure 27.** Data obtained on OMEGA campaign MULTIIION-23A in support of qualification of the CryoPXTD diagnostic. The four-channel streaked image shows the ability to simultaneously record implosion generated D-<sub>3</sub>He protons, DT-neutrons and X-rays within the streak camera's dynamic range for a single shot.

## References

- [1] L. J. Waxer et al., Proc. SPIE 10898, 108980F (2019).
- [2] W. Theobald et al., RSI 91, 023505 (2020).
- [3] R. Forties and F.J. Marshall, RSI 76, 073505 (2005).
- [4] S. Sampat et al., Applied Optics 57, 9571 (2018).
- [5] S. P. Regan et al., JOSA B 17, 1883 (2000).
- [6] W. Seka et al., POP 15, 056312 (2008).
- [7] P. Celliers et al., RSI 75, 4916 (2004).
- [8] A. Kar et al., POP 26, 032705 (2019).
- [9] S. P. Regan et al. PRL 109, 265003 (2012).
- [10] M. P. Valdivia et al., Appl. Opt. 57, 138 (2018).
- [11] P. Celliers et al., RSI 81, 035101 (2010); Peebles et al., PRE 99, 063208 (2019).
- [12] V. Smalyuk et al., PRL 81, 5342 (1998).
- [13] W. Seka et al., PRL 112, 145001 (2012).
- [14] I.A. Begishev et al., Optics Letters 43, 2462 (2018).
- [15] A. Howard et al., Rev. Sci. Instrum. 89, 10B107 (2018).
- [16] D. Haberberger et al., Phys. Plasmas 21, 056304 (2014).
- [17] D. Turnbull et al., Nature Physics 16, 181 (2020).
- [18] A.L. Milder et al. POP 26, 022711 (2019).
- [19] W. Stoeckl et al., RSI 92, 1197 (2001).
- [20] P. Michel et al., RSI 83, 10E530 (2012).
- [21] F.J. Marshall et al. submitted for publication.
- [22] P. Michel et al., PRL 120, 125001 (2018).
- [23] K. Churnetski et al., RSI 93, 093530 (2022).
- [24] F.J. Marshall et al., Rev. Sci. Instrum. 88, 093702 (2017).
- [25] W. Theobald et al., RSI 89, 10G117 (2018).

- [26] O.M. Mannion et al., Nucl. Instrum. Methods Phys. Res. Sect. A 964, 163774 (2020); O. M. Mannion et al., Rev. Sci. Instrum. 92, 033529 (2021); O. M. Mannion et al., Phys. Plasmas 28, 042701 (2021).
- [27] C.R. Danly et al., RSI 86, 043503 (2015).
- [28] H. Rinderknecht et al., RSI 93, 093507 (2022); J. Kunimune et al., Phys. Plasmas 29, 072711 (2022).
- [29] W. Stoeckl et al., POP 24, 056304 (2017).
- [30] D. Cao et al., POP 26, 082709 (2019).
- [31] P. Adrian et al., RSI 92, 043548 (2021).
- [32] H. Sio et al., RSI 87, 11D701 (2017).
- [33] P. Nilson et al., RSI 87, 11D504 (2016).
- [34] S.P. Regan et al., PRL 111, 045001 (2013).
- [35] T. Ma et al., PRL 111, 085004 (2013); Epstein et al., Phys. Plasmas 22, 022707 (2015).
- [36] V. Yu. Glebov et al., RSI 81, 10D325 (2010).
- [37] O. Landoas et al., RSI 82, 073501 (2011).
- [38] W. Stoeckl et al., RSI 87, 053501 (2016).
- [39] C.K. Li et al., POP 8, 4902 (2001).
- [40] C. Forrest et al., RSI 83, 10D919 (2012).
- [41] J. A. Frenje et al., Phys. Plasmas 17, 056311 (2010).
- [42] R. Tomassini et al., Phys. Plasmas 18, 056309 (2011).
- [43] E. J. Gamboa et al., RSI 83, 10E108 (2012).
- [44] J. E. Miller et al., RSI 78, 034903 (2007).
- [45] N. Kabadi et al., APS DPP 2022.
- [46] G. Bruhaug et al., RSI 93, 123502 (2022).
- [47] F. H. Seguin et al., RSI 83, 10D908 (2012).
- [48] J. R. Rygg et al., RSI 83, 113904 (2012).
- [49] C.J. Forrest et al., RSI 93, 103505 (2022).
- [50] S. T. Ivancic et al., RSI 93, 113521 (2022).
- [51] A. LaPierre et al., APS DPP 2022.
- [52] J. Katz et al., RSI 95, 093513 (2024).
- [53] D. Polsin et al., RSI 96 063510 (2025).
- [54] K. Churnetski et al., RSI 95, 103521 (2024).
- [55] K. Woo et al., Phys. Rev. Research 7, 023272 (2025).
- [56] P. Nilson et al., Phys. Plasmas 32, 082705 (2025).
- [57] N. Kabadi et al., RSI 93 103538 (2022).

## Appendix:

**Scattered light diagnostic for direct drive (DD) - five systems:** Scattered light diagnostic to measure angular distribution of scattered laser light principally from Direct Drive laser illumination experiments on NIF.

**Upgrade DISC:** The existing DIM Insertable Streak Camera (DISC) will be upgraded with improved electron optics to improve the spatial resolution over the whole 24mm active area of the cathode. The microchannel plate fiber optic detector will also be replaced with a direct electron detection CMOS detector.

**CBI:** Crystal Backlit Imaging; this diagnostic uses spherical Bragg crystals to provide narrow band ( $dE/E < 0.5\%$ ) high resolution imaging (<10 micron) at discrete photon energies (6keV – 16keV) for ICF and HED applications.

**HGXD-Rad Hard Camera:** Replace the optical film that is used in the current Hardened Gated X-ray framing camera Diagnostic (HGXD) with radiation hardened CMOS sensors to increase useful neutron yield ceiling of these x-ray imaging cameras to  $\sim 10^{17}$  neutrons per shot.

**Z\_VISAR:** This is 1-D imaging open-beam VISAR system developed in collaboration between SNL and LLNL for use on Z. The primary application is measuring current delivery to MDD-ICF targets.

**Prec.nToF/Quartz Detector:** Precision Neutron time of Flight diagnostic will replace existing Bibenzyl scintillator as the neutron detector with device using Cherenkov emission in quartz crystals. This fast optical signal reduces the instrument response function (IRF) from its current many nanoseconds to  $\sim 350$  of pico-seconds. This effectively reduces the DT Tion systematic uncertainty due to the IRF to around 50 eV. Further, since the crystal is also sensitive to gammas produced at bangtime, the detector will also improve the accuracy of fluid velocity measurements by through direct measurement of the neutron-gamma flight time difference along a given flight path.

**RTNADS:** The real time Nuclear Activation Diagnostic uses in situ Zirconium activation coupled to photomultipliers to provide a real time spatial measurement of the neutron flux at the NIF target chamber after a high yield shot ( $>5e14$  neutrons). This diagnostic will provide a spatial map of relative un-scattered neutron flux at least 24 locations around the NIF target chamber. This data is designed to be used to infer the uniformity of the compressed DT fuel in an ICF implosion.

**Contaminated Control VISAR:** This diagnostic modifies the VISAR debris shield so that VISAR can be used whenever NIF is used to study hazardous material such as “high Z”.

**SPBT upgrade:** South-Pole Bang-Time will be upgraded to provide new HAPG crystals and Indium Phosphide detectors that will characterize the time of peak x-ray capsule emission at both 15 and 30keV. This will be used to obtain a slope temperature measurement at x-ray energies that are transparent to the imploded shell in high convergence implosions.

**Crystal calibration facility:** X-ray calibration station inside NIF facility, to measure absolute sensitivity and sensitivity vs x-ray energy of NIF spectrometer snouts in the geometry in which they are used and to track performance vs time.

**U.V. Interferometry-polarimetry:** Optical diagnostic for measure density profiles and magnetic fields in low density plasmas, relevant for discovery science and hohlraum science.

**EXAFS spectrometer:** High resolution spectrometer for measuring Absorption Fine Structure near absorption edges. This is a sensitive temperature diagnostic in shock heated plasmas. This design allows crystals to be changed to look at the different absorption edges.

**DIXI Polar:** “Dilation Imager for X-rays at Ignition”. A DIXI high temporal resolution x-ray imager will be mounted on the Polar DIM of the NIF target chamber. This diagnostic utilizes a time dilation drift tube to obtain x-ray images of high yield implosions from the pole with a time resolution better than 10 ps. This kind of time resolution is necessary because as the yield increases, the duration of x-ray emission reduces to 100 ps.

**Toroidal x-ray imager:** Toroidal curved x-ray imaging microscope for quasi monochromatic radiography of plasmas and shocked material with <10um resolution and  $dE/E \sim 0.5\%$

**HRV:** NIF High Resolution Velocity Interferometer. This is a 2-Dimensional diagnostic for measuring shock uniformity in ICF ablators such as CH, HDC and Be at pressures in 1 to >20 Mbar range with gate times < 40 ps.

**Imaging x-ray spectrometer:** High spatial and spectral resolution imaging spectrometer for characterizing temperature gradients in HED plasmas.

**SPEC5 nToF:** 5<sup>th</sup> Neutron time of flight diagnostic in a location opposite to existing to nToF detectors. This diagnostic will help to increase accuracy of fluid velocities in high convergence ICF and HED implosions

**SPEC6 nToF:** 6<sup>th</sup> Neutron time of flight diagnostic in a location opposite to existing to nToF detectors. This diagnostic will help to increase accuracy of fluid velocities in high convergence ICF and HED implosions

**VIRGIL time resolved spectrometer:** Adding time resolution to the VIRGIL X-ray spectrometer for characterizing hohlraum emission spectrum in soft x-ray regime.

**4 $\omega$  FIDU:** This is a replacement for the optical 4 $\omega$  (263nm) timing Fiducial that serves SPIDER and DISC streak cameras to improve reliability and energy output.

**HEXI:** The High Energy X-ray Imager is a DIM insertable direct detection diagnostic built using dual hCMOS gated sensors for nanosecond time scale imaging of x-rays in the range of 10keV to 50keV.

**ISS:** Will allow x-ray spectra to be recorded along the polar axis with simultaneous neutron imaging and x-ray pinhole imaging; the spectral data will still have 1D spatial resolution and may be recorded in time-resolved snapshots.

**NEPPS:** A new NEPPS design for use on Cryotarpos or 90-348 for use as a diagnostic for ARC beam studies

**SSII:** New replacement Qtz or PET crystals in the existing SSII snout to look at backlighter and Compton

**AXIS Snout (DRI):** New snout to use on ARC dual backlighting on image plate to radiograph large field of view targets. New snout shall leverage existing AXIS snout design.

**EHXI 90-110 Electronic Readout:** The addition of an electronic readout system for the existing equatorial hard x-ray imager (eHXI) will eliminate the cost and time associated with processing of image plates and enable data from shots to be available in real time.

**dHiRes II:** This is a high-resolution time resolved x-ray spectrometer utilizing conical crystals to measure line emission from Ar.

**DIXI3:** “Dilation Imager for X-rays at Ignition”. A DIXI high temporal resolution x-ray imager will be mounted at the equator of the NIF target chamber.

**FBIT:** Full Beam In-Tank (UV intensity at TCC)

**Beamlets:** Gated Optic Imager to measure relative changes in 60+TOP9 refracted beam intensity (CBET)

**T-OPA TBD:** Transmitted Beam Diagnostic for the Tunable Optical Parametric Amplifier beam (EP UV beam injected into port P9 on the OMEGA target chamber for LPI studies)

**NIF Scattered Light:** Fiber-based, compact spectroscopic measurements for SBS and SRS (add ~5 units per year)

**FABS:** Full Aperture Back Scatter (streaked SBS and SRS)

**OTS:** Optical Thomson Scattering (5 $\omega$  is being pursued currently on the NIF with significant

**TS:** Thomson Scattering

**ROSS:** Rochester Optical Streak System (camera)

**PXTD:** Particle and X-ray Temporal Diagnostic (simultaneous proton, neutron and x-ray burn history)

**2<sup>nd</sup> LOS (nTOF):** Shielded neutron Time-Of-Flight for simultaneous DD/DT yields, T<sub>ion</sub> and  $\rho R$  (via n,T backscatter 10-12 MeV Down Scattered Ratio, DSR)

**3D nTOF:** 3 axes of antipodal neutron time-of-flight (nTOF)

**3<sup>rd</sup> LOS (nTOF):** Third shielded nTOF; challenge is finding a suitable line-of-sight

**NIS:** Neutron Imaging System (scoping feasibility initially)

**KoDI:** Knock-on Deuteron Imager (extension of existing Proton Core Imaging System)

**CherenTOF:** nTOF diagnostic based on a Cherenkov radiator rather than a conventional scintillator

**GCD:** g-ray Cherenkov Detector (time-integrated and time-resolved versions to be pursued)

**SLOS-TRXI:** Single Line-of-Sight Time-Resolved X-ray Imager

**PXRDP(t):** Time-resolved diffraction

**XRPHC:** X-Ray PinHole Camera

**HOTSPEC:** Hard x-ray spectrometer to infer electron temperature

**Spec-Te:** Low energy x-ray spectrometer to infer electron temperature

**GXSC:** “Generic” X-ray Streak Camera (use existing tubes and modern pulsers, package for use in a TIM, add configuration options)

**EXAFSvH:** New crystals in existing von Hamos spectrometer for EXAFS measurements of various materials (initially FeO and Fe)

**XANES:** New crystal(s) in EP High Resolution Spectrometer to measure XANES modulations

**3<sup>rd</sup> LOS GXI:** Time-resolved imager (likely a KBFramed front-end with a DIXI readout)

**UFXRSC:** Ultra-Fast (<ps) X-Ray Streak Camera

**ZP:** Zone Plates (<few microns resolution x-ray imager)

**SCI:** Spherical Crystal Imager (updated crystal configurations to image specific lines/ranges)

**CCPt:** This is a convex crystal spectrometer coupled to an hCMOS camera in the axial diagnostic package. The primary application is time-gated opacity measurements.

**Line VISAR:** This is 1-D imaging open-beam VISAR system developed in collaboration between SNL and LLNL. The primary application is measuring current delivery to MDD-ICF targets.

**HE-diodes:** This is a high energy filtered diode array. The primary application is measuring the time-dependent x-ray output spectrum from >15 keV x-ray sources.

**CRS:** This is a time-integrating spectrometer that measures recoil protons from DD or DT neutrons. The primary application is measuring the burn-averaged neutron spectrum from the stagnation in MDD-ICF.

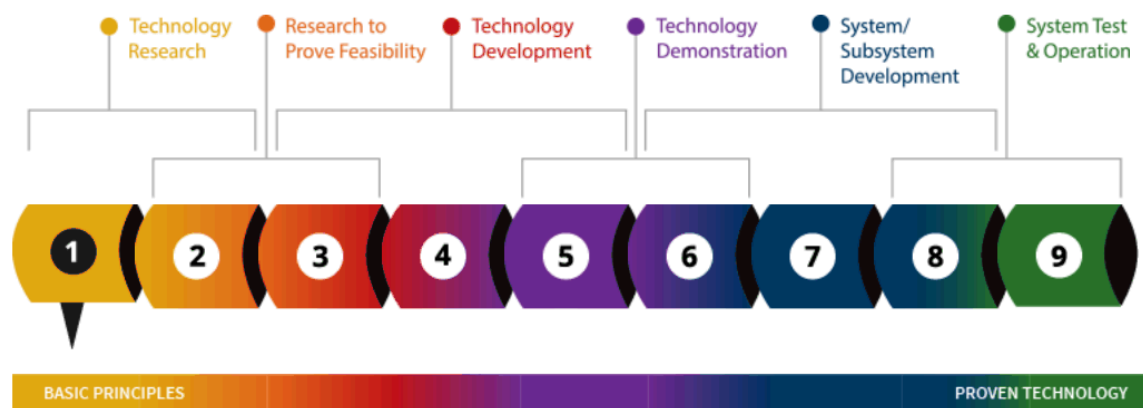
**Gated Backlighting:** This is a spherical crystal backlighter coupled to an hCMOS camera. The primary application is measuring the liner mass distribution near stagnation in MDD-ICF.

**GRH:** This is a gamma reaction history diagnostic to measure the time-history of the DT fusion production in MDD-ICF (requires ~1% tritium on Z).

**DT-nImager:** This is a time-integrating 2-D neutron imager optimized for primary DT neutrons from the stagnation in MDD-ICF.

**MRS:** This is a time-integrating spectrometer that measures the recoil protons from DT neutrons. The primary application is measuring the neutron spectrum from the stagnation in MDD-ICF with higher resolution and range than the CRSLocal Diagnostic Efforts on OMEGA

## Technical Readiness Levels



This work was performed under the auspices of the U.S. Department of Energy by Lawrence Livermore National Laboratory under Contract DE-AC52-07NA27344.